R006-01
A 会場 ：11/25　PM2 （15:30-18:15）
15:30〜15:45

ヌルーセパレーター構造に基づくテーターオーロラの説明

#田中 高史 [1)]
([1]REPPU 研

Interpretation of the Theta Aurora Based on the Null-Separator Structure

#Takashi Tanaka[1)]
([1]REPPU code institute

The theta aurora is reproduced by global simulation. First, we construct a solution for the stationary northward interplanetary magnetic field (IMF) forming the separatrices, the separators, the nulls, and the stemlines. From the drawing of last-closed field lines, the overall structure under this condition is summarized as the northern lobe is generated by a separatrix emanating from the southern null. In this paper, all variations are antisymmetric in the southern hemisphere. Afterward, the IMF By is switched to reproduce the theta aurora. The ionospheric theta aurora is reproduced as closed magnetic field regions. The polar cap is divided to old and new parts, by the theta bar. In the magnetosphere, two dayside nulls occur corresponding to the new IMF and two nulls corresponding to the old IMF retreat tailward. The four nulls form a structure connected by four separators, constructing the magnetospheric topology corresponding to the theta aurora. In this topology, old and new nulls in the southern hemisphere generate old and new lobes in the northern hemisphere. Each lobe is projected onto northern old and new polar caps. The origin of the theta bar is the stagnating closed magnetic field region that occurs between old and new lobes. Separator reconnection occurs between the old lobe in the southern and the new lobe in the northern hemispheres, reducing southern old polar caps. This is the cause of the movement of the theta bar. The theta aurora is the phenomenon that demonstrates the existence of the null-separator structure.

R006-02
A 会場 ：11/25　PM2 （15:30-18:15）
15:45〜16:00

北向き IMF における太陽風磁気圏系での基本物理過程

#藤田 茂 [1)], 田中 高史 [2)], 渡辺 正和 [3)], 蔡 東生 [4)]
[(1] データサイエンスセンター/統数研, [(2]REPPU 研, [(3] 九大・理・地惑, [(4] 筑波大・シス情

Fundamental physical processes of the solar wind-magnetosphere system in the northward IMF condition

#Shigeru Fujita[1)], Takashi Tanaka[2)], Masakazu Watanabe[3)], DongSheng Cai[4)]
[(1]Joint-support center for data science research/The Institute of Statistical Mathematics, [(2]REPPU code institute, [(3]Department of Earth and Planetary Sciences, Graduate School of Science, Kyushu University, [(4]Institute of System and Information, University of Tsukuba

The physical processes in the solar wind-magnetosphere region are usually studied as interactions between independent magnetized plasmas in the two regions across the interface (the magnetopause). We propose an alternative approach that treats the solar wind and the magnetosphere as a single system, wherein the magnetopause is regarded as an internal structure. This approach entails studying the physical processes as interactions between the magnetic field and plasmas within this integrated system. In this approach, we should recall the magnetic field that is not affected by plasmas. It is the vacuum magnetic field which is a superposition of the Earth's main magnetic field and a uniform interplanetary field (IMF). Because the vacuum magnetic field does not have free energy, this field is the definitive ground state of the solar wind-magnetosphere system. Moreover, because the vacuum magnetic field has null points where two different magnetic fields meet [e.g., Cowley, 1973; Lau and Finn, 1990; Watanabe et al., 2005; Xiong et al., 2024], the stage is already set for the reconnection between the IMF and the magnetospheric magnetic field. Therefore, the vacuum field can be called the skeletal magnetic field of the solar wind-magnetosphere system. On the other hand, the solar-wind plasmas just pass the Earth and create a cylindrical shadow behind the Earth in the environment without the magnetic field. Therefore, the behavior of the solar wind-magnetosphere system is determined by the balance between the force that plasma exerts on the skeletal magnetic field and the restoring force caused by the deformed magnetic field (“the mechanical principle”). At this time, the vacuum magnetic field structure has two null points and two separator lines that connect the null points. This two-null two-separator topology is conserved when plasmas deform the skeletal magnetic field in the northward IMF condition (“the topology conservation property”). Therefore, our approach to the physical processes in the solar wind-magnetosphere system in the northward IMF condition is to manifest behaviors of the magnetic field and plasmas in terms of the mechanical principle under the constraints of the topology conservation property. Furthermore, the reconnection process transports magnetic flux and plasma from the solar wind into the magnetosphere, inducing magnetospheric convection. The convection of the plasmas and the magnetic field lines occurs to satisfy the mechanical principle and the topology conservation property. Based on these fundamental principles, we can explain that the lobe is generated as a consequence of the mechanical principle. In addition, the topology conservation property leads to the closed field line region extending long in the magnetotail. Furthermore, we will show that the mechanical principle and the topology conservation property control the generation of the plasma bulge in the lobe, energy transport from the solar wind to the plasma sheet, and formation of the current systems around the magnetosphere.

References

Cowley, S. W. H. (1973), A qualitative study of the reconnection between the Earth's magnetic field and an interplanetary field of arbitrary orientation, Radio Sci., 8(11), 903-913, doi:10.1029/RS008i011p00903.

Lau, Y.-T. and Finn, J. M. (1990), Three-dimensional kinematic reconnection in the presence of field nulls and closed field lines, Astrophysical Journal, 350, 672-691.

Watanabe, M., K. Kabin, G. J. Sofko, R. Rankin, T. I. Gombosi, A. J. Ridley, and C. R. Clauer (2005), Internal reconnection for northward interplanetary magnetic field, J. Geophys. Res., 110, A06210, doi:10.1029/2004JA010832.

Xiong, P., Fujita, S., Watanabe, M., Tanaka, T. and Cai, D. (2024), Identifying and Visualizing Terrestrial Magnetospheric Topology using Geodesic Level Set Method. Computer Graphics Forum, 43: e14994. https://doi.org/10.1111/cgf.14994

R006-03
A 会場 ：11/25　PM2 （15:30-18:15）
16:00〜16:15

#田口 聡 [1)], 今城 峻 [2)], 細川 敬祐 [3)], 原田 裕己 [1)], 松岡 彩子 [2)], 小池 春人 [1)], 品川 裕之 [4)]
([1] 京大理, [2] 京大地磁気センター, [3] 電通大, [4] 九州大学国際宇宙惑星環境研究センター

Abrupt changes in Pc1 pulsations observed at the cusp with the arrival of high-density solar wind: A event on 5 November 2023

#Satoshi Taguchi[1)], Shun Imajo[2)], Keisuke Hosokawa[3)], Yuki Harada[1)], Ayako Matsuoka[2)], Haruto Koike[1)], Hiroyuki Shinagawa[4)]
([1]Department of Geophysics, Graduate School of Science, Kyoto University, [2]DACGSM, Graduate School of Science, Kyoto University, [3]Graduate School of Communication Engineering and Informatics, University of Electro-Communications, [4]International Research Center for Space and Planetary Environmental Science, Kyushu University

We have installed an induction magnetometer at Longyearbyen, Svalbard (˜75.5 MLAT), and started continuous observations at a sampling rate of 64 Hz from 8 September 2023. In this paper we report on the characteristics of the abrupt changes in Pc1 pulsations observed at the cusp by this magnetometer. We focus on the observation at the time of the arrival of the high-density solar wind associated with the coronal mass ejection that occurred on 5 November 2023. At 09:02 UT on that day, the high-density solar wind produced a sudden commencement. Almost at the same time as this sudden commencement, the wideband Pc1 pulsations are abruptly intensified, and then intermittently further intensified. We present the detailed characteristics, including associated signatures of lower-frequency pulsations, and discuss the cause of the abrupt changes in the wideband Pc1 pulsations.

R006-04
A 会場 ：11/25　PM2 （15:30-18:15）
16:15〜16:30

プラズマ圏界面の位置と太陽風電場 Ey の関係: Arase 衛星 PWE 観測に基づく解析

#尾花 由紀 [1)], 海老原 祐輔 [2)], 新堀 淳樹 [3)], 土屋 史紀 [4)], 熊本 篤志 [5)], 笠原 禎也 [6)], 松岡 彩子 [7)], 寺本 万里子 [8)], 堀 智昭 [9)], 三好 由純 [10)], 篠原 育 [11)]
([1] 九州大学 国際宇宙惑星環境研究センター, [2] 京大生存圏, [3] 名古屋大学宇宙地球環境研究所, [4] 東北大・理・惑星プラズマ大気, [5] 東北大・理・地球物理, [6] 金沢大, [7] 京都大学, [8] 九工大, [9] 名大 ISEE, [10] 名大 ISEE, [11] 宇宙機構／宇宙研

Relationship Between Plasmapause Position and Solar Wind Electric Field Ey: Analysis Based on Arase Satellite PWE Observations

#Yuki Obana[1)], Yusuke Ebihara[2)], Atsuki Shinbori[3)], Fuminori Tsuchiya[4)], Atsushi Kumamoto[5)], Yoshiya Kasahara[6)], Ayako Matsuoka[7)], Mariko Teramoto[8)], Tomoaki Hori[9)], Yoshizumi Miyoshi[10)], Iku Shinohara[11)]
([1]International Research Center for Space and Planetary Environmental Science, Kyushu University, [2]Research Institute for Sustainable Humanosphere, Kyoto University, [3]Institute for Space-Earth Environmental Research, Nagoya University, [4]Planetary Plasma and Atmospheric Research Center, Graduate School of Science, Tohoku University, [5]Department of Geophysics, Graduate School of Science, Tohoku University, [6]Emerging Media Initiative, Kanazawa University, [7]Graduate School of Science, Kyoto University, [8]Kyushu Institute of Technology, [9]Institute for Space-Earth Environmental Research, Nagoya University, [10]Institute for Space-Earth Environement Research, Nagoya University, [11]Japan Aerospace Exploration Agency/Institute of Space and Astronautical Science

Using the electric field spectral data obtained by the Plasma Wave Experiment (PWE) onboard the Arase satellite, we calculated in-situ electron density to determine the plasmapause (Lpp) locations, in which we examined its dependence on Ey, SYM-H, and Kp. The plasmapause was defined as a region where the electron density (ne) changed by a factor of 5 or more within Δ L <0.1, and we identified a total of 348 plasmapause crossings. Our primary analysis focused on the 180 events detected on the nightside (18-6 MLT), in which we examined its dependence on Ey, SYM-H, and Kp.

We found that the average Ey over the past 48 hours had the highest correlation with Lpp. Specifically, when the average Ey was less than 1.8 mV/m, we observed the strongest correlation, resulting in the approximate formula Lpp $\approx$ 2.41 $\times$ Ey + 6.8. However, when the average Ey exceeded 2 mV/m, Lpp became more dispersed, suggesting a potential saturation.

We also investigated the correlation between Lpp and Ey across six different MLT bins. The best correlation was observed in the 22-2 MLT bin. When varying the averaging time of Ey from 1 to 48 hours, the optimal correlations were found with approximately 45 hours for the 22-6 MLT bin, 10 hours for the 6-14 MLT bin, and 20 hours for the 14-22 MLT bin. The ˜45-hour averaging time seems unexpectedly long, given that the nightside plasmapause is known to respond to IMF polarity changes within approximately 30 minutes and undergo erosion (e.g., Goldstein et al., 2003). It is also unusual that Lpp on the nightside shows a better correlation with longer averaging times of Ey compared to Lpp on the dayside. These phenomena warrant further detailed research.

あらせ衛星搭 Plasma Wave Experiment (PWE) で得られた電場スペクトルデータを使用して電子密度を算出し、プラズマ圏界面（Lpp）の位置を特定した。これを 3 つの異なる地磁気指標、すなわち Ey、SYM-H、Kp と比較した。プラズマ圏界面は、電子密度（ne）がΔ L <0.1 の範囲で 5 倍以上変化する領域として定義され、合計で 348 回のプラズマ圏界面通過イベントを検出した。まず初めに、夜側（18-6 MLT）で検出された 180 件のイベントを分析し、Lpp と Ey、SYM-H、Kp との比較を行った。その結果、過去 48 時間の平均 Ey が Lpp と最も高い相関を示した。特に、平均 Ey が 1.8 mV/m 未満の場合に最も強い相関が観測され、Lpp $\approx$ 2.41 $\times$ Ey + 6.8 という近似式が得られた。しかし、平均 Ey が 2 mV/m を超えると、Lpp はより分散し、飽和の兆候が示唆された。

さらに、Lpp と Ey の相関を 6 つの異なる MLT ビンに分けて調査した。その結果、22-2 MLT ビンで最も高い相関が確認された。Ey の平均化時間を 1 時間から 48 時間まで変動させたところ、22-6 MLT ビンでは約 45 時間、6-14 MLT ビンでは約 10 時間、14-22 MLT ビンでは約 20 時間の平均化時間で最適な相関が得られた。しかし、約 45 時間という平均化時間は予想外に長く、夜側のプラズマ圏界面が IMF（太陽風磁場）の極性変化に対して約 30 分で反応し、侵食することが知られている（Goldstein et al., 2003）。さらに、夜側の Lpp が昼側の Lpp に比べて、より長い時間平均化された Ey と高い相関を示す結果は一見、奇妙であり、さらなる詳細な研究が必要である。

R006-05
A 会場 ：11/25　PM2 （15:30-18:15）
16:30〜16:45

#長田 知大 [1)], 関 華奈子 [1)], 山川 智嗣 [2)], 山本 和弘 [2)], 桂華 邦裕 [1)], 海老原 祐輔 [3)], 天野 孝伸 [1)], 三好 由純 [2)]
([1] 東大理・地球惑星科学専攻, [2] 名古屋大学 ISEE, [3] 京大生存圏

Magnetic storms of a weakly magnetized planet based on global inner magnetospheric simulations

#Kazuhiro Osada[1)], Kanako Seki[1)], Tomotsugu Yamakawa[2)], Kazuhiro Yamamoto[2)], Kunihiro Keika[1)], Yusuke Ebihara[3)], Takanobu Amano[1)], Yoshizumi Miyoshi[2)]
([1]Department of Earth and Planetary Science, Graduate School of Science, University of Tokyo, [2]Institute for Space-Earth Environmental Research, Nagoya University, [3]Research Institute for Sustainable Humanosphere, Kyoto University

Intrinsic magnetic field of terrestrial planets is one of the important factors that determine the space environment near the planet and the magnetospheric structure. Earth's intrinsic magnetic field strength has decreased by 9% over the past 150 years and by ˜30% over the past 2000 years [Olson and Amit, 2006]. The decrease may change not only the quasi-static state of near-Earth space environment but also the development of magnetic storms. A previous study examined the influence of the intrinsic magnetic field on auroral substorms using global MHD simulations [Ebihara et al., 2020]. However, the effect of intrinsic magnetic field strength on the development of magnetic storms is still unclear, because kinetic processes, which are not included in the MHD approximation, are dominant in the inner magnetosphere.

We investigated the development of magnetic storms and ring current, using the magnetosphere-ionosphere coupled model [Yamakawa et al., 2023], which combines GEMSIS-RC [Amano et al., 2011], cold plasmaspheric module, and GEMSIS-POT [Nakamizo et al., 2012]. In GEMSIS-RC, the 5D drift kinetic equation is solved self-consistently with Maxwell equations. GEMSIS-POT solves ionospheric potential for the height-integrated ionosphere. In the coupled model, motions of cold plasma in the plasmasphere are also included based on a continuity equation. Simulations were conducted for three cases: the present Earth (Case 1), a planet with a weak (2/3 of Case 1) intrinsic magnetic field and high ionospheric conductivity (Case 2), and with the weak magnetic field and standard (the same as Case 1) ionospheric conductivity (Case 3). Case 1, 2, and 3 correspond to Run 1, 3, and 5 in Ebihara et al. [2020], respectively. For each case, we applied R1-FAC to the ionosphere and set the temperature and density of the plasma sheet, according to the corresponding run.

The development of the ring current was investigated in detail for Cases 1-3. SYM-H index was calculated with the Dessler-Parker-Sckopke equation. The results show that the intensities of magnetic storms are in the following order: Case 3 >Case 2 >Case 1. We also found that SYM-H declines more rapidly in Cases 2 and 3 compared to Case 1. This is because the ring current development in the azimuthal direction is faster in the weak magnetic field cases than Case 1, because the distance from the planet is smaller at the same magnetic field strength. In Case 3, the ionospheric conductivity and plasma convection are as strong as in Case 1, although the scale of the dipole is smaller, which allows ions to inject more efficiently and results in the most intense and rapidly developing magnetic storm. Because the outer boundary conditions on the nightside, i.e., the temperature and density of the plasma sheet, were derived from the results of the MHD simulation runs corresponding to each case [Ebihara et al., 2020], changes in the size of the simulation box can alter the properties of the injected ions, which may affect the results. By comparing the results from two different simulation boxes, the characteristics of the model and the validity of the conclusions will be also discussed.

R006-06
A 会場 ：11/25　PM2 （15:30-18:15）
17:00〜17:15

#三好 由純 [1)], チェン ルイ [2)], 田 采祐 [1)], 栗田 怜 [3)], 松田 昇也 [4)], 齊藤 慎司 [5)], 加藤 雄人 [6)], 浅村 和史 [7)], 寺本 万里子 [8)], 山本 和弘 [1)], Kumar Sandeep[1)], Porunakatu Radhakrishna Shreedevi[1)], 風間 洋一 [9)], ウォング シャンユー [9)], 堀 智昭 [1)], 篠原 育 [7)], 笠原 禎也 [4)], 笠原 慧 [10)], 横田 勝一郎 [11)], 桂華 邦裕 [10)], 三谷 烈史 [7)], 高島 健 [7)], 土屋 史紀 [6)], 熊本 篤志 [6)], 新堀 淳樹 [1)], 松岡 彩子 [3)]
([1] 名大 ISEE, [2]Auburn University, [3] 京都大学 生存研, [4] 金沢大学, [5] 情報通信研究機構, [6] 東北大・理・地球物理, [7] 宇宙研, [8] 九工大, [9]ASIAA, [10] 東京大学, [11] 大阪大

Origins of chorus waves in the inner magnetosphere

#Yoshizumi Miyoshi[1)], Rui Chen[2)], ChaeWoo Jun[1)], Satoshi Kurita[3)], Shoya Matsuda[4)], Shinji Saito[5)], Yuto Katoh[6)], Kazushi Asamura[7)], Mariko Teramoto[8)], Kazuhiro Yamamoto[1)], Sandeep Kumar[1)], Shreedevi Porunakatu Radhakrishna[1)], Yoichi Kazama[9)], Shiangu Yu Wang[9)], Tomoaki Hori[1)], Iku Shinohara[7)], Yoshiya Kasahara[4)], Satoshi Kasahara[10)], Shoichiro Yokota[11)], Kunihiro Keika[10)], Takefumi Mitani[7)], Takeshi Takashima[7)], Fuminori Tsuchiya[6)], Atsushi Kumamoto[6)], Atsuki Shinbori[1)], Ayako Matsuoka[3)]
([1]Institute for Space-Earth Environemental Research, Nagoya University, [2]Auburn University, [3]Research Institute for Sustainable Humanosphere, Kyoto University, [4]Kanazawa University, [5]National Institute of Information and Communications Technology, [6]Department of Geophysics, Graduate School of Science, Tohoku University, [7]Japan Aerospace Exploration Agency, [8]Kyushu Institute of Technology, [9]Academia Sinica Institute of Astronomy and Astrophysics, [10]The University of Tokyo, [11]Osaka University

Non-linear whistler mode waves, known as chorus waves, are commonly observed in the inner magnetosphere. These waves play a crucial role in the dynamics of energetic electrons, including their acceleration, which contributes to the formation of radiation belts, and the scattering of electrons across a wide energy range, leading to phenomena such as pulsating auroras and relativistic electron microbursts. Recent studies suggest that non-linear processes are significant in the generation of these waves, particularly through the formation of electron holes in phase space. Theoretical threshold amplitudes have been proposed as a proxy for estimating the conditions necessary to trigger these non-linear processes. In this study, we investigate the generation of chorus waves in the inner magnetosphere in association with 1) substorm injections, 2) Pc5 pulsations, and 3) solar wind dynamic pressure enhancements. Using data from the Arase satellite (LEPe/MEPe/HEP, PWE and MGF), we analyze the time variations in threshold amplitudes before and after chorus wave generation. In all three cases, it is expected that the linear growth rate increases due to temperature anisotropy resulting from betatron acceleration. A decrease in the threshold amplitude, which is essential for triggering the generation of chorus waves, is observed. This decrease is attributed to the enhancement of hot electron density through injections in case 1) and Pc5 modulation in case 2) and changes in field line topology in case 3). We conclude that both an increased linear growth rate and decreased threshold amplitudes contribute to the non-linear triggering of chorus waves.

R006-07
A 会場 ：11/25　PM2 （15:30-18:15）
17:15〜17:30

あらせ衛星観測に基づくコーラス波動強度の経験モデルの構築

#栗田 怜[1)], 三好 由純[2)], 加藤 雄人[3)], 齊藤 慎司[4)], 松田 昇也[5)], 笠原 禎也[6)], 松岡 彩子[7)], 堀 智昭[8)], 寺本 万里子[9)], 山本 和弘[10)], 篠原 育[11)]
([1] 京都大学 生存研, [2] 名大 ISEE, [3] 東北大・理・地球物理, [4] 情報通信研究機構, [5] 金沢大学, [6] 金沢大, [7] 京都大学, [8] 名大 ISEE, [9] 九工大, [10] 名大 ISEE, [11] 宇宙機構／宇宙研

Construction of empirical wave power model of whistler-mode chorus waves based on the Arase observation

#Satoshi Kurita[1)], Yoshizumi Miyoshi[2)], Yuto Katoh[3)], Shinji Saito[4)], Shoya Matsuda[5)], Yoshiya Kasahara[6)], Ayako Matsuoka[7)], Tomoaki Hori[8)], Mariko Teramoto[9)], Kazuhiro Yamamoto[10)], Iku Shinohara[11)]
([1]Research Institute for Sustainable Humanosphere, Kyoto University, [2]Institute for Space-Earth Environement Research, Nagoya University, [3]Department of Geophysics, Graduate School of Science, Tohoku University, [4]National Institute of Information and Communications Technology, [5]Kanazawa University, [6]Emerging Media Initiative, Kanazawa University, [7]Graduate School of Science, Kyoto University, [8]Institute for Space-Earth Environmental Research, Nagoya University, [9]Kyushu Institute of Technology, [10]Institute for Space-Earth Environmental Research (ISEE), Nagoya University, [11]Japan Aerospace Exploration Agency/Institute of Space and Astronautical Science

Whistler-mode chorus waves play crucial roles in the Earth's inner magnetosphere dynamics through wave-particle interactions. In particular, stochastic acceleration by chorus waves is considered to be responsible for the creation of relativistic electrons in the Earth's outer radiation belt during geomagnetic disturbances. The quasi-linear diffusion regime can describe the stochastic acceleration, and modeling works based on the regime successfully reproduce observed flux increase in radiation belt electrons during geomagnetic disturbances. The quasi-linear diffusion model of chorus waves requires information on wave power and the normal angle of chorus waves, which significantly changes the timescale for the acceleration of relativistic electrons. The model describes the wave power distribution as a function of frequency using a Gaussian function. Since the magnetic latitude dependence of this distribution has not been clarified very well, it needs to be incorporated into the model to correctly evaluate the stochastic acceleration of electrons during the propagation of chorus waves from the magnetic equator to higher latitudes.

We aimed to develop the empirical chorus wave model based on the Arase satellite observation, which describes the wave power distribution as a function of frequency as well as MLAT and MLT dependence of the distribution. We have statistically studied the frequency spectra of wave magnetic fields obtained by the Onboard Frequency Analyzer (OFA), a part of the Plasma Wave Experiment onboard the Arase satellite. The wave power of chorus waves is derived from the OFA-SPEC dataset, and the wave power is modeled so that the parameter can be used as inputs of the quasi-linear diffusion model. We report on the integrated wave power distribution of lower-band and upper-band chorus waves as a function of L^*, MLAT, and MLT. The input parameters of the quasi-linear diffusion model are derived from the obtained distributions, and diffusion rates will be calculated using the parameters derived from the Arase observation.

R006-08
A 会場 ：11/25　PM2 （15:30-18:15）
17:30〜17:45

あらせによって観測された低周波ホイッスラーコーラス波動の空間分布と伝搬特性

#玉村 優剛 [1)], 松岡 彩子 [1)], 寺本 万里子 [2)], 笠原 禎也 [3)], 尾崎 光紀 [4)], 松田 昇也 [5)], 三好 由純 [6)], 堀 智昭 [6)], 篠原 育 [7)], 土屋 史紀 [8)], 熊本 篤志 [9)], 笠羽 康正 [10)]
([1] 京都大学理学研究科, [2] 九工大, [3] 金沢大, [4] 金沢大, [5] 金沢大学, [6] 名大 ISEE, [7] 宇宙機構／宇宙研, [8] 東北大・理・惑星プラズマ大気, [9] 東北大・理・地球物理, [10] 東北大・理

Analysis of space distribution and propagation properties of low frequency whistler chorus waves observed by Arase

#Yugo Tamamura[1)], Ayako Matsuoka[1)], Mariko Teramoto[2)], Yoshiya Kasahara[3)], Mitsunori Ozaki[4)], Shoya Matsuda[5)], Yoshizumi Miyoshi[6)], Tomoaki Hori[6)], Iku Shinohara[7)], Fuminori Tsuchiya[8)], Atsushi Kumamoto[9)], Yasumasa Kasaba[10)]
([1]Graduate School of Science, Kyoto University, [2]Kyushu Institute of Technology, [3]Emerging Media Initiative, Kanazawa University, [4]Institute of Science and Engineering, Kanazawa University, [5]Kanazawa University, [6]Institute for Space-Earth Environement Research, Nagoya University, [7]Japan Aerospace Exploration Agency/Institute of Space and Astronautical Science, [8]Planetary Plasma and Atmospheric Research Center, Graduate School of Science, Tohoku University, [9]Department of Geophysics, Graduate School of Science, Tohoku University, [10]Planetary Plasma and Atmospheric Research Center, Graduate School of Science, Tohoku University

In the Earth's inner magnetosphere, the radiation belts are torus-shaped zones at 2-6 Earth radii distance from the center of the Earth, where high energy particles are trapped by the Earth's magnetic field. It is known that the acceleration and loss of the energetic particles in the radiation belts are deeply related with the energy transfer by electromagnetic waves. Whistler chorus waves are electromagnetic wave often observed in the low-density region outside the plasmasphere. The frequencies are generally ranging 0.1 - 0.8 fce (fce is the equatorial electron cyclotron frequency). Whistler chorus waves are typically divided into lower band chorus of 0.1 - 0.5 fce and upper band chorus of 0.5 -0.8 fce, with a clear gap in wave power at 0.5 fce. The contribution of chorus waves to the acceleration and loss of the radiation belt particles has been examined by many studies. They suggested that chorus waves are generated by an anisotropic distribution of energetic electrons (a few – hundred keV) injected from the plasma sheet during substorms and energize the electrons in the radiation belt. Cattell et al. (2015) statically investigated the whistler chorus waves during moderate geomagnetic storms observed by Van Allen Probes (VAPs) and found that their frequencies often dramatically dropped and became much lower than the commonly observed frequencies of whistler chorus waves. Analysis of the Poynting flux of such chorus waves suggested that low-frequency chorus waves originated in the magnetic equator region and propagated along the magnetic field lines to high latitudes. Then, the cyclotron resonance kinetic energy may exceed the rest mass energy of the electron (~0.5 MeV) at low frequency below 0.1fce, and chorus emissions below 0.1fce can play an important role in discussing the dynamics of radiation band electrons. Thus, recently, VAPs observations have led to a study of the excitation mechanism by low frequency chorus waves and their effect on relativistic electrons.

We investigated the distribution of L-value, magnetic local time (MLT), and magnetic latitude (MLAT) of low-frequency chorus waves observed by the Arase satellite during the period from March 2017, when the satellite began regular observations, to October 2018. Similar to the VAPs results, low-frequency whistler chorus waves were often observed by the Arase satellite, while these waves were also observed at MLAT higher than 20° , outside the area of the VAPs observation. In addition, while previous studies such as Cattell et al. (2015) limited their analysis to days when Dst was below -50 nT, we investigated all periods regardless of the geomagnetic activity and found that low-frequency whistler chorus waves were observed even when Dst was relatively quiet. Focusing on the spatial distribution and propagation characteristics of low-frequency whistler chorus waves observed by the Arase satellite, we discuss the effect on the dynamics of radiation belt electrons and the propagation to high latitude regions.

地球内部磁気圏には、2-6 地球半径の距離に、高エネルギープラズマが地球磁場によって捕捉されている放射線帯と呼ばれるトーラス状の領域が存在している。放射線帯を形成している高エネルギープラズマの生成・消滅には、電磁波によるエネルギー授受が深く寄与していることが知られている。プラズマ圏外側の低密度領域で観測される電磁波であるホイッスラーコーラス波は、一般的に周波数が赤道電子サイクロトロン周波数 fce の 0.1-0.8 倍の範囲である。また、典型的には 0.1-0.5fce の周波数帯の低域コーラスと 0.5-0.8fce の周波数帯の高域コーラスに分かれており、0.5fce 付近に明瞭なギャップが存在する。コーラス波による放射線帯粒子の生成・消滅への寄与は多くの研究により明らかになってきており、コーラス波はサブストーム時にプラズマシートから流入される異方性をもつ高エネルギー電子 (数 keV-100keV) によって発生し、電子放射線帯を活性化する働きをすることが示唆されている。Cattell et al. (2015) では、Van Allen Probes (VAPs) で観測された中程度の地磁気嵐時のホイッスラーコーラス波を統計的に調査した結果、一般的によく観測されるホイッスラーコーラス波の周波数よりも極端に低い周波数をもつ低周波ホイッスラーコーラス波がしばしば観測されることが報告されている。このコーラス波のポインティングフラックスを調査した結果、低周波コーラス波は磁気赤道付近で発生し、磁力線に沿って高緯度領域に伝播していることが見出された。また、0.1fce を下回るような低い周

波数のコーラス波は、サイクロトロン共鳴運動エネルギーが電子の静止質量エネルギー (~0.5MeV) に近づくため、放射線帯電子のダイナミクスを議論する上で重要な役割を果たす可能性が示唆されている。近年では、VAPs による観測から、低周波ホイッスラーコーラス波の励起メカニズムや相対論的電子に与える影響について研究が行われている。本研究では、あらせ衛星に搭載されているサーチコイル磁力計のデータを使用して、2017 年 3 月から 2018 年 10 月までの期間において、あらせ衛星で観測された低周波コーラス波の L 値、磁気地方時 (MLT)、磁気緯度 (MLAT) について調査を行った。あらせ衛星による観測でも、VAPs の結果と同様に、低周波ホイッスラーコーラス波がしばしば観測された一方、VAPs の観測領域外の、MLAT が 20° を超える領域でも低周波コーラス波が観測されることがわかった。また、Cattell et al.(2015) 等の先行研究では、Dst が-50nT 以下の日に限定して解析を行っていたが、今回の研究では、Dst による制限を無くしたところ、Dst が比較的静穏な時でも、低周波ホイッスラーコーラス波が観測されることが判明した。あらせ衛星で観測された低周波ホイッスラーコーラス波の空間分布や伝搬特性に着目し、放射線帯電子のダイナミクスに与える影響や高緯度領域への伝搬について議論する。

R006-09
A 会場 ：11/25　PM2 （15:30-18:15）
17:45〜18:00

あらせ衛星で観測されたNWC送信局信号を用いた伝搬方向推定手法の検討

#牛山 大洋 [1)], 梅澤 祐伊 [1)], 笠原 禎也 [1)], 松田 昇也 [1)], 太田 守 [2)], 土屋 史紀 [3)], 熊本 篤志 [3)], 松岡 彩子 [4)], 三好 由純 [5)], 篠原 育 [6)]
([1] 金沢大, [2] 富山高専, [3] 東北大, [4] 京都大学, [5] 名古屋大, [6] 宇宙機構／宇宙研

Evaluation of a direction finding method using NWC transmitter signals observed by the Arase satellite

#Taiyo Ushiyama[1)], Yui Umezawa[1)], Yoshiya Kasahara[1)], Shoya Matsuda[1)], Mamoru Ota[2)], Fuminori Tsuchiya[3)], Atsushi Kumamoto[3)], Ayako Matsuoka[4)], Yoshizumi Miyoshi[5)], Iku Shinohara[6)]
([1]Kanazawa university, [2]NIT(KOSEN), Toyama College, [3]Tohoku University, [4]Kyoto University, [5]Nagoya University, [6]ISAS/JAXA

Propagation direction of plasma waves is crucial for understanding the environment of the terrestrial inner magnetosphere. Analyzing the propagation characteristics of plasma waves, which change under the influence of the medium during the propagation process, leads to a better understanding of the three-dimensional plasma environment along the propagation paths. Several methods have been proposed to determine the wave normal angle (WNA) of plasma waves using electromagnetic field data obtained by scientific satellites. However, the estimation primarily requires the three components of the magnetic field. If one component is missing due to sensor degradation or other issues, it becomes difficult to perform the estimation using single plane wave models like the Means' method or the SVD method, which assume all three magnetic field components are available. Since October 2018, the Arase satellite has been unable to measure one component of the magnetic field due to the degradation of the onboard triaxial search-coil magnetometer. Therefore, it is necessary to explore other methods for estimating the WNA for the data measured after October 2018. This study aims to establish a reliable method to determine the WNA in an environment under only four components of the electromagnetic field (two components of electric field and two components of magnetic field) are available.

In this study, we evaluate the estimation accuracy of the MUSIC (Multiple Signal Classification) method by using the amplitude and phase information among electromagnetic fields calculated from the dispersion relation of plasma waves. Since the MUSIC method can estimate the WNA using smaller number of components due to the estimation principle, it is expected that it works with four components of the electromagnetic field. We apply this method to the waveform data measured by the waveform capture (WFC), which is one of the receivers of the Plasma Wave Experiment (PWE) on board the Arase satellite. We analyze the WNA of artificial signals from the NWC (North West Cape) transmitter in Australia and statistically evaluate the propagation characteristics to verify the validity of the estimation results. First, we define the accuracy of the estimated WNA as the angular width derived from the MUSIC spectrum in the zenith angle (θ) and in the azimuth angle (ϕ). These angular widths are determined within a range of -10 dB from the maximum value of the MUSIC spectrum. Next, using four observation events of the NWC signal during periods when all five electromagnetic field components were available, we draw scatter plots showing the absolute error between the four-component and five-component estimates on the horizontal axis and the accuracy of the four-component estimates on the vertical axis. We then determine the threshold for the accuracy of the four-component estimates that satisfies an absolute error within 10 degrees. Next, for events after October 2018, we derive four-component estimates where the estimated error is within 10 degrees after applying the above-mentioned threshold and investigate the relationship between amplitudes and WNAs, revealing a positive correlation between the signal amplitude and the stability of the WNA. Finally, we determine a typical WNA by taking a moving average of the sum of squares of the amplitudes with a 5-degree interval and normalized it by the observation time length. Investigating the relationship between the determined WNA and the magnetic latitude of the observation point, we find that the zenith angle (θ) of the WNA decreases from the transmission station towards the magnetic equator and then increases again towards the conjugate point.

In this presentation, we will show the statistical evaluation results of the estimation accuracy using the four electromagnetic field components from the NWC transmitter signals, along with a comparison to simulations conducted using ray tracing.

地球近傍の宇宙空間は内部磁気圏と呼ばれ，その環境の理解にプラズマ波動の伝搬方向は重要な情報となる．伝搬過程において媒質の影響を受け変化するプラズマ波動の伝搬特性を解析することは、伝搬経路に沿った 3 次元的なプラズマ環境の理解につながる．科学衛星による電磁界計測データからプラズマ波動の WNA（Wave normal angle）を求める様々な手法が提案されているが，推定には主に磁界 3 成分を要し，磁界センサの劣化等によって 1 成分が欠損した場合，Means 法や SVD 法のような磁界 3 成分を前提とした単一平面波モデルのアルゴリズムでは推定が困難となる．2018 年 10 月以降，あらせ衛星は搭載された三軸サーチコイル磁力計の劣化により，磁界 1 成分が使用できない状態にあり，これ以後のデータについて WNA 推定を行う方法の検討が必要である．そのため，本研究では電界 2 成分，磁界 2 成分の計 4 成分の観測情報のみで信頼性のある伝搬方向推定手法の確立を目的とする．

本研究では，電磁界間の振幅・位相情報をプラズマ波動の分散関係を用いて求め， MUSIC (Multiple Signal Classification) 法を利用して WNA 推定を行う方法について，推定精度を評価する．MUSIC 法は推定手法の原理上少ない成分

数でも推定が可能であるため，電磁界 4 成分でも推定できることが期待できる．評価にはあらせ衛星搭載のプラズマ波動・電場観測器 (PWE) の受信器の 1 つである波形捕捉受信器 (WFC) で取得された電界 2 成分，磁界 3 成分の波形データを用い，オーストラリアの NWC(North West Cape) 局からの人工信号の WNA 解析を行い，伝搬特性を統計的に評価することで，推定結果の妥当性を検証する．

まず，磁力線に対する WNA の天頂角を示す θ 方向，方位角を示す φ 方向における MUSIC スペクトルから，最大値-10 dB より得られる角度幅を推定角度に対する精度として定義する．次に，電磁界 5 成分が使用可能な期間の NWC 信号観測イベント 4 件より，電磁界 5 成分を用いた推定結果と 4 成分を用いた推定結果の絶対誤差を横軸に，4 成分を用いて推定した際の精度を縦軸にとった散布図を作成し，絶対誤差 10° 以内となる 4 成分推定時の精度の閾値を決定する．次に 2018 年 10 月以降のイベントについて電磁界 4 成分推定を行い，前述した閾値を適用後に推定誤差が 10° 以内となるデータについて，振幅-WNA の散布図を作成したところ，振幅が大きいほど WNA が安定する傾向があることを確認した．そこで，この散布図をもとに，振幅の 2 乗和を 5 度幅で移動平均をとり，観測時間で正規化することで，振幅を重みとした各イベントの最も支配的な WNA を決定した．最後に，すべてのイベントに対し，決定した WNA と観測地点の磁気緯度の関係を調査し，送信局から磁気赤道にかけて WNA が減少し，その後共役地点に向けて WNA が増加する傾向を確認した．

本発表では，NWC 局からの信号を用いた電磁界 4 成分での推定精度を統計的に評価した結果を，レイトレーシングによるシミュレーションとの比較とともに示す．

R006-10
A 会場 ：11/25　PM2 （15:30-18:15）
18:00〜18:15

あらせ衛星が観測した中緯度プラズマ圏低域混成波の統計的研究

#山本 和弘 [1)], 三好 由純 [2)], 新堀 淳樹 [3)], 松岡 彩子 [4)], 寺本 万里子 [5)], 笠原 禎也 [6)], 松田 昇也 [7)], 堀 智昭 [8)], 熊本 篤志 [9)], 土屋 史紀 [10)], 篠原 育 [11)]
([1] 名大 ISEE, [2] 名大 ISEE, [3] 名古屋大学宇宙地球環境研究所, [4] 京都大学, [5] 九工大, [6] 金沢大, [7] 金沢大学, [8] 名大 ISEE, [9] 東北大・理・地球物理, [10] 東北大・理・惑星プラズマ大気, [11] 宇宙機構／宇宙研

A statistical study on energy sources of mid-latitude plasmaspheric lower hybrid waves observed by the Arase satellite

#Kazuhiro Yamamoto[1)], Yoshizumi Miyoshi[2)], Atsuki Shinbori[3)], Ayako Matsuoka[4)], Mariko Teramoto[5)], Yoshiya Kasahara[6)], Shoya Matsuda[7)], Tomoaki Hori[8)], Atsushi Kumamoto[9)], Fuminori Tsuchiya[10)], Iku Shinohara[11)]
([1]Institute for Space-Earth Environmental Research (ISEE), Nagoya University, [2]Institute for Space-Earth Environement Research, Nagoya University, [3]Institute for Space-Earth Environmental Research, Nagoya University, [4]Graduate School of Science, Kyoto University, [5]Kyushu Institute of Technology, [6]Emerging Media Initiative, Kanazawa University, [7]Kanazawa University, [8]Institute for Space-Earth Environmental Research, Nagoya University, [9]Department of Geophysics, Graduate School of Science, Tohoku University, [10]Planetary Plasma and Atmospheric Research Center, Graduate School of Science, Tohoku University, [11]Japan Aerospace Exploration Agency/Institute of Space and Astronautical Science

The lower hybrid resonance frequency (f_{LHR}) is an important plasma parameter to know because the lower hybrid resonance appears near f_{LHR} for perpendicularly propagating waves (θ_{WNA} ~90°, where θ_{WNA} is the wave normal angle). In the Earth's magnetosphere, f_{LHR} also controls the reflection of whistler mode waves and is related to the generation of plasmaspheric hiss. The lower hybrid waves can heat thermal electrons and ions through Landau resonance (e.g., Lashkul et al., 2001; Cairns & McMillan, 2005) and probably play a role in particle acceleration.

While plasma wave emissions near f_{LHR} were reported as lower hybrid cavities in the auroral region of the topside ionosphere (e.g., Smith et al., 1966; Kintner et al., 1992) and as lower hybrid drift waves at the magnetopause (e.g., Graham et al., 2017, 2019), few studies have reported lower hybrid resonance emissions in the inner magnetosphere. Recently, Liu et al. (2021) have shown that Van Allen Probes often (up to ~10% of the dwelling time) detect lower hybrid waves within 5° around the magnetic equator. They proposed a couple of possible energy sources for wave excitation including ring current protons, density gradients, and mode conversion from whistler mode waves for each local time sector. However, they could not investigate lower hybrid waves at mid-latitudes due to the limitation of Van Allen Probes orbits. Therefore, the relation between lower hybrid waves and ionospheric energy sources like lightning whistlers is still unclear. Xia et al. (2022) have investigated ionospheric lower hybrid waves observed by the DEMETER satellite. They ruled out the possibility of mode conversion from lightning whistlers on the basis of the AE dependence of the lower hybrid waves that they analyzed.

In this presentation, we report a statistical study on lower hybrid waves observed by the Arase satellite observations from 27 March 2017 to 31 Dec 2022 to reveal the off-equator distribution of lower hybrid waves and identify their energy sources. We mainly analyzed wave electric and magnetic field data from 64 Hz to 19.5 kHz obtained by PWE/OFA (Matsuda et al., 2018; Kasahara et al., 2017). We automatically detected spectral peaks in the electric field spectra which are not accompanied by peaks in the magnetic field spectra near f_{LHR}. We find that most of the detected lower hybrid waves occur in the off-equator region of |MLAT|>20° inside the plasmasphere, where MLAT is the magnetic latitude. Their occurrence rate reaches ~70% at L = 2-3 on the dayside. Compared with the result of Liu et al. (2021), this result indicates that the mid-latitude plasmaspheric population dominates in the inner magnetosphere. We also examine MLT, SYM-H, F10.7, and seasonal dependences of the detected lower hybrid waves. The variations of the occurrence rate and the wave power at L = 1-2 show different trends from those at L >3, suggesting different energy sources at lower L-shells. We compare our results with past statistical studies of lightning whistlers (Oike et al., 2014) and hiss waves (Li et al., 2015; Meredith et al., 2021). The MLT and seasonal dependences of lower hybrid waves at L = 1-2 are similar to that of lightning whistlers, while the SYM-H dependence at L >3 is similar to that of hiss waves. According to Yu et al. (2017), the wave normal angles of hiss waves rapidly become large at |MLAT|>20°. Because the mode conversion from whistler mode waves to lower hybrid waves can occur at large θ_{WNA}, the latitudinal distributions of lower hybrid waves can be attributed to the wave normal angle of hiss waves. We conclude that mode conversion from lightning whistlers and hiss waves is the most likely process of lower hybrid wave excitation in the plasmasphere.

低域混成周波数 fLHR）は重要なプラズマパラメータのひとつである。磁化プラズマ中の伝搬角９０度の電磁波は fLHR 周辺で共鳴を起こす。光線追跡法の数値計算では、磁力線に沿って高緯度に向かって伝搬するホイッスラー波が徐々に伝搬角を変えながら波動振動数が fLHR と等しくなるところで反射することが示されており、プラズマ圏ヒスの生成メカニズムを考えるうえで重要である。また、低域混成はランダウ共鳴などを通して 100 eV 程度の電子やイオンを加熱することが指摘されており、磁気圏での粒子加速に寄与していると考えられる。

電離圏上部の極光領域や磁気圏界面にて低域混成波の観測例が報告されている一方、内部磁気圏における低域混成波の

研究は長らく行われていなかった。近年になって、Liu et al. (2021) が赤道付近を飛翔する Van Allen Probes 衛星のデータを解析した結果、磁気赤道から± 5° の範囲に集中して最大 10% の頻度で発生していることが分かった。しかしながら、Van Allen Probes 衛星は赤道付近のみを飛翔するため中高緯度の分布を把握することができなかった。低域混成波の励起源としては、リングカレント陽子のリング分布や他のプラズマ波動からのモード変換が考えられている。そのため、電離圏から伝搬してくる雷ホイッスラーなども考慮すると、励起源の解明には磁気圏で広範囲な緯度分布を求める必要がある。

本研究では、磁気緯度 45° までの観測が可能な磁気圏衛星「あらせ」のデータを用いて、低域混成波の発生頻度や振幅の統計解析を行った。「あらせ」の PWE/OFA の電磁場スペクトルの中から、fLHR 周辺のスペクトルピークのうち、静電波として電場スペクトルのみ急峻なピークをもつ場合を低域混成波が観測された時間として抽出した。その結果、PWE/OFA が測定している 64 Hz から 19.5 kHz の間で検出された低域混成波は、主にプラズマ圏内の磁気緯度 20° 以上でみられ、発生頻度は 70% にのぼることが分かった。これは、Liu et al. (2021) の結果に比べると非常に高い頻度で現れており、内部磁気圏における低域混成波の大部分はプラズマ圏の中緯度で生じていることが明らかとなった。また、低域混成波の地方時、F10.7 指数、SYM-H 指数、季節依存性を調査したところ、L = 1-2 の領域では雷ホイッスラーの変動と類似する地方時・季節依存性がみられた。一方で、L >3 においてはプラズマ圏ヒスと類似する地磁気擾乱依存性がみられた。これらのことから、低域混成波の励起源には L-shell 依存性があり、プラズマ圏における内側の L-shell では雷ホイッスラー、外側の L-shell ではプラズマ圏ヒスのモード変換で低域混成波が生じていると考えられる。

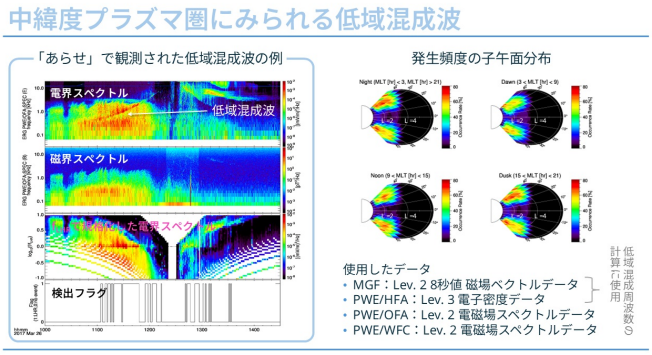

R006-11
A 会場 ：11/27　AM1 （9:00-10:15）
9:00〜9:15

#細川 敬祐 [1)], 片岡 龍峰 [2)], ホワイター ダニエル [3)], 小川 泰信 [2)], パルタミース ノーラ [4)], シガーネス フレッド [4)], 津田 卓雄 [5)], 田口 聡 [6)], 塩川 和夫 [7)]
([1] 電通大, [2] 極地研, [3] サウスハンプトン大学, [4] スバールバル北極大学, [5] 電通大, [6] 京大理, [7] 名大宇地研

Multi-instrument observations of polar rain aurora

#Keisuke Hosokawa[1)], Ryuho Kataoka[2)], Daniel Whiter[3)], Yasunobu Ogawa[2)], Noora Partamies[4)], Fred Sigernes[4)], Takuo Tsuda[5)], Satoshi Taguchi[6)], Kazuo Shiokawa[7)]
([1]University of Electro-Communications, [2]National Institute of Polar Research, [3]University of Southampton, [4]The University Centre in Svalbard, [5]University of Electro-Communications, [6]Department of Geophysics, Graduate School of Science, Kyoto University, [7]Institute for Space-Earth Environmental Research, Nagoya University

Recently, we documented an extraordinarily large-scale aurora that encompassed the entire polar cap region during a period of nearly 28 hours when the solar wind almost completely vanished on December 25 – 26, 2022. By integrating data from ground-based and satellite observations, we demonstrated that this remarkable aurora was caused by the precipitation of field-aligned “strahl” electrons streaming directly from the Sun, a phenomenon known as “polar rain.” High-sensitivity ground-based imaging revealed complex spatial structures within the polar rain aurora, potentially reflecting the internal patterns of the solar wind or even the structure of the surface of the Sun.

Approximately a month later, on January 19 – 20, 2023, another case of polar rain aurora occurred in the northern hemisphere. This event lasted around five hours, shorter than the one observed in December 2022. However, during this interval, the EISCAT Svalbard Radar (ESR) in Longyearbyen, Norway, was operated as part of a special UK experiment. The radar detected intense ionization with a cut-off altitude as low as 90 km, suggesting that the electron precipitation was more energetic than typical polar rain events. Additionally, an all-sky airglow imager from OMTIs (Optical Mesosphere Thermosphere Imagers) in Eureka, Canada, captured corresponding diffuse greenish and reddish auroral signatures over the central polar cap, although the green line images were saturated most of the time, possibly due to the intense polar rain precipitation.

In this paper, we present a detailed analysis of these two polar rain aurora events, utilizing a comprehensive array of optical instruments in Svalbard and Eureka, along with ionospheric plasma parameters obtained from ESR. Specifically, we examine the mechanisms behind the unusually intense electron precipitations during the large-scale polar rain aurora and their connection to the origin of strahl electrons on the surface of the Sun.

R006-12
A 会場 ：11/27　AM1 （9:00-10:15）
9:15〜9:30

オーロライメージングのためのハイパースペクトルカメラ (HySCAI) の開発と初期結果

#居田 克巳 [1)], 吉沼 幹朗 [1)], 海老原 祐輔 [2)]
([1] 核融合研, [2] 京大生存圏

Development of Hyperspectral Camera for Auroral Imaging (HySCAI) and first light results

#Katsumi Ida[1)], Mikirou Yoshinuma[1)], Yusuke Ebihara[2)]
([1]National Institute for Fusion Science, [2]Research Institute for Sustainable Humanosphere, Kyoto University

The Hyperspectral Camera for Auroral Imaging (HySCAI), which can provide a two-dimensional (2D) aurora image with full spectrum, was developed to study auroral physics. HySCAI consists of an all-sky lens, monitor camera, galvanometer scanner, grating spectrograph, and Electron Multiplying Charge Coupled Device (EM-CCD). The galvanometer scanner can scan a slit image of the spectrograph on the all-sky image plane in the direction perpendicular to the slit. HySCAI has two gratings; one is 500 grooves/mm for a wide spectral coverage of 400 - 800 nm with a spectral resolution (FWHM) of 2.1 nm, and the other is 1500 grooves/mm for a higher spectral resolution of 0.73 nm with a narrower spectral coverage of 123nm. The absolute sensitivity is 2.1 count/s/R with 4x4 binning (256 x 340 image) at 557.7 nm. The exposure time depends on the brightness of the aurora emission and is typically 64 sec for a 2D image (0.2 seconds per line scan). This system has been installed at the KEOPS (Kiruna Esrange Optical Platform Site) of the SSC (Swedish Space Corporation) in Kiruna, Sweden. All-sky images with a Liquid Crystal Filter and a sky color camera have also been installed to compensate for the poor time resolution of HySCAI. 2D aurora monochromatic images for given wavelength are obtained by reconstructing the EM-CCD image over the scan period. HySCAI has the advantage of providing a 2D image of intensity for a weak emission line, which appears on top of a high background emission without the contamination from other emissions, which is usually difficult in a system with a bandpass filter. As the first light results, monochromatic images of N_2^+ 1NG (0,1) (427.8nm), N_2^+ 1NG (0,2) (470.9nm), H_{beta} (486.1nm), N II (500. 1nm), N I (^{2}D) (520.0nm), O I (^{1}S) (557.7nm), NaD (589.3nm), O I (^{1}D) (630.0nm), N_2^+ 1NG (670.5nm) emission intensity were measured. We estimated the precipitating electron energy from a ratio of I(630.0nm)/I(427.8nm) to be 1.6 keV.

オーロラ観測用ハイパースペクトルカメラ（Hyperspectral Camera for Auroral Imaging: HySCAI）を、オーロラを研究するために開発した。HySCAI は、全天レンズ、モニターカメラ、ガルバノスキャナー、回折格子分光器、電子増倍電荷結合素子 (EM-CCD) から構成されている。ガルバノスキャナは、全天像面上の分光器のスリット像をスリットに垂直な方向に走査することができる。HySCAI には 2 つのグレーティングがあり、1 つは 500 溝/mm で 400〜800 nm の広いスペクトルを 2.1 nm のスペクトル分解能（FWHM）でカバーし、もう 1 つは 1500 溝/mm で 0.73 nm の高いスペクトルを 123 nm の狭いスペクトルでカバーする。絶対感度は、557.7 nm で 4x4 のビニング（256 x 340 イメージ）で 2.1 count/s/R である。露光時間はオーロラ発光の明るさに依存し、通常 2D 画像で 64 秒（1 ラインスキャンあたり 0.2 秒）。このシステムは、スウェーデンのキルナにある SSC（スウェーデン宇宙公社）の KEOPS（キルナ・エスレンジ・オプティカル・プラットフォーム・サイト）に設置した。HySCAI の時間分解能の低さを補うために、液晶フィルターによる全天画像とスカイ・カラー・カメラも設置した。与えられた波長に対する 2 次元オーロラ単色画像は、EM-CCD 画像をスキャン期間にわたって再構成することにより得られた。HySCAI は、バンドパスフィルタを用いたシステムでは通常困難な、高いバックグラウンド発光の上に現れる弱い発光線の強度の 2 次元画像を、他の発光のコンタミネーションなしに得られるという利点がある。ファーストライトの結果として、N_2^+ 1NG (0,1) (427.8nm), N_2^+ 1NG (0,2) (470.9nm), H_{beta} (486.1nm), N II (500. 1nm), N I (^{2}D) (520.0nm), O I (^{1}S) (557.7nm), NaD (589.3nm), O I (^{1}D) (630.0nm), N_2^+ 1NG (670.5nm) の発光強度を測定した。I(630.0nm)/I(427.8nm) の比から電子の振り込みエネルギーを 1.6keV と見積もった。

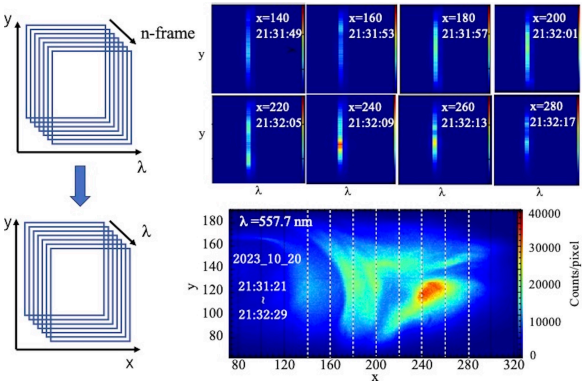

R006-13
A 会場 ：11/27　AM1 （9:00-10:15）
9:30〜9:45

あらせ衛星と高感度地上カメラに基づくサブオーロラ帯に広がるディフューズ発光領域の磁気圏ソース領域の初観測

#五味 優輝 [1)], 塩川 和夫 [1)], 三好 由純 [1)], 大塚 雄一 [1)], 大山 伸一郎 [1)], 新堀 淳樹 [1)], 堀 智昭 [1)], 田 采祐 [1)], 山本 和弘 [1)], 篠原 育 [2)], 浅村 和史 [2)], 桂華 邦裕 [3)], 横田 勝一郎 [4)], 土屋 史紀 [5)], 熊本 篤志 [5)], 笠原 禎也 [6)], 風間 洋一 [7)], Wang Shiang-Yu[7)], Tam Sunny W.Y.[8)], 松岡 彩子 [9)], Martin Connors[10)]
([1 名大・宇地研, [2 宇宙機構／宇宙研, [3 東大・理, [4 大阪大, [5 東北大・理・惑星プラズマ大気, [6 金沢大, [7ASIAA, [8NCKU, [9 京都大学, [10 アサバスカ大学

First observation of magnetospheric source of diffuse auroral emission at subauroral latitudes using Arase and ground imagers

#Masaki Gomi[1)], Kazuo Shiokawa[1)], Yoshizumi Miyoshi[1)], Yuichi Otsuka[1)], Shin ichiro Oyama[1)], Atsuki Shinbori[1)], Tomoaki Hori[1)], ChaeWoo Jun[1)], Kazuhiro Yamamoto[1)], Iku Shinohara[2)], Kazushi Asamura[2)], Kunihiro Keika[3)], Shoichiro Yokota[4)], Fuminori Tsuchiya[5)], Atsushi Kumamoto[5)], Yoshiya Kasahara[6)], Yoichi Kazama[7)], Shiang-Yu Wang[7)], Sunny W.Y. Tam[8)], Ayako Matsuoka[9)], Connors Martin[10)]
([1Institute for Space-Earth Environmental Research, Nagoya University, [2Japan Aerospace Exploration Agency/Institute of Space and Astronautical Science, [3Department of Earth and Planetary Science, Graduate School of Science, The University of Tokyo, [4Osaka University, [5Planetary Plasma and Atmospheric Research Center, Graduate School of Science, Tohoku University, [6Emerging Media Initiative, Kanazawa University, [7Academia Sinica Institute of Astronomy and Astrophysics, [8Institute of Space and Plasma Sciences, National Cheng Kung University, Tainan, [9Graduate School of Science, Kyoto University, [10Athabasca University

At latitudes just below the auroral oval, discrete auroras, such as the STEVE and SAR arc, and diffuse auroras, such as the Evening Corotating Patch (ECP; Kubota et al., GRL, 2003), are known to appear. Measurements of the magnetospheric source plasma of the STEVE and SAR arcs have been reported. However, the magnetospheric source plasma of diffuse auroras in this latitudinal region has not yet been investigated. In this study, we report two cases of magnetospheric source plasma measurements of the diffuse emission regions at latitudes lower than the auroral oval, based on observations by the Arase satellite and the highly sensitive all-sky cameras installed at subauroral latitudes in the northern hemisphere by the PWING project. Event 1 was observed in Kapuskasing, Canada (magnetic latitude: 59.0° N, geographic latitude and longitude: 49.4° N, 277.8° E) in the evening sector (19-21 MLT). A diffuse emission region extended from the poleward oval to the southern edge of the camera field-of-view. The emission intensity was approximately 500 R in the region where the Arase footprint passes. Event 2 was observed in Athabasca, Canada (magnetic latitude: 62.5° N, geographic latitude and longitude: 54.6° N, 246.4° E), in the morning sector (3-5 MLT). A diffuse emission region extended in an east-west direction with a brightness of approximately 600 R. These low-latitude emission regions were observed at a wavelength of 557.7 nm during geomagnetic quiet time, whereas emissions at 630.0 nm were not observed. When the auroral intensity in the high-latitude oval was enhanced due to substorms, the intensity of these low-latitude emissions did not increase. Patch structures, such as ECPs, were not clearly observed in these diffuse emissions. From the Arase satellite observations, we found that the plasmasheet electrons with energies of 0.5-10 keV were responsible for the diffuse emission of event 1. For event 2, plasma waves at frequencies of ˜7 kHz and plasmasheet electrons at energies of 0.1-20 keV were observed in the magnetospheric source region, suggesting that the precipitation due to pitch angle scattering associated with prasmapause hiss (Ondoh, RS, 1993) can be responsible for the emission. In these two cases, the equatorward boundary of the auroral oval was located at one of the inner boundaries of the plasmasheet electron population. The source regions of the diffuse emissions at the subauroral latitudes correspond to another population of plasmasheet electrons in the inner magnetosphere. They are also located in the plasmasphere, suggesting that pitch-angle scattering in the plasmasphere generates the observed diffuse emissions.

オーロラオーバルよりも低緯度側に広がるオーロラとして、STEVE や SAR アークのようなディスクリートオーロラや、ディフューズでパッチ状の構造をもち、同じ位置で発光を維持する Evening Corotating Patch (ECP, Kubota et al., GRL, 2003) が知られている。しかし特にディフューズな低緯度側発光の磁気圏ソース領域の直接観測はこれまで行われていない。本研究では、内部磁気圏を飛翔するあらせ衛星と、PWING プロジェクトで北半球のサブオーロラ帯に設置された高感度の全天カメラを用いて、オーロラオーバルよりも低緯度側に広がるディフューズなオーロラの磁気圏側のソース領域を観測した 2 例を報告する。

イベント 1 は、カナダの Kapuskasing 観測点 (磁気緯度：59.0N、地理緯度・経度：49.4N, 277.8E) で、夕方 (19-21 MLT) にかけてオーロラオーバルの低緯度側からカメラ視野の南端まで広がり、あらせ衛星の通過部分における明るさは約 500 R であった。イベント 2 はカナダの Athabasca 観測点 (磁気緯度：62.5N、地理緯度・経度：54.6N, 246.4E) で、朝 (3-5 MLT) にかけてオーロラオーバルよりも低緯度側に東西方向に伸びた発光領域が観測され、あらせ衛星の通過部分における明るさは約 600 R であった 。これらの低緯度側の発光領域は、どちらも地磁気静穏時に波長 557.7 nm の発光で観測さ

れ、波長 630.0 nm では観測されなかった。さらに、高緯度側でサブストームによるオーロラオーバルの増光があっても、この低緯度側の発光は強度の増加が観測されなかった。どちらもディフューズな発光であり、STEVE や SAR アークのような特徴は見られなかった。また、ECP のようなパッチ状の構造ははっきりと見られなかった。この発光領域の磁気圏共役点を通過したあらせ衛星の粒子データから、イベント 1 では、エネルギーが 0.5 – 10 keV のプラズマシートの電子がこの発光を引き起こしている可能性がある。 また、イベント 2 では、磁気圏で約 7 kHz の電場波動と 0.1-20 keV のプラズマシート電子が観測されており、プラズマポーズヒス (Ondoh, RS, 1993) に伴うピッチ角散乱によるプラズマシート電子の降り込みが発光の原因と推測される。これら 2 例の場合、オーロラオーバルの低緯度側境界はプラズマシートの低緯度側境界の一つに位置していた。オーバルよりも低緯度側の発光領域のソース領域は、このプラズマシートの低緯度側境界よりもさらに内側に存在する別の一連のプラズマシート電子に対応していた。この領域はプラズマ圏の中 に位置しており、プラズマ圏内でもオーロラが発生するピッチ角の散乱メカニズムがはたらいていることが示唆された。

R006-14
A 会場 ：11/27　AM1 （9:00-10:15）
9:45〜10:00

サブストームオンセットに伴うオーロラ形態の時間発展とオンセット位置からの距離依存性に関する研究

#松岡 桃伽 [1)], 大山 伸一郎 [2)], 細川 敬祐 [3)], 三好 由純 [4)], 小川 泰信 [5)], 栗田 怜 [6)]
([1] 名大 ISEE, [2] 名大 ISEE, [3] 電通大, [4] 名大 ISEE, [5] 極地研, [6] 京都大学 生存研

Temporal development of auroral morphology associated with substorm onset and its dependence on distance from the onset location

#Momoka Matsuoka[1)], Shin ichiro Oyama[2)], Keisuke Hosokawa[3)], Yoshizumi Miyoshi[4)], Yasunobu Ogawa[5)], Satoshi Kurita[6)]
([1]Institute for Space-Earth Environmental Research, Nagoya University, [2]Institute for Space-Earth Environmental Research, Nagoya University, [3]Graduate School of Informatics and Engineering, University of Electro-Communications, [4]Institute for Space-Earth Environemental Research, Nagoya University, [5]National Institute of Polar Research, [6]Research Institute for Sustainable Humanosphere, Kyoto University

Previous studies have extensively explored the spatial and temporal development of auroras during substorm events. It has been observed that auroras that drift equatorward at the substorm growth phase typically exhibit rapid expansion poleward at the substorm onset, which leads to enhancement of the emission intensity through the expansion phase. Subsequently, diffuse auroras, including pulsating auroras, are observed predominantly on the morning side of the magnetic local time. In contrast, in case where the ground-based all-sky imager is operated east (i.e., dawn side) of the substorm onset location, the auroral intensity tends to increase with the onset, but a diffuse aurora may develop in the field-of-view of the imager. Although it has been observed that the auroral morphology coinciding with a substorm onset depends on the relative distance from the onset location, it has not been fully confirmed yet. This study aims to clarify variations in the auroral morphology seen before and after the substorm onset with respect to the zonal distance from the onset location by analyzing auroral images captured by all-sky imagers at several ground-based locations.

By applying four specific criteria to the 1949 substorm events that occurred between 2016 and 2022 (with the majority taking place during the northern hemisphere's winter months from September to March only), we identified 34 distinct events that presented clearer visibility of auroras.

1. The weather conditions at the all-sky imager installation site indicate a clear night, along with substorm onsets taking place after 22 MLT. There are no other onset occurrences with a 2-hour window before and 30 minutes after each substorm onset.
2. The minimum value of the SML index (the minimum value attained at each time of the N-component of the magnetic field measured by magnetometers located at 40º-80º magnetic latitude in the northern hemisphere, as defined by SuperMAG) reaches -400 nT or lower within one hour following the initiation of a substorm onset.
3. The SML index has a single minimum for one hour after the substorm onset.
4. The MLT difference between the time at which the substorm onset occurred and the MLT at the location where the SML minimum was recorded is within one hour.

At the SGEPSS 2023 Fall meeting, we visually confirmed the 34 events and classified them as diffuse or discrete auroras. We investigated the trends in auroral morphology relative to the onset location and found that the diffuse aurora was distributed over a wider range in longitude from the onset location. Additionally, both type of auroras was distributed in a wider latitudinal range at the east side of the onset location. The latitudinal standard deviation of the substorm onset location showed that discrete auroras tended to occur at latitudes closer to the onset location. To improve the accuracy of the results and to provide objectivity in discriminating auroral morphology, we developed a program that is mechanically capable of discriminating the auroral morphology. We focused on the auroral meridional width as an indicator, which depends on the auroral morphology, retrieved from the analysis of the 34 events. To increase the number of events analyzed, the criteria 2 and/or 3 are relaxed, resulting in more events with relatively small substorm activities and with repetition of auroral brightening within a short period of time. In this presentation, we will apply the developed program to more events and report the results of an analysis that improves the accuracy of the statistical analysis.

サブストームの時間発展とオーロラの時空間発展の関係は先行研究によって報告されている。サブストームの成長相に低緯度側にシフトしたオーロラは、オンセットの後に爆発相へ移行すると、短時間で増光し、高緯度側へ急速に拡大する傾向がある。その後、特に磁気地方時の朝側で脈動オーロラを含むディフューズオーロラが発生する。一方、サブストームオンセットの発生場所に対して東側（即ち明け方側）で地上全天イメージャーによる観測を行った場合、オンセットに伴ってオーロラの輝度は増加するものの、ディフューズオーロラが視野内に発生することがある。しかし、サブストームオンセットに伴い発生するオーロラの形態が、オンセット発生場所からの相対距離にどのように依存しているかは

十分に確認されていない。そこで本研究では、サブストームオンセット前後に見られるオーロラの形態がオンセット位置からの東西距離に対してどのように異なるかを明らかにすることを目的とし、地上複数箇所に設置された全天イメージャーで撮影されたオーロラ画像を解析した。

解析には、スカンジナビア北部と米国アラスカ州に設置された計 8 台の全天イメージャーが取得したオーロラ画像データと、SuperMAG が提供するサブストームオンセットのリストおよび磁場データを使用した。

2016 年から 2022 年の 7 年間（主に 9 月から 3 月までの北半球冬期のみ）に発生したサブストームイベント（計 1949）に以下 4 つの条件を適用して、オーロラをより鮮明に視認できる明瞭なサブストームに特化したイベントを抽出した。その結果、計 34 イベントが選出された。

1. 全天イメージャー設置地点の上空が晴天暗夜であり、サブストームオンセットが 22 磁気地方時 (magnetic local time: MLT) 以降に発生し、かつ、各オンセットの 2 時間前から 30 分後に別のオンセットがない。
2. SML 指数 (SuperMAG に集約された北半球磁気緯度 40º-80º に分布した磁力計で測定された磁場の北向き成分の各時刻における最小値) の最小値が、サブストームオンセットから 1 時間以内に − 400 nT 以下に到達している。
3. サブストームオンセットから 1 時間以内に SML 指数の極小値が 1 つのみである。
4. サブストームオンセットが発生した MLT と SML 指数極小値を観測した観測所の MLT との差が 1 時間以内である。

2023 年度 SGEPSS 秋季年会では、本 34 イベントを目視で確認し、ディフューズオーロラとディスクリートオーロラを選別して、オンセット位置からの相対距離に対するオーロラ形態の傾向を調べた。その結果、ディフューズオーロラの方がオンセットに対してより広い経度範囲に分布しており、緯度差はディスクリートオーロラとディフューズオーロラどちらに関しても、オンセットより東側の方が広い緯度範囲に分布していた。また、サブストームオンセットの緯度方向の標準偏差を考慮すると、ディスクリートオーロラの方がオンセットに近い緯度で発生する傾向にあった。今回は、オーロラ形態の判別に客観性を持たせることと、より大量のイベントに対して同様の解析をし、結果の精度を高めるためにオーロラ形態を機械的に判別するプログラムを開発した。その際、前述の 34 イベントの解析から得られた、オーロラ形態に依存する南北方向の幅を指標として活用した。大量のイベント解析が可能になったので、上記の条件 2 または条件 3 を緩和することで、比較的小規模なサブストームや短時間にオーロラ増光が繰り返されるイベントも解析対象に含めてイベント数を増やした。本発表では、より多くのイベントに対して開発したプログラムを適用し、統計解析の確度を高めた解析結果を報告する。

R006-15
A 会場 ：11/27　AM1 （9:00-10:15）
10:00〜10:15

#八島 和輝 [1)], 田口 聡 [1)], 小池 春人 [1)], 細川 敬祐 [2)]
([1] 京大理, [2] 電通大

2D distribution of the low-energy electron precipitation derived from 630-nm all-sky auroral images and its characteristics

#Kazuki Yashima[1)], Satoshi Taguchi[1)], Haruto Koike[1)], Keisuke Hosokawa[2)]
([1]Department of Geophysics, Graduate School of Science, Kyoto University, [2]Graduate School of Communication Engineering and Informatics, University of Electro-Communications

The discrete red aurora near the nightside polar cap boundary frequently exhibits dynamic motion. This type of dynamic feature is the manifestation of the rapid deformation of two-dimensional spatial distribution of the intense low-energy electron precipitation, which is believed to be accelerated by the Alfvén waves along the magnetic field lines connected to the plasma sheet boundary layer. Previous studies utilizing satellite data have shown the energy distribution and spatial characteristics of the low-energy electron precipitation. However, the characteristics of the temporal evolution of the low-energy electron precipitation, which play an important role in the rapid deformation of the spatial distribution of the intense low-energy electron precipitation, have not yet been clarified. To understand the temporal characteristics of the intense low-energy electron precipitation, we have established an automated method that can estimate the two-dimensional distribution of the energy flux of the precipitating low-energy electrons by combining 630-nm all-sky auroral image data with the Global Airglow (GLOW) model. Specifically, we have constructed a model in which GLOW can be applied to a three-dimensional domain up to an altitude of 500 km along the magnetic field lines within the imager's field of view so that the auroral intensity calculated from GLOW can be compared with the auroral intensity observed by the all-sky imager at Longyearbyen, Svalbard. We have applied our method to a large number of continuous all-sky images obtained near the nightside polar cap boundary. The processes responsible for the temporal characteristics revealed by this method are discussed.

R006-16
A 会場 ：11/27　AM2 （10:30-12:00）
10:30〜10:45

地球磁気圏における kinetic Alfvén wave による効率的な電子加速過程の理論・数値的検討

#齋藤 幸碩 [1)], 加藤 雄人 [1)], 川面 洋平 [2)], 熊本 篤志 [1)]
([1] 東北大・理・地球物理, [2] 宇都宮大

Theoretical and numerical study of efficient electron acceleration process by kinetic Alfvén waves

#Koseki Saito[1)], Yuto Katoh[1)], Yohei Kawazura[2)], Atsushi Kumamoto[1)]
([1]Dept. Geophys., Grad. Sch. Sci., Tohoku Univ., [2]Utsunomiya Univ.

Kinetic Alfvén waves (KAWs) are electromagnetic waves with a long wavelength parallel to the magnetic field lines and a perpendicular wavelength on the order of the ion Larmor radius. KAWs possess a parallel electric field component (δ E_{jj}) and are known to accelerate electrons along the field line [e.g., Hasegawa, 1976]. KAWs are associated with substorms and auroral beads in the magnetosphere and can accelerate electrons to energies ranging from a few hundred eV to a few keV along the field line, leading to enhancing auroral brightness [e.g., Duan et al., 2022; Tian et al., 2022]. In the process of electron acceleration by KAWs, Landau resonance occurs between electrons and the KAWs when the electron velocity (v_{jj}) is equal to the wave phase speed (V_{phjj}). When the electron enters the trapped region $v_{jj} \in [V_{phjj} \pm V_{tr}]$, where V_{tr} is a nonlinear trapping width and depends on δ E_{jj}, the electron is trapped by the KAWs and transported to higher latitudes while being accelerated to a speed close to V_{phjj} [e.g., Artemyev et al., 2015; Damiano et al., 2016]. Previous studies have focused on this trapped process, but in the actual magnetospheric environment, the gradient of the background field, including magnetic flux density, plays a significant role, and the transition processes between trapped and non-trapped states due to the mirror force are important. However, these transition processes have not been sufficiently investigated.

In this study, we apply the second-order resonance theory of charged particles trapped by coherent electromagnetic waves [e.g., Omura et al., 2008] to the electron acceleration process by KAWs. We can describe the motion of electrons trapped by KAWs in the velocity phase space by considering a simple harmonic motion of the wave phase as viewed from the electron (ψ) and the inhomogeneity factor (S) due to the background magnetic field gradient. As the trapped move parallel to magnetic field lines, the background magnetic field gradient and S, as viewed from the electron, change accordingly. As S increases, V_{tr} decreases, causing the trapped region to shrink as the electron moves toward higher latitudes. This makes it easier for the electron to be detrapped from KAW. From theoretical calculations, we find that electrons can be trapped by KAWs up to approximately 36° of magnetic latitude on the L=9 magnetic field line in the terrestrial magnetosphere, assuming δ E_{jj} is approximately 1 mV/m at the magnetic equator. We perform test particle simulations and confirm that while v_{jj} of trapped electrons remain at around V_{phjj}, the energy of electrons significantly changes after they escape from the trapped region. In particular, we find that electrons transitioning from the trapped state to the non-trapped state with ψ near -π, the electrons are accelerated to up to approximately 10.5 keV at the ionosphere while located at $\psi \in (-\pi, 0)$ where the wave accelerates the electron [Saito et al., P-EM17-07, JpGU Meeting, 2024]. Additionally, when non-trapped electrons move toward lower latitudes, the kinetic energy changes due to δ E_{jj} and the background magnetic field gradient make it difficult to be re-trapped near ψ=0, but more likely near ψ=-π. The electrons trapped near ψ=-π are greatly accelerated through the aforementioned process and precipitate into the ionosphere. This process of accumulating un-trapped electrons near ψ=-π can be an important process in the electron acceleration process by KAWs, which efficiently accelerates the electrons. In this presentation, we discuss the above theoretical considerations and calculation results in detail.

Kinetic Alfvén wave (KAW) は、磁力線平行方向の波長が長く、磁力線垂直方向の波長がイオン Larmor 半径程度の電磁波動である。KAW は磁力線平行方向の電場成分 δ E_{jj} を持ち、電子を磁力線に沿って加速することが知られている [e.g., Hasegawa, 1976]。KAW は地球磁気圏のサブストームやオーロラビーズ現象と関連があり、KAW が電子を磁力線平行方向に数百 eV から数 keV 程度のエネルギーに加速し、オーロラ増光を引き起こすと考えられている [e.g., Duan et al., 2022; Tian et al., 2022]。KAW による電子加速過程では、電子の速度 v_{jj} が波の位相速度 V_{phjj} の時に電子と KAW の間で Landau 共鳴が生じる。特に δ E_{jj} によって捕捉速度 V_{tr} だけ拡がった捕捉領域 $v_{jj} \in [V_{phjj} \pm V_{tr}]$ に電子が入った場合に、KAW に捕捉され、V_{phjj} 程度の速度に加速されながら高緯度に向けて輸送されると考えられている [e.g., Artemyev et al., 2015; Damiano et al., 2016]。従来の研究では、この捕捉過程に焦点が当てられてきたが、実際の磁気圏環境では磁束密度をはじめとした背景場の勾配が存在し、ミラー力による電子の捕捉状態から非捕捉状態への遷移が重要になる。これらの遷移過程を考慮した調査は十分に行われていない。

本研究では、KAW による電子加速過程に対して、コヒーレントな電磁波動に捕捉された荷電粒子の加速過程の研究で用いられてきた 2 次共鳴理論 [e.g., Omura et al., 2008] を導入し、電子加速過程の詳細を調査する。KAW に捕捉された電子の運動は、V_{phjj} 近傍に形成される捕捉領域により特徴づけられ、電子から見た KAW の位相ψについての単振動

と、背景磁場勾配に起因する不均一性因子 S による影響との重畳として記述される。捕捉電子が磁力線平行方向に移動することで、その位置に応じて背景磁場勾配と S が変化する。V_{tr} は S が増加することで小さくなることから、電子が高緯度に向かうにつれて捕捉領域が縮小し、電子は波の捕捉から外れやすくなる。理論計算では、地球磁気圏 L=9 の磁力線上で δE_{jj} が磁気赤道で 1 mV/m 程度であり伝播中に減衰しない場合、電子は磁気緯度 36° 程度まで KAW に捕捉され得ることが示された。また、テスト粒子計算の結果、捕捉電子は V_{phjj} 程度の速度を持つが、捕捉から外れた後、その運動エネルギーが大きく変化することが確認された。特に、ψが-π付近で捕捉状態から非捕捉状態に遷移した電子は、速度位相空間上で波が電子を加速するψ∈(-π, 0) に位置しながら、最大で約 10.5 keV まで加速されて電離圏に降り込むことが明らかになった [Saito et al., P-EM17-07, JpGU Meeting, 2024]。さらに、非捕捉状態の電子が低緯度に移動する際、δE_{jj} によるエネルギー変化と背景磁場勾配の影響で、ψ=0 の周囲では電子は波に捕捉されにくく、ψ=-π付近で捕捉されやすいことが分かった。ψ=-πの近くで捕捉された電子は、前述の過程を通して大きく加速されて電離圏に降り込むことから、非捕捉電子をψ=-πの近くに集積するこの過程は、KAW の電子加速過程において効率的に電子を加速して電離圏降下させる重要な過程である可能性がある。本発表では、以上の理論検討と計算結果について詳細に報告する。

R006-17
A 会場 ：11/27　AM2 （10:30-12:00）
10:45〜11:00

2 次元 ideal MHD シミュレーションによる IAR 領域における低プラズマ密度領域の再現
—ポンデロモチーブ力の評価—

#川上 航典 [1)], 吉川 顕正 [2)], 深沢 圭一郎 [3)], 樋口 颯人 [1)]
[(1] 九大, [(2] 九大/理学研究院, [(3] 京大・メディアセンター

The Reproduction of Low Plasma Density Region in IAR with 2-dimensional MHD Simulation
-Evaluation of Ponderomotive Force-

#Kousuke Kawakami[1)], Akimasa Yoshikawa[2)], Keiichiro Fukazawa[3)], Hayato Higuchi[1)]
[(1]Kyushu University, [(2]Department of Earth and Planetary Sciences, Kyushu University, [(3]Academic Center for Computing and Media Studies, Kyoto University

Auroral acceleration regions (AARs) are quasi-static upward electrostatic structures typically located at altitudes of 3,000 to 10,000 km, and they play a crucial role in the production of auroral particles. Observations of Auroral Kilometric Radiation (AKR) have shown that AARs develop from lower to higher altitudes. Additionally, theoretical and numerical studies have been conducted to investigate these electrostatic structures by solving the Vlasov-Poisson system of equations. While these and other studies have elucidated the structures of AARs, the processes underlying their formation and development remain unclear. In particular, the low plasma density regions known as auroral cavity regions, which are one of the key observational features of AARs, are essential for understanding current continuity, AKR generation conditions, and the solutions of the Vlasov-Poisson system of equations; however, their formation process remains a mystery. To understand the formation and development of electrostatic AARs, it is necessary to consider an electromagnetic perspective, particularly the time evolution associated with Alfvén wave propagation.

Therefore, we focus on Ionospheric Alfvén Resonators (IARs), which exist at altitudes that partially correspond to low-altitude AARs and confine Alfvén waves. Previous research has reported the existence of cavity regions, distinct from auroral cavity regions, and particle acceleration within these cavity regions in IARs. Based on these observations, we hypothesize that the cavity regions in IARs are key to the formation of AARs, and we investigate their formation process.

Previous research [Streltsov and Lotko 2008, Sydorenko et al., 2008] reported that the parallel ponderomotive force in IAR standing wave structures is crucial for cavity formation. However, in their simulation, while the density depletion consistent with the cavity region is confirmed, regions of density enhancement, which are not observed in practice, were also formed.

Therefore, we considered that not only the parallel but also the perpendicular ponderomotive force plays an important role in density variation in the IAR and conducted 2-dimensional ideal MHD simulations to investigate this. As a result, we obtained outcomes consistent with observations, showing only density depletion along the magnetic field lines. In the presentation, we will discuss our research background and objectives, provide an overview of the simulation setup, and present the results along with future work.

オーロラ加速領域は典型的に高度 3,000km-10,000km において、準定常的に存在する上向き静電場構造であり、オーロラ粒子を生成する重要な領域である。加速領域は AKR(Auroral Kilometric Radiation) 観測から低高度側（3,000km）から高高度側へと発展していくことが知られている。また、理論・数値計算の観点からも Vlasov-Poisson 方程式系の定常解を求めることで、その静電場構造について研究が進められてきた。これらをはじめとした多くのオーロラ加速領域に関する研究が行われ、その構造について明らかにされてきた一方で、加速領域自体の形成・発展プロセスについては多くが未解明のままである。特に Auroral Cavity 領域と呼ばれる低プラズマ密度領域は、加速領域の観測的特徴の 1 つであり加速領域内での電流の連続性、AKR の発生条件、そして Vlasov-Poisson 方程式系の定常解を考える上で重要であるのが、その形成プロセスについては現在でも明らかでない。このような electrostatic な構造を持つ加速領域の形成・発展プロセスを明らかにするためには electromagnetic な観点、すなわち Alfven 波の伝搬に伴う時間発展について理解する必要がある。

そこで、我々はオーロラ加速領域初期形成過程解明を目的として、低高度加速領域 (3,000km) と一部一致する高度に存在し、Alfven 波を閉じ込める役割を持つ IAR(Ionospheric Alfven Resonator) における発展に注目した。IAR では Auroral Cavity 領域とは別の低プラズマ密度領域 (Cavity 領域)、並びにその内部における電子・イオンの加速が観測されている。これらの観測結果をもとに、本研究ではこの IAR 高度において生じる Cavity 領域が Auroral Cavity 領域ひいてはオーロラ加速領域の形成につながると着想し、その形成過程について調査を行った。

IAR 高度での Cavity 領域の形成については、先行研究 [Streltsov and Lotko 2008, Sydorenko et al., 2008] から IAR 中の定在 Alfven 波構造において働く平行方向のポンデロモチーブ力が重要になることが報告されていた。しかしこのモデルでは、磁力線と平行方向に対して Cavity 領域に相当するプラズマ密度が減少する領域だけでなく、観測では確認されていないプラズマ密度が増加する領域も同時に形成されてしまっている。

そこで本研究では IAR 構造中でのプラズマ密度の変動では平行方向だけでなく、垂直方向のポンデロモチーブ力も

考慮することが必要であると考え、これらの物理を含んだ 2 次元 ideal MHD シミュレーションを用いて数値計算を行った。その結果、磁力線方向に関してはプラズマ密度の減少のみが生じ、観測と一致する特徴が得られた。発表では、研究背景、研究目的について整理したのち、今回用いたシミュレーションに関する概観、そして結果と今後の展望について報告する予定である。

R006-18
A 会場 ：11/27　AM2 （10:30-12:00）
11:00〜11:15

#石丸 宏樹 [1)], 今城 峻 [1)], 三好 由純 [2)], 風間 洋一 [3)], 浅村 和史 [4)], 松岡 彩子 [1)], Wang Shiang-Yu[3)], Tam Sunny, W.Y.[5)], 田 采祐 [2)], 堀 智昭 [2)], 篠原 育 [6)], 土屋 史紀 [7)], 熊本 篤志 [8)], 笠原 禎也 [9)], 新堀 淳樹 [2)], 寺本 万里子 [10)], 山本 和弘 [2)]
([1] 京都大学, [2] 名大 ISEE, [3]ASIAA, [4] 宇宙研, [5] 国立成功大学, [6] 宇宙機構／宇宙研, [7] 東北大・理・惑星プラズマ大気, [8] 東北大・理・地球物理, [9] 金沢大, [10] 九工大

The source altitude distribution and heating property of electron conic estimated with the Arase satellite

#Hiroki Ishimaru[1)], Shun Imajo[1)], Yoshizumi Miyoshi[2)], Yoichi Kazama[3)], Kazushi Asamura[4)], Ayako Matsuoka[1)], Shiang-Yu Wang[3)], Sunny, W.Y. Tam[5)], ChaeWoo Jun[2)], Tomoaki Hori[2)], Iku Shinohara[6)], Fuminori Tsuchiya[7)], Atsushi Kumamoto[8)], Yoshiya Kasahara[9)], Atsuki Shinbori[2)], Mariko Teramoto[10)], Kazuhiro Yamamoto[2)]
([1]Graduate School of Science, Kyoto University, [2]Institute for Space-Earth Environement Research, Nagoya University, [3]Academia Sinica Institute of Astronomy and Astrophysics, [4]Japan Aerospace Exploration Agency, [5]National Cheng Kung University, [6]Japan Aerospace Exploration Agency/Institute of Space and Astronautical Science, [7]Planetary Plasma and Atmospheric Research Center, Graduate School of Science, Tohoku University, [8]Department of Geophysics, Graduate School of Science, Tohoku University, [9]Emerging Media Initiative, Kanazawa University, [10]Kyushu Institute of Technology

We examined the source altitude of electron conics by analyzing high-angular resolution electron data obtained by the Arase satellite. We surveyed electron conic events between 2017 and 2021 and identified electron conics with ion beams observed at an altitude of ˜30,000 km above the auroral acceleration region. Assuming that the observed electron conics have adiabatically moved upward from the source altitude and undergone a potential difference along the dipole field line, we fitted energy-dependent loss cone curves to the electron flux distribution of the conics to estimate the mirror ratio and the potential difference between the source and the satellite altitude. The electron conic source altitude approximately matched the simultaneously observed auroral kilometeric radiation (AKR) source altitude, at which a parallel electric field is formed. In particular, the coincidence of the middle of the source altitude with the bottom altitude of the AKR suggests that heating is related to the time spent in the acceleration region. This result suggests two hypotheses for the generation of electron conics: electron heating due to time-varying electric fields that accelerate auroral electrons, and diffusive heating due to waves, such as electrostatic waves seen around this altitude. We also compared the phase space densities of downward and upward electrons to determine their heating property. We found that the number fluxes of upward and downward electrons were comparable, while the upward energy fluxes increased. This implies that the magnetospheric electrons just outside the loss cone are heated at low altitude and reflected. Using the estimated heating altitude and potential difference, we reproduced the observed electron conic distribution by a Monte Carlo simulation.

R006-19
A 会場 ：11/27　AM2 （10:30-12:00）
11:15〜11:30

脈動オーロラの発光強度変化と降下電子エネルギースペクトルの相関: LAMP 観測ロケットと EMCCD 全天カメラによる同時観測

#平野 晶也 [1)], 細川 敬祐 [1)], 三好 由純 [2)], 浅村 和史 [3)], Lessard Marc[4)], Mcharg Matthew[5)], Jaynes Allison[6)], Shumko Mykhaylo[7)], Ledvina Vincent[8)], Hampton Don[8)], 坂野井 健 [9)], 三谷 烈史 [3)], 滑川 拓 [10)], 能勢 正仁 [11)], 小川 泰信 [12)], Halford Alexa[13)]
([1] 電通大, [2] 名大 ISEE, [3] 宇宙研, [4] ニューハンプシャー大学, [5] アメリカ合衆国空軍士官学校, [6] アイオワ大学, [7] ジョンズ・ホプキンズ大学応用物理研究所, [8] アラスカ大学フェアバンクス校, [9] 東北大・理・PPARC, [10]NICT, [11] 名市大・DS 学部, [12] 極地研, [13]NASA ゴダード宇宙飛行センター

The correlation between the luminosity variation of pulsating aurora and energy spectra of precipitating electrons

#Masaya Hirano[1)], Keisuke Hosokawa[1)], Yoshizumi Miyoshi[2)], Kazushi Asamura[3)], Marc Lessard[4)], Matthew Mcharg[5)], Allison Jaynes[6)], Mykhaylo Shumko[7)], Vincent Ledvina[8)], Don Hampton[8)], Takeshi Sakanoi[9)], Takefumi Mitani[3)], Taku Namekawa[10)], Masahito Nose[11)], Yasunobu Ogawa[12)], Alexa Halford[13)]
([1]University of Electro-Communications, [2]Institute for Space-Earth Environement Research, Nagoya University, [3]Japan Aerospace Exploration Agency, [4]University of New Hampshire, [5]the United States Air Force Academy, [6]University of Iowa, [7]Johns Hopkins University Applied Physics Laboratory, [8]University of Alaska Fairbanks, [9]Planetary Plasma and Atmospheric Research Center, Graduate School of Science, Tohoku University, [10]The National Institute of Information and Communications Technology, [11]School of Data Science, Nagoya City University, [12]National Institute of Polar Research, [13]NASA Goddard Space Flight Center

Aurorae observed in the nightside auroral zone are primarily classified into two broad categories. The one is discrete aurorae, which have clear and distinct spatial structures, and the other is diffuse aurorae, characterized by vague and indistinct patchy shapes. It is known that most of diffuse aurorae show a quasi-periodic luminosity modulation called pulsating aurora (PsA). The energy of the precipitating electrons causing PsA tends to be higher than those causing typical discrete aurorae, and we sometimes refer to these precipitating electrons as ”PsA electrons”. The tail of the energy spectra of PsA electrons often extends to a few tens/hundreds of keV. Such sub-relativistic electron precipitations can be explained in association with whistler-mode chorus waves that originate near the equatorial plane of the magnetosphere. These waves propagate along the magnetic field lines and scatter electrons through the wave-particle interaction in the high-latitude regions of the magnetosphere. Regarding the relationship between PsA electrons and auroral emissions, simultaneous observations using electron detectors and multi-spectral auroral camera onboard the Reimei satellite suggested that a flux modulation, whose energy is above a few keV, is the primary cause of the luminosity modulation of PsA [Miyoshi et al., 2015]. However, the detailed correlation between the luminosity modulation of PsA and the energy spectrum of PsA electrons during relatively longer time interval (e.g., over several minutes) has not yet been clarified. In addition, the spatial extent of the region showing a strong correlation between PsA electrons and auroral emissions has not been visualized through actual observations. These issues fundamentally stem from the absence of spacecraft missions capable of conducting continuous electron measurements in the regions where PsA occur.

To address this issue, this study analyzes the correlation between the in-situ low-energy electron data obtained from the EPLAS low-energy electron sensor onboard the LAMP sounding rocket and the PsA emission intensity data obtained from the EMCCD all-sky camera operated in Alaska during the launch window. The launch window of the LAMP sounding rocket was from 11:29 to 11:38 UT on March 5, 2022, and the onboard low-energy electron sensor, EPLAS, covered an energy range of 5 eV to 15 keV. Additionally, the EMCCD all-sky camera in Venetie, Alaska, observed the region containing the magnetic footprint of the rocket during the launch window with a temporal resolution of 100 Hz. This allowed us to conduct a longer time interval correlation analysis between the time-series data of the precipitating electron energy flux and the optical intensity from the ground-based camera, covering the downrange area of the rocket trajectory. As a result, we successfully visualized the correlation coefficients between the two datasets and confirmed that, during most of the time, higher correlation coefficients were obtained in a limited area near PsA patches. It was also revealed that the correlation between PsA luminosity modulation and low-energy electron flux is not always high and can be unclear depending on the time interval. Furthermore, the spatial extent of regions showing high correlation coefficients varied in time. In the presentation, we will show a video visualizing the spatial distribution of the correlation coefficients, where it changes with the motion of the rocket (shift of the observation region) and discuss the relationship between the PsA luminosity variation and the temporal changes in the PsA electron energy spectrum during the launch window. Based on this, we will consider the factors controlling the degree of correlation between PsA electrons and auroral emissions.

夜側オーロラ帯で観測されるオーロラは主に次の二つに分類される．一つ目は明瞭な空間構造を持つディスクリートオーロラである．二つ目はぼんやりとした空間構造を持つディフューズオーロラである．ディフューズオーロラの多く

は，準周期的な輝度変調を示すことが知られており，脈動オーロラ（Pulsating Aurora: PsA）と呼ばれる．PsA を引き起こす降下電子のエネルギーは典型的なディスクリートオーロラを引き起こすものよりも高いことが知られており，それらの降下電子をここでは「PsA 電子」と呼ぶ．PsA 電子のエネルギースペクトルは，その裾野が数十から数百 keV にまで及ぶこともある．このような準相対論的な電子降下は，磁気赤道面付近で発生する自然電磁波「ホイッスラーモードコーラス波」が磁力線に沿って伝搬し，磁気圏の高緯度領域において波動粒子相互作用によって電子を散乱することによって説明できる．PsA 電子とオーロラ発光の関連については，科学衛星「れいめい」に搭載された電子観測器と多波長オーロラカメラによる同時観測から数 keV 以上の変調が PsA の輝度変調の主原因であることが示唆されている（Miyoshi et al., 2015）．しかし，数分間に渡る長時間の PsA の輝度変調と PsA 電子のエネルギースペクトルとの間の詳しい相関関係は明らかになっていない．また，PsA 電子とオーロラ発光の相関が良い領域がどれくらいの空間的な広がりを持っているのかについて，実観測から明らかにすることも成されていなかった．これらの問題は，PsA が発生している領域において長時間継続的に電子計測を行う飛翔体ミッションが存在しなかったことに本質的に起因する．

この問題を解決するために，本研究では，LAMP 観測ロケットに搭載された低エネルギー電子観測器（EPLAS）のデータと，アラスカに設置されている EMCCD 全天カメラから得られた打ち上げウィンドウ中の PsA の発光強度データとの間の相関を解析した．LAMP 観測ロケットの打ち上げウィンドウは 2022 年 3 月 5 日 11:29 — 11:38 UT であり，搭載された低エネルギー電子観測器「EPLAS」は 5 eV から 15 keV までのエネルギー範囲をカバーしている．また，アラスカのベネタイに設置されている EMCCD 全天カメラは，LAMP ロケットの打ち上げウィンドウ中のロケットのフットプリントを含む領域を 100 Hz の時間分解能で観測していた．そのため，降下電子エネルギーフラックスの時系列データと地上カメラの発光強度の時系列データとの間で相関解析を長時間にわたって，かつ地上カメラの全視野を対象として行うことができた．その結果，両者の間の相関係数の可視化に成功し，多くの時間帯において，相関が良い領域が PsA パッチの近傍のみに限定されていることが確認された．また，PsA の輝度変調と低エネルギー電子フラックスの相関が常に高い訳ではなく，時間帯によって明瞭な相関が見えないことも明らかになった．さらに，高い相関係数を示す領域の空間的な広がりも時間帯によって変化することがわかった．発表では，ロケットの移動（観測領域の移動）に伴って変化する相関係数の空間分布を可視化した動画を示し，打ち上げウィンドウ中の数分間の PsA 発光強度変化と PsA 電子のエネルギースペクトルの時間変化の間の関係性について議論する．それを踏まえ，PsA 電子とオーロラ発光の間の相関の程度を決めている要因について考察を行う予定である．

R006-20
A 会場 ：11/27　AM2 （10:30-12:00）
11:30〜11:45

あらせ衛星と地上光学カメラによるオメガバンドオーロラ観測

#長縄 一輝[1)], 三好 由純[2)], 栗田 怜[3)], 細川 敬祐[4)], 大山 伸一郎[5)], 小川 泰信[6)], 笠原 禎也[7)], 松田 昇也[8)], 堀 智昭[5)], 風間 洋一[9)], Wang Shiang-Yu[9)], 田 采祐[10)], 笠原 慧[11)], 横田 勝一郎[12)], 桂華 邦裕[13)], 松岡 彩子[14)], 寺本 万里子[15)], 山本 和弘[16)], 篠原 育[17)]
([1] 名大 ISEE, [2] 名大 ISEE, [3] 京都大学 生存研, [4] 電通大, [5] 名大 ISEE, [6] 極地研, [7] 金沢大, [8] 金沢大学, [9]ASIAA, [10] 名大 ISEE 研, [11] 東京大学, [12] 大阪大, [13] 東大・理, [14] 京都大学, [15] 九工大, [16] 名大 ISEE, [17] 宇宙機構／宇宙研

Investigation of Omega Band Auroras: Ground and Magnetospheric Conjugate Observations

#Itsuki Naganawa[1)], Yoshizumi Miyoshi[2)], Satoshi Kurita[3)], Keisuke Hosokawa[4)], Shin ichiro Oyama[5)], Yasunobu Ogawa[6)], Yoshiya Kasahara[7)], Shoya Matsuda[8)], Tomoaki Hori[5)], Yoichi Kazama[9)], Shiang-Yu Wang[9)], ChaeWoo Jun[10)], Satoshi Kasahara[11)], Shoichiro Yokota[12)], Kunihiro Keika[13)], Ayako Matsuoka[14)], Mariko Teramoto[15)], Kazuhiro Yamamoto[16)], Iku Shinohara[17)]
([1]Institute for Space-Earth Environmental Research,Nagoya University, [2]Institute for Space-Earth Environemental Research, Nagoya University, [3]Research Institute for Sustainable Humanosphere, Kyoto University, [4]University of Electro-Communications, [5]Institute for Space-Earth Environmental Research, Nagoya University, [6]National Institute of Polar Research, [7]Emerging Media Initiative, Kanazawa University, [8]Kanazawa University, [9]Academia Sinica Institute of Astronomy and Astrophysics, [10]Institute for Space-Earth Environmental Research, [11]The University of Tokyo, [12]Osaka University, [13]Department of Earth and Planetary Science, Graduate School of Science, The University of Tokyo, [14]Graduate School of Science, Kyoto University, [15]Kyushu Institute of Technology, [16]Institute for Space-Earth Environmental Research ([ISEE), Nagoya University, [17]Japan Aerospace Exploration Agency/Institute of Space and Astronautical Science

The Omega band aurora is a type of aurora that appears just after auroral breakup and drifts eastward from midnight towards the early morning hours. It is characterized by a distinctive structure resembling an inverted Ω shape. Previous studies on Omega band auroras have proposed several hypotheses regarding their origins. It is suggested that Omega band is caused by velocity shear resulting from a hybrid of Kelvin-Helmholtz and Rayleigh-Taylor instabilities. Another model, the streamer model, proposes that the poleward auroral streamer directly evolves into the Omega band torch. The Omega band auroras consist of various type of aurora, including diffuse aurora, pulsating aurora, and discrete aurora within the torch. However, due to the limited number of simultaneous observations with magnetospheric satellites, the magnetospheric mechanisms responsible for triggering Omega band auroras remain unclear. In this study, we analyzed ground-based observations at two wavelengths, 427.8 nm and 844.6 nm, using two EMCCD cameras installed in Tromsø, Norway, along with conjugate observations by the Arase satellite on the magnetospheric side. On September 30, 2017, and March 25, 2021, Omega band auroras were observed in Tromsø, with the Arase satellite's orbital footprint located within the field of views of the cameras. These events occurred during dawn local time, and the Arase satellite detected strong chorus waves along with injections of electrons in the tens of keV range, which may have contributed to the diffuse and pulsating auroras within the Omega band auroras. In this presentation, we will report on these two events, focusing on the spatial characteristics of precipitating electrons within the Omega band auroras and their correspondence with magnetospheric phenomena.

オメガバンドオーロラとは、オーロラブレークアップ直後に発生し真夜中から朝方にかけて東側にドリフトするオーロラであり、特徴的なΩを上下反転させたような構造を持つ。
オメガバンドオーロラの先行研究では、その成因に関していくつかの説が提案されており、ケルビンヘルムホルツ/レイリー・テイラー不安定性のハイブリッドによって発生する速度シアを起因とした説や、極側オーロラストリーマがオメガバンドのトーチに直接進化するストリーマモデルが提案されている。また、オメガバンドオーロラはさまざまなオーロラで構成されていることが明らかとなっており、トーチ中にディフューズオーロラ、脈動オーロラ、ディスクリートオーロラが存在していることが確認されている。しかし、磁気圏側の衛星との同時観測例がほとんどないため、オメガバンドオーロラを起こす磁気圏側の機構については、明らかになっていない。本研究では、ノルウェーのトロムソに設置された 2 台の EMCCD カメラによる 427.8nm と 844.6nm の 2 波長の地上観測と、あらせ衛星による磁気圏側共役観測イベントの解析を行った。2017 年 9 月 30 日、2021 年 3 月 25 日において、トロムソでオメガバンドオーロラが観測された際に、あらせ衛星の軌道フットプリントが光学観測視野内にあった。これらのイベントは、朝側の地方時で発生しており、あらせ衛星では数十 keV の電子のインジェクションとともに、強いコーラス波動が観測され、オメガバンドオーロラ中のディフューズ/脈動オーロラの起源となっている可能性がある。本発表では、この 2 つのイベントについて、オメガバンドオーロラ内部における空間的な降込み電子特性と、磁気圏側現象との対応について報告する。

R006-21
A 会場 ：11/27　AM2 （10:30-12:00）
11:45〜12:00

リオメータとカメラ観測による磁気嵐時の降下電子エネルギーの推定

#高野 向陽 [1)], 細川 敬祐 [1)], 大山 伸一郎 [2,3)], 田中 良昌 [3)], Kero Antti[4)], 三好 由純 [2)], 小川 泰信 [3)], 吹澤 瑞貴 [3)], 栗田 怜 [5)]
([1] 電通大, [2] 名大 ISEE, [3] 極地研, [4] ソダンキラ地球物理観測所, [5] 京都大学 生存研

Estimation of energy of precipitation electrons during magnetic storms by riometer and camera observations

#Koyo Takano[1)], Keisuke Hosokawa[1)], Shin ichiro Oyama[2,3)], Yoshimasa Tanaka[3)], Antti Kero[4)], Yoshizumi Miyoshi[2)], Yasunobu Ogawa[3)], Mizuki Fukizawa[3)], Satoshi Kurita[5)]
([1]The University of Electro Communications, [2]Institute for Space-Earth Environmental Research, Nagoya University, [3]National Institute of Polar Research, [4]Sodankylä Geophysical Observatory, [5]Research Institute for Sustainable Humanosphere, Kyoto University

Auroras are broadly classified into two categories: discrete auroras, which have clear and distinct shapes, and diffuse auroras, which have vague and blurred shapes. Among diffuse auroras, those that exhibit quasi-periodic brightness modulations are known as ”Pulsating Aurora (PsA).” The appearance of PsA is often accompanied by a large-scale wavy auroral structure called the ”omega band.” Recent studies have shown that highly energetic electrons of radiation belt origin sometimes precipitate into the atmosphere during the appearance of PsA. To further investigate this phenomenon, we examine the correlation between auroral emission intensities and Cosmic Noise Absorption (CNA). Additionally, by using an atmospheric model to quantitatively calculate CNA and the absorption spectral index, we will explore the relationship between the index, the energy of precipitating electrons, and the ionization altitude. Through this approach, we aim to estimate the energy of precipitating electrons at riometer observation sites, using CNA as a proxy, and then visualize the characteristics of the energy of precipitating electrons in a two-dimensional fashion within the observation area where cameras can detect emission intensity during the occurrence of omega bands.

In this study, we investigated the spatiotemporal variations of CNA associated with substorms that occurred during a geomagnetic storm by combining observations from high-speed EMCCD all-sky cameras installed at four locations in Scandinavia (Tromsø, Tjautjas, Sodankylä, and Kevo) and spectral riometers located at five stations in the same region (Abisko, Kilpisjärvi, Sodankylä, Kevo, and Oulu). Specifically, we analyzed two substorms that occurred during a Coronal Mass Ejection (CME) type large geomagnetic storm on March 23-24, 2023. We found that the torch structures of the omega bands drifted eastward quasi-periodically across the cameras' fields of view of the cameras. A comparison between the temporal variations in CNA and optical data indicated that CNA significantly increased when the torch structures passed through the riometers' sensing areas. Additionally, by directly comparing the spatial structure of the omega bands with CNA variations at the five locations, we discovered that CNA increased not in regions of discrete auroras along the omega band's edge, but within and outside the torch structures filled with diffuse auroras. Furthermore, during the substorm on the 24th, ground-based observations from the European Incoherent Scatter radar (EISCAT) revealed stepwise variations in the altitude distribution of electron density, suggesting the presence of high-energy electron precipitation causing ionization at lower altitudes. In the presentation, we will focus on the latitudinal distribution of auroras during geomagnetic storms, with a particular emphasis on omega bands, through visualizing them through wide-area imaging, and highlighting the increase in CNA observed during such events. Additionally, using the GLOW model, we will theoretically calculate CNA and derive the absorption spectral index in relation to characteristic energy, thereby clarify the relationship between the absorption spectral index, the specific energy of precipitating electrons, and the ionization altitude caused by these electrons. Finally, we will estimate the energy of precipitating electrons based on observation data from multiple riometers and discuss its validity as well as its relationship with the spatial structure of auroras.

オーロラは、明瞭な形をしたディスクリートオーロラと、曖昧な形をしたディフューズオーロラに分類される。ディフューズオーロラの中でも準周期的に明滅を繰り返すものを「脈動オーロラ (Pulsating Aurora: PsA)」と呼ぶ。PsA の出現に伴い「オメガバンド」と呼ばれる波状のオーロラ構造が見られることがある。近年の研究によって、PsA の発生に伴って PsA を光らせる電子だけでなく、放射線帯に起源を持つ高エネルギー電子が降下していることが明らかとなった。しかし、これまでの研究では、オメガバンド発生時の放射線帯電子降下のエネルギーや時空間分布が十分に明らかとなっているとは言えない。本研究では、2023 年 3 月に発生した大規模な磁気嵐時に観測されたオメガバンドについて、スペクトルリオメータを用いた銀河電波吸収 (Cosmic Noise Absorption: CNA) の同時観測を行い、カメラによって観測された発光強度との相関を調査する。また、大気モデルを用いて、CNA および吸収スペクトル指数を定量的に算出することにより、指数と降下電子エネルギー、電離高度の関係を検討する。これにより、CNA を仲介とすることでリオメータ設置地点における降下電子のエネルギーを推定し、オメガバンド発生時にカメラが発光強度を検出できる観測領域の降下電子のエネルギー特性を二次元的に可視化することを目的とする。

本研究では、北欧の 4 地点（Tromsoe, Tjautjas, Sodankyla, and Kevo）に設置されている EMCCD 高速撮像全天カメラと、同じく北欧の 5 地点 (Abisko, Kilpisjarvi, Sodankyla, Kevo, and Oulu) に設置されているスペクトルリオメータの観測

を組み合わせることによって、磁気嵐時に発生したサブストームに伴う CNA の時空間変動を調べた。具体的には、2023 年 3 月 23-24 日にかけて発生したコロナ質量放出 (Coronal Mass Ejection: CME) 型の規模の大きい磁気嵐の主相から回復相にかけて発生した二つのサブストームの事例について解析を行った。まず、真夜中から明け方のローカルタイムにかけて、オメガバンドを構成するトーチ構造が準周期的に発生し東向きにドリフトしていたことが分かった。EMCCD 全天カメラによって得られた全天画像から作成したケオグラムとスペクトルリオメータから得られた CNA 強度の時間変化を比較した結果、トーチ構造がリオメータの観測領域を通過するタイミングで CNA が顕著に増大していたことが明らかになった。また、オメガバンドの空間構造と 5 地点で得られた CNA 観測データを直接的に比較することにより、観測領域の低緯度側は高緯度側に比べ CNA の増強が激しいことが分かった。さらに、3 月 24 日に発生した二つ目のサブストームでは、欧州非干渉散乱レーダー (European Incoherent SCATer rader: EISCAT) による地上観測から、電子密度の高度分布の段階的な変動が確認された。これは、低高度で電離を引き起こす高エネルギー電子降下の存在を示唆する。発表では、磁気嵐発生時のオーロラの緯度分布を、オメガバンドに焦点を当てながら広域撮像により可視化し、イベント中に発生する CNA の増大現象との関連について報告する。また、多流体発光計算モデル (GLOW モデル) を用いて CNA を理論的に算出し、特性エネルギーと吸収スペクトル指数の関係を導出することにより、吸収スペクトル指数と降下電子の具体的なエネルギー、降下電子が引き起こす電離高度の関係を示す。それらに基づいて、多地点リオメータの観測データから降下電子エネルギーを推定し、その妥当性やオーロラの空間構造との関係性について議論する。

R006-22
A 会場 ：11/27　PM1 （13:15-15:15）
13:15〜13:30

オーロラ降下電子計測を目的としたCubeSat搭載用小型広視野電子計測器の開発

#籔本 将基 [1)], 浅村 和史 [2)], 三谷 烈史 [3)], 寺本 万里子 [1)], 岩瀬 智哉 [1)], 北村 健太郎 [4)], 宮里 健太郎 [1)]
([1] 九工大, [2] 宇宙研, [3] 宇宙研, [4] 九州工大

Development of a small-size and wide-field of view electron analyzer for CubeSat to measure auroral precipitating electrons

#Shoki Yabumoto[1)], Kazushi Asamura[2)], Takefumi Mitani[3)], Mariko Teramoto[1)], Tomoya Iwase[1)], Kentarou Kitamura[4)], Kentarou Miyazato[1)]
([1]Kyushu Institute of Technology, [2]Japan Aerospace Exploration Agency, [3]Japan Aerospace Exploration Agency, Institute of Space and Astronautical Science, [4]Kyushu Institute of Technology

In recent years, nano-satellites called CubeSats have been actively used. We are developing a small-size electron analyzer to be mounted on CubeSat in order to observe the multi-scale structure of the auroral emission layer through simultaneous multi-point observations of auroral precipitating electrons using CubeSats. However, while CubeSat can be developed quickly and inexpensively, it has the disadvantage of having a small onboard volume. For this reason, we will use an APD (Avalanche Photodiode) as the sensor of the electron detector instead of an MCP (Micro Channel Plate), which has been conventionally used for observations of low-energy electrons from 10 eV to a few tens of keV. APDs are considered to have relatively small uncertainty in detection efficiency. However, since APDs are not sensitive to electrons below a few keV, + several kV is applied to the entire APD to accelerate the incident electrons to detectable energies. In this study, the measurement performance of the APDs was verified using an experimental setup that enables the installation and signal processing of up to eight floating APDs within a 10-cm cube, assuming that the APDs will be installed on an actual CubeSat.

In addition, to enable observations that do not require satellite attitude control, the electrode structures of the field-of-view control unit, which is angle-resolvable and has an ultra-wide field of view of 3 π [sr], and the electrostatic energy analysis unit are being investigated through computer simulations.

We will report on the current status of the development and future plans.

近年 CubeSat と呼ばれる超小型衛星の利用が活発に行われている。我々はこの CubeSat を用いてオーロラ降下電子を同時多点で観測することでオーロラ発光層のマルチスケール構造の成因解明のため、CubeSat に搭載する超小型の電子計測器の開発を目指している。CubeSat は短期間かつ低コストの開発が可能である一方、搭載可能容積が小さい欠点がある。我々は電子計測器のセンサに従来 10eV-数 10keV 帯の低エネルギー電子観測に用いられてきた MCP（Micro Channel Plate）ではなく比較的検出効率の不確定性が比較的小さく、取り扱いが容易な APD(Avalanche Photodiode) を用いることで機器の小型化を行う。ただし、APD はそのままでは数 keV 以下の電子に感度を持たないため、APD 全体を周囲から絶縁し、+ 数 kV の電圧を印加することで入射電子を加速し計測する。本研究では実際の CubeSat への搭載を想定し、10cm 立方に収まるサイズで最大 8 個のフローティングさせた APD の搭載と信号処理が可能な実験セットアップを用いて APD の計測性能を確認した。

また、衛星の姿勢制御を必要としない観測を可能にするため、角度分解可能で 3 π [sr] の超広視野をもつ視野制御部、静電エネルギー分析部の電極構造を計算機シミュレーションによって検討している。本発表では、開発の現状と今後の計画について報告する。

R006-23
A 会場 ：11/27　PM1 （13:15-15:15）
13:30〜13:45

#寺澤 賢哉 [1)], 浅村 和史 [2)], 永谷 朱佳理 [1)], 三好 由純 [1)]
([1 名大 ISEE, ([2 宇宙研

Newly development of an ion energy-mass spectrometer for observations of suprathermal ions

#Kenya Terasawa[1)], Kazushi Asamura[2)], Akari Nagatani[1)], Yoshizumi Miyoshi[1)]
([1]Institute for Space-Earth Environmental Research, Nagoya University, ([2]Japan Aerospace Exploration Agency

In the inner magnetosphere, oxygen ions, nitrogen ions, and molecular ions flow out from the ionosphere along the Earth's magnetic field lines. The mechanism for accelerating these thermal ions (about 1 eV) in the ionosphere to suprathermal ions (about 10 eV) remains unclear. To clarify the mechanism, we develop a new suprathermal ion energy-mass spectrum analyzer for the next sounding rocket experiment "LAMP-2" and the future geospace satellite mission "FACTORS". One of the scientific objectives is to observe the 3D distribution function for each ion species from the ionosphere to the magnetosphere. To achieve this, several functions are required to observe these ions, including a sensitivity adjustment function to prevent saturation in case of high ion flux. The instrument consists of mainly two components: an electrostatic energy-per-charge analyzer and a mass analyzer using a Time-Of-Flight (TOF) method with the linear-electric field (LEF) system. Using a dedicated electrode system, the field-of-view (FOV) of the instrument is expanded by controlling the looking direction sequentially and the sensitivity is also controllable. We report on the design of the instrument and outline our plans.

R006-24
A 会場 ：11/27　PM1 （13:15-15:15）
13:45〜14:00

デジタル方式フラックスゲート磁力計における FPGA コーディングの検討と開発

#田中 颯 [1)], 松岡 彩子 [2)]
[(1] 京都大学 理学研究科 地球惑星科学専攻, [(2] 京都大学 理学研究科 地磁気世界資料解析センター

Investigation and development of FPGA coding for digital-type fluxgate magnetometer

#Hayato Tanaka[1)], Ayako Matsuoka[2)]
[(1]Division of Earth and Planetary Sciences, Graduate School of Science, Kyoto University, [(2]Data Analysis Center for Geomagnetism and Space Magnetism, Kyoto University

Digital-type fluxgate magnetometers have been developed and installed on satellites and sounding rockets in Japan and other countries because they have advantages in reducing power consumption and weight compared to conventional analog-type fluxgate magnetometers. In this study, the frequency characteristics of a digital-type magnetometer are numerically modeled and compared with those of manufactured hardware. The improvement of the digital-type fluxgate magnetometer can expand the possibilities for advanced magnetic field measurement in the future space-science mission.

The fluxgate magnetometer measures the external magnetic field strength and direction by the non-linearity characteristics of magnetic field in a soft-magnetic core in the sensor. Artificial magnetic field is excited by alternating current flowing through a drive coil wound around the core, and the induced voltage in another coil, pickup coil, wound around the same core, is detected as the signal corresponding to the external field. For the digital-type fluxgate magnetometer, developed for use on spacecraft, a Field Programmable Gate Array (FPGA), a digital logical processor, is used to perform most of the pickup signal processing. Therefore, the weight and power consumption of its circuit can be reduced compared to analog-type fluxgate magnetometer. Recently the target of space exploration is expanded to the wider area in the solar system. As a result, observation instruments of wider variety are installed on a single spacecraft and the technology for the in-situ observation has been developed to suit that condition. Digital-type fluxgate magnetometer, which is small and power-saving compared with the conventional analog-type, is more suitable for the future exploration by spacecraft, on which more various and smaller observation instruments would be installed. Meanwhile the devices and materials used in instruments on spacecraft require a high degree of reliability and must be tolerant of the severe space environment, e.g., high and low temperatures and radiation. The reliability and environment tolerance strictly restrict the available device, material and design of the instruments. The goal of this research is to develop a digital-type magnetometer with improved performance over conventional one while overcoming these limitations.

This study and development are based on the design of a digital-type fluxgate magnetometer developed for the SS-520-3 sounding rocket experiment. Since the output data from the magnetometer to the magnetic-field input depend on the frequency of the magnetic field time variation, the frequency characteristics of the response of the magnetometer should be evaluated with high accuracy. We numerically simulated and modeled the frequency characteristics and derived the overall transfer function of the digital-type fluxgate magnetometer. When comparing the obtained frequency response of our first model with the frequency response of the manufactured hardware, there was a significant difference between the model and the actual hardware. Since the circuit of the digital-type fluxgate magnetometer consists of both analog and FPGA digital circuit, the model must be the combination of transfer functions for continuous and discrete time-series signals. In our first model, to implement this combination easily, the digital signal processing in the FPGA was modeled in a simplified form. It led to the considerable inaccuracy of the modeled transfer function of the digital signal processing, and caused the discrepancy of the overall frequency characteristics. In the next step we revised the model for the digital signal processing, which accurately expresses the processing in the FPGA and can be combined with the analog data processing model. We constructed the overall transfer function of the digital-type fluxgate magnetometer by implementing the revised model, and examined the consistency of its frequency characteristics with the actual hardware.

We will present the frequency response model of the digital-type magnetometer based on our examination of the FPGA coding in detail, and discuss its characteristics. Moreover, we are investigating the parameter in the FPGA coding to improve the performance of the digital-type fluxgate magnetometer.

In the future, based on the results of this study, we will design the parameter of the digital-type fluxgate magnetometer that could detect higher frequency magnetic field fluctuations in the space.

デジタル方式フラックスゲート磁力計はアナログ方式に比べて消費電力、重量を抑えられるという利点から、国内外で開発、宇宙機に搭載されている。本研究ではデジタル方式フラックスゲート磁力計の利点を生かしつつ更に幅広い磁場測

定への可能性の開拓に向けて開発を行っている。

フラックスゲート磁力計はコアの周りに巻いたドライブコイルに交流電流を流すことによりコアを励磁し、外部磁場の強度と方向に応じて生じた起電力を検出することにより、外部磁場を計測する。宇宙機への搭載を目的に開発されたデジタル方式のフラックスゲート磁力計では、デジタル演算素子の Field Programmable Gate Array (FPGA) でピックアップ信号の処理の大半を行うため、アナログ方式のフラックスゲート磁力計に比べ回路の重量や消費電力を抑えることができる。近年の探査技術の向上により、太陽系における直接探査の領域や対象が広がりつつある。これに伴い、一つの宇宙機に多種多様な観測機器を搭載する傾向にある。小型化・省電力化したデジタルフラックスゲート磁力計は、観測機器の増加、小型化の進む近年の宇宙機での観測に適している。しかし、宇宙機に搭載する機器で使用する部品には高度な信頼性が要求され、また熱や放射線等の過酷な宇宙環境に耐える必要があることから、設計は制約を受ける。この制約を克服しつつ、従来よりも性能を向上させた磁力計を開発することが本研究の最終的な目標である。

本研究では観測ロケット SS-520-3 号機に搭載されたデジタル方式フラックスゲート磁力計の設計をベースに検討と開発を行う。磁場の入力に対する磁力計の出力は磁場変動の周波数に依存するため、入力信号に対する出力信号の応答の周波数特性を精度よく評価することが求められる。そこで磁力計の伝達関数を計算機でシミュレーションして求め、周波数特性をモデル化した。そしてこの周波数特性モデルを実機の周波数特性と比較したところ、モデルと実機の周波数特性には大きな乖離があった。フラックスゲート磁力計の回路はアナログ回路と FPGA によるデジタル回路が混在しており、モデルでは連続的な時間信号の伝達関数と離散的な時間信号の伝達関数を組み合わせる必要がある。組み合わせを容易に行うためにモデルのデジタル回路の動作を単純化し、FPGA で実際に行っている信号処理を厳密に反映していなかったために乖離が生じたと考えられる。そこで、FPGA が行っている演算を正確にモデル化した上でアナログ回路との組み合わせが可能な形式の伝達関数を導出し、デジタル方式フラックスゲート磁力計全体の伝達関数を構築することにより、モデルと実機の周波数特性の一致をはかった。

今回の発表においては FPGA のコーディングを詳細に検討し、これを反映した周波数特性のモデルを提示し、考察する。また、デジタル方式フラックスゲート磁力計の性能を向上させるための、FPGA コーディングにおけるパラメータ設計を検討する。

将来的には、本研究の結果を元に、デジタル方式フラックスゲート磁力計のパラメータ設計を行い、より高周波の磁場変動を捉えることを目指す。

R006-25
A 会場 ：11/27　PM1 （13:15-15:15）
14:00〜14:15

#小池 春人 [1)], 田口 聡 [1)]
([1] 京大理

Ion heating asymmetry between the tailward and earthward sides of lobe reconnection X-line

#Haruto Koike[1)], Satoshi Taguchi[1)]
([1]Department of Geophysics, Graduate School of Science, Kyoto University

For the northward interplanetary magnetic field, reconnection can occur at high latitudes of the Earth's magnetopause, where the earthward outflow jet from the reconnection X-line has an antiparallel component to the tailward magnetosheath flow, while the tailward outflow jet has a parallel component to the magnetosheath flow. Recent simulation studies suggest that the Hall electric field exhibits a turbulent structure on the earthward side where counterstreaming ion distributions are formed, leading to efficient ion heating there. In this study, we investigate the kinetic effects of the counterstreaming ions in the reconnection outflow jets using data from the Cluster satellites observing high-latitude lobe reconnection regions. We performed a statistical analysis of lobe reconnection events where Cluster detected both tailward and earthward outflow jets, and examined how the increase in ion temperature depends on the inflow conditions. Our results indicate that ion heating is more pronounced on the earthward side of the reconnection X-line than on the tailward side. We will discuss the possible mechanisms of the ion heating, focusing on turbulent electric field generation.

R006-26
A 会場 ：11/27　PM1 （13:15-15:15）
14:15〜14:30

昼側地球磁気圏の軟 X 線イメージングによる磁気リコネクションレートの推定

#百瀬 遼太 [1)], 松本 洋介 [2)], 三好 由純 [3)]
([1] 千葉大学大学院融合理工学府, [2] 千葉大高等研究基幹, [3] 名大 ISEE

An Estimation of Magnetic Reconnection Rate from Soft X-ray Emission in the Earth's Dayside Magnetosphere

#Ryota Momose[1)], Yosuke Matsumoto[2)], Yoshizumi Miyoshi[3)]
([1]Graduate School of Science and Engineering, Chiba University, [2]Institute for Advanced Academic Research, Chiba University, [3]Institute for Space-Earth Environement Research, Nagoya University

Magnetic reconnection is a physical mechanism that converts magnetic energy into plasma internal and kinetic energies in various astrophysical phenomena. The reconnection rate is a physical quantity that characterizes the energy conversion efficiency during the reconnection process. The reconnection rate can be measured by the time variation of the magnetic flux, the reconnection electric field, the Alfvén Mach number of the inflow speed toward the diffusion region, or the aspect ratio of the diffusion region (Cassak et al., 2017). This rate has been estimated by various numerical, experimental, and observational data. From observational data, they have been estimated from plasma inflow and outflow velocities estimated by solar flare imaging (Takasao et al., 2011) and from reconnection electric fields measured by in-situ observations in the Earth's magnetosphere (Nakamura et al., 2018; Burch et al., 2020).

In addition to these methods, we propose a new approach to estimating the rate geometrically by using soft X-ray emission in the Earth's magnetopause. The X-rays are emitted during charge exchange between high charge-state ions in the solar wind and the Earth's exosphere (geocorona). This emission process, termed SWCX (Solar Wind Charge eXchange), is useful for visualizing the dayside magnetosphere and its response to solar wind variations. The SMILE and GEO-X missions have been proposed to provide soft X-ray images of the magnetosheath and cusps and will contribute to a better understanding of the dynamic response of the Earth's magnetosphere.

For this purpose, we have developed a global magnetohydrodynamic simulation model of the magnetosphere (Matsumoto and Miyoshi, 2022). The model can provide three-dimensional distributions of the soft X-ray intensity from the plasma parameters. Then line-of-sight integrations of the intensity distribution give a two-dimensional X-ray map as a virtual observation in the simulation domain. By using this model, we examined the SWCX emission around the dayside magnetopause under a coronal mass ejection event. We found that the current sheet around the dayside reconnection region is bright as 10 keV/cm^2/s/str so that we could identify the reconnection outflow region. By calculating the opening angle of the reconnection region estimated from the bright area, we obtained the reconnection rate as R˜0.13. This value is close to the aspect ratio δ/L˜0.1, as assumed in a previous study (Cassak and Shay, 2007) and consistent with values obtained by PIC simulations (Zenitani et al., 2011). Furthermore, we confirmed that there is a difference in emission intensity depending on the dipole tilt; we expect that the larger the tilt, the clearer the bright reconnection region will be. In this presentation, we present a new approach to estimating the reconnection rate geometrically by the soft X-ray imaging of the dayside magnetosphere and discuss its seasonal dependence.

R006-27
A 会場 ：11/27　PM1 （13:15-15:15）
14:30〜14:45

水星磁気圏夜側領域にみられる特徴的な磁場の窪み構造の統計解析

#小川 琢郎 [1)], 篠原 育 [2)], 村上 豪 [3)], 相澤 紗絵 [4)]
[(1] 東大, [(2] 宇宙機構／宇宙研, [(3]ISAS/JAXA, [(4] プラズマ物理学研究所

Statistical analysis of the characteristic magnetic depression structure in Mercury's nightside magnetosphere

#Takuro Ogawa[1)], Iku Shinohara[2)], Go Murakami[3)], Sae Aizawa[4)]
[(1]University of Tokyo, [(2]Japan Aerospace Exploration Agency/Institute of Space and Astronautical Science, [(3]Institute of Space and Astronautical Science, Japan Aerospace Exploration Agency, [(4]Laboratoire de Physique des Plasmas, CNRS

Mercury, the closest planet to the Sun, is known to possess an internal magnetic field similar to Earth's. Combination of the weaker magnetic field of Mercury compared to Earth and harsher solar wind, the magnetosphere formed is significantly smaller than that of Earth. This smaller magnetosphere is more responsive to variations in the solar wind, making the magnetotail, or nightside region, particularly important for understanding the magnetospheric response to the solar wind. NASA's MESSENGER mission (2011-2015) has observed this magnetotail and found characteristic dip structures across a wide region in the nightside. Previous studies have identified this structure as a result of tail current sheet crossing, and no in-depth studies have been conducted. In this study, we have focused on the major magnetic field components that form this depression structure,

and we found that the main components are different between those observed near Mercury and those observed on the magnetotail side. This suggests that not all depression structures can be explained by neutral sheet crossing. We propose that solar wind variations play an important role in the development of a type of depression that appears closer to Mercury, which cannot be explained solely by neutral sheet crossing. In this study, we refer to these structures as "dips" and conduct more detailed analysis of its spatial distribution and the conditions under which they form, considering the magnetospheric current structure and solar wind conditions using both the magnetic field and plasma data. The presentation reports on the current status of our research.

太陽に最も近い惑星である水星は、地球と同様に内部磁場を持つことが知られている。水星固有磁場は地球と比べて弱いため、太陽風との相互作用によって形成される水星磁気圏は、地球の磁気圏と比べてはるかに小さいことが明らかになっている。小さい磁気圏は太陽風変動の影響を受けやすく、その中でも磁気圏尾部は磁気圏の太陽風への応答を理解するのに重要な領域であると考えられている。NASA の MESSENGER 探査機（2011-2015）はこの磁気圏尾部の観測を行っており、広い領域において磁気圏夜側領域に特徴的な窪み構造が確認されている．複数の先行研究でこの構造は neutral sheet crossing によるものであると結論付けられており，踏み込んだ研究はされていない．しかし，この窪み構造をつくっている磁場成分に注目すると，水星近傍で観測されるものと磁気圏尾部側で観測されるものでは主成分が異なっていることがわかり，全ての窪み構造を neutral sheet crossing で説明できるわけではないことがわかる．我々は，neutral sheet crossing では説明できない，より水星近傍でこの構造が生じるタイプの窪みの形成には，太陽風変動が重要な役割を果たしていると考えている．本研究ではこの構造を「dip」とよび，dip 構造が空間的にどのような場所で生じているのか，この構造がどのような条件下で生じているのかについて，磁気圏の電流構造，太陽風状態の観点から，プラズマのデータも活用してより詳細な解析を行っている．本講演では研究の現状について報告する．

R006-28
A 会場 ：11/27　PM1 （13:15-15:15）
14:45〜15:00

磁気圏近尾部におけるプラズモイドと磁気再結合の夕側への偏在

#家田 章正 [1)], 宮下 幸長 [2)]
([1] 名大宇宙地球研, [2]KASI

Duskward displacement of plasmoids and reconnection in the near-Earth magnetotail

#Akimasa Ieda[1)], Yukinaga Miyashita[2)]
([1]Institute for Space-Earth Environmental Research, Nagoya University, [2]Korea Astronomy and Space Science Institute

Magnetic reconnection in the near-Earth magnetotail is responsible for explosive release of energy during substorms and auroral breakups. This near-tail reconnection was previously assumed to occur around the midnight meridian, where earthward flows were typically observed. Based on observations of tailward-moving plasmoids, the Geotail spacecraft mission discovered that the reconnection location was displaced toward dusk. This dusk preference is presumably caused by the Hall electric field, as was suggested later in simulations. However, recent spacecraft observations have indicated that the reconnection was displaced toward dawn, and not dusk, in Mercury's magnetotail.

In response to this controversy, our study aims to clarify the dawn − dusk location of fast plasma flows in the near-Earth magnetotail. Through a comprehensive reinterpretation and integration of previous statistical results, we found that the dusk preference is generally evident for tailward flows but is often absent for earthward flows. These results indicate that the statistical results of earthward flows are sensitive to event selection criteria. We conclude that the dawn − dusk location of earthward flow is statistically unclear at the time of substorm onset. Similarly, in the magnetotail of other planets, the dawn − dusk location of planetward flow may be sensitive to event selection criteria. Hence, reconnection may occur predominantly on the duskside in Mercury's magnetotail. This hypothesis will be tested using observations of tailward-moving plasmoids by the BepiColombo Mio satellite, which will begin orbiting Mercury in the year 2025.

Ieda and Miyashita, EPS, 2024, doi:10.1186/s40623-024-02003-w
in special issue "Symposium on the Future of Heliospheric Science: From Geotail and Beyond"

地球磁気圏の近尾部における磁気再結合は、尾部に蓄積された磁気エネルギーの爆発的解放を起こす。この磁気再結合が開始する位置の解明は、オーロラ爆発の開始過程を理解するために必要である。以前は、磁気再結合は真夜中付近で生ずると想定された。この想定は、AMPTE 衛星や ISEE-2 衛星の、地球向き高速プラズマ流の観測と整合した。現在は、磁気再結合は夕方側に偏ると考えられている。この夕方偏在は、Geotail 衛星が尾部向きプラズモイドの観測により発見し、後にシミュレーションが原因はホール電場であることを説明した。しかし、近年の水星観測は、磁気再結合が夕側ではなく朝側に偏在することを示唆している。磁気再結合の位置が、このように地球と水星で異なる原因は不明である。

本研究では、地球近尾部の高速プラズマ流の朝夕位置について、過去の統計結果を整理して再解釈した。その結果、夕方偏在は、尾部向き高速流では普遍的だが、地球向き高速流では統計的な一貫性がなく不明瞭であった。従って、磁気再結合は水星においても夕側に位置している可能性がある。この仮説は、2025 年に水星周回を開始する BepiColombo Mio 衛星の、尾部向きプラズモイドの観測により検証することができる。

Ieda and Miyashita, EPS, 2024, doi:10.1186/s40623-024-02003-w
in special issue "Symposium on the Future of Heliospheric Science: From Geotail and Beyond"

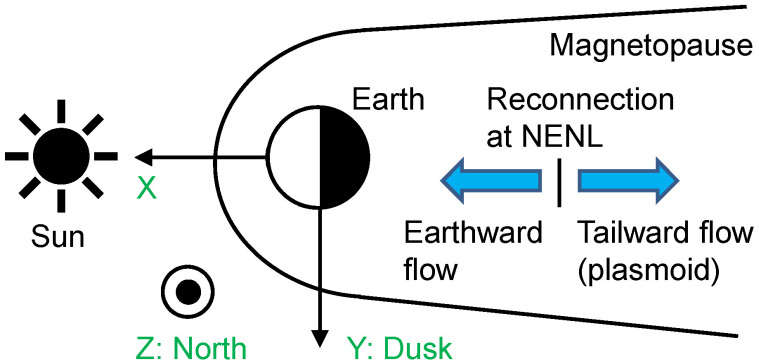

Fig. 1 Pair of earthward and tailward flows in the Earth's magnetotail. These fast plasma flows are generated by magnetic reconnection on the near-Earth neutral line (NENL). Not to scale

R006-29
A 会場 ：11/27　PM1 （13:15-15:15）
15:00〜15:15

#カリオコスキ ミラ [1)], キスラー リン [1,2)], 三好 由純 [1)], 浅村 和史 [3)], 篠原 育 [3)], 松岡 彩子 [4)], 横田 勝一郎 [5)], 笠原 慧 [6)], 桂華 邦裕 [7)], 堀 智昭 [1)], 寺本 万里子 [8)], 山本 和弘 [1)]
([1 名大 ISEE, ([2 ニューハンプシャー大学, ([3 宇宙研, ([4 京都大学, ([5 大阪大, ([6 東京大学, ([7 東大・理, ([8 九工大

Energy and pitch angle dispersed ion injections from the magnetotail during geomagnetic storms observed by Arase

#Milla M H Kalliokoski[1)], Lynn M Kistler[1,2)], Yoshizumi Miyoshi[1)], Kazushi Asamura[3)], Iku Shinohara[3)], Ayako Matsuoka[4)], Shoichiro Yokota[5)], Satoshi Kasahara[6)], Kunihiro Keika[7)], Tomoaki Hori[1)], Mariko Teramoto[8)], Kazuhiro Yamamoto[1)]
([1Institute for Space-Earth Environmental Research, Nagoya University, ([2University of New Hampshire, USA, ([3Japan Aerospace Exploration Agency, ([4Graduate School of Science, Kyoto University, ([5Osaka University, ([6The University of Tokyo, ([7Department of Earth and Planetary Science, Graduate School of Science, The University of Tokyo, ([8Kyushu Institute of Technology

During geomagnetic storms, energetic ions are injected from the Earth's magnetotail into the plasma sheet boundary layer (PSBL) and the inner magnetosphere. Owing to its off-equatorial, inclined orbit the Arase satellite is in the prime position to observe these injections in the PSBL on the nightside at apogee. Arase can also observe dispersions in pitch angle better than low-latitude satellites. There are two main ion sources into the PSBL: low-energy (<˜1 keV) ionospheric outflow and high-energy (>˜5 keV) injections. The injections are observed as energy and pitch angle dispersed features in the Arase LEP-i and MEP-i data. H+ dispersions are common, but O+ dispersions are predominantly seen during storm times. The energy dispersion can be used to estimate the location and timing of the ion injections, by deriving the inversed velocity distribution and fitting the identified dispersion features. Our study of dispersed structures during storms shows that distances to the injection location range from ˜20 to 40 Earth radii, which is in agreement with the expected origin in the near-Earth neutral line. We will discuss the correspondence between H+ and O+ dispersions and injections, and the association with concurrent plasma waves and ion outflow in the PSBL. We will also study the effect of injections on the plasma sheet ion composition.

R006-P01
ポスター 1 ：11/24　PM1/PM2 （13:15-18:15）

#ギルギス キロロス [1)], 羽田 亨 [1)], 汪 愷悌 [2)], 大塚 史子 [3)], 吉川 顕正 [1,4)]
([1] 九大国際宇宙, [2] 淡江大学 航空宇宙工学科, [3] 九大総理工, [4] 九大/理学研究院

Numerical Modelling of Particle Energization during Dipolarization Substorm Events by Test Particle Simulations

#Kirolosse Girgis[1)], Tohru Hada[1)], Kaiti Wang[2)], Fumiko Otsuka[3)], Akimasa Yoshikawa[1,4)]
([1]International Research Center for Space and Planetary Environmental Science, Kyushu University, [2]Department of Aerospace Engineering, Tamkang University, [3]Department of Advanced Environmental Science and Engineering, Faculty of Engineering Sciences, [4]Department of Earth and Planetary Sciences, Kyushu University

During certain dipolarization substorm events, particles originating from the magnetotail can undergo significant acceleration, leading to their transport into the inner magnetosphere. This phenomenon, observed by various spacecraft such as THEMIS, is marked by a substantial increase in particle flux. The energy enhancement during these events is believed to be driven by an intensified magnetic field, coupled with induced and polarized electric fields, which together energize and transport particles earthward.

To better understand the particle energization mechanisms from the magnetotail to the inner magnetosphere, we developed a hybrid test particle simulation code. This code was used to study the dynamics of particles during specific dipolarization events observed by the THEMIS mission during substorm periods in 2008 and 2009. Our simulations calculated the trajectories of electrons, protons, and oxygen ions across an energy range from 0.1 keV to 1 MeV, considering a variety of initial pitch angles and L-shells. The code integrates two particle tracing methods: the Tao-Chan-Brizard guiding center model and full Lorentz particle motion, with transitions between the two governed by the evaluation of the adiabaticity condition.

To replicate the time-dependent magnetic field, we utilized the Tsyganenko TS05 and IGRF models, which also account for computing the associated inductive and polarized electric fields. Preliminary results indicate significant energy enhancement levels, and a comparison of these numerical findings with observational data supports their consistency.

R006-P02
ポスター 1 ：11/24　PM1/PM2 （13:15-18:15）

北向き惑星間空間磁場におけるダンジーサイクルと交換サイクルの共起

#渡辺 正和 [1)], 蔡 東生 [2)], 熊 沛坤 [2)], 藤田 茂 [3)], 田中 高史 [4)]
([1] 九大・理・地惑, [2] 筑波大・シス情, [3] データサイエンスセンター/統数研, [4]REPPU 研

Concurrence of the Dungey and interchange cycles during northward interplanetary magnetic field periods

#Masakazu Watanabe[1)], DongSheng Cai[2)], Peikun Xiong[2)], Shigeru Fujita[3)], Takashi Tanaka[4)]
([1]Department of Earth and Planetary Sciences, Graduate School of Science, Kyushu University, [2]Institute of System and Information, University of Tsukuba, [3]Joint-support center for data science research/The Institute of Statistical Mathematics, [4]REPPU code institute

When the interplanetary magnetic field (IMF) is southward, the geomagnetic field lines on the dayside magnetopause transmute from closed to open and transported tailward. They become closed again in the magnetotail and transported sunward to finally return to the dayside, thus forming a magnetic flux circulation called the Dungey cycle. The two reconnection processes associated with the Dungey cycle are both called Dungey-type. Topologically, in Dungey-type reconnection, four distinct regions meet together on a separator. In contrast, when the IMF is close to due north, another magnetic flux circulation called the interchange cycle is formed. The interchange cycle is characterized by a pair of ”reverse” convection cells on the dayside ionosphere whose circulation directions are opposite to those driven by the Dungey cycle. The name ”interchange” comes from the fact that the magnetic flux circulation consists of two interchange-type reconnection processes (i.e., IMF-to-lobe reconnection and lobe-to-closed reconnection). The interchange-type reconnection is a process in which two topological regions meet together on a separatrix excluding the separators. Although the Dungey cycle for southward IMF and the interchange cycle for northward IMF appear to be mutually exclusive, they can coexist One example is the IMF By-dependent ionospheric convection that appears occasionally on the nightside when the IMF is northward. This convection system is interpreted as a manifestation of the partial Dungey cycle, and is concurrent with the twin reverse cells on the dayside that characterize the interchange cycle. From global magnetohydrodynamic (MHD) simulations, we reproduced the IMF By-dependent convection system on the nightside and investigated how the two magnetic flux circulations can coexist. The magnetic topology of the magnetosphere for northward IMF consists of two magnetic nulls and two separators connecting them. When the IMF is close to due north, the two separators bend sharply in the vicinity of the magnetic nulls. This bend enables both types of reconnection to coexist in the neighborhood of the null point. However, the geometry of Dungey-type reconnection is quite different from that for southward IMF. In our talk, we discuss the separator configuration in detail that allows the concurrence of the two magnetic flux circulations.

惑星間空間磁場（interplanetary magnetic field, IMF）南向き時には、昼間側で地球の閉磁力線が開き夜側で再び閉じる、いわゆるダンジーサイクル（磁束循環）が形成される。ダンジーサイクルに関与する２つのリコネクションはダンジー型リコネクションと呼ばれ、いずれも４つのトポロジー領域がセパレータ上で会するリコネクションである。一方、IMF が真北に近い時には交換サイクルと呼ばれる磁束循環が形成され、昼間側電離圏にダンジーサイクルとは逆向きの対流が現れる。交換サイクルの名称は、磁束循環が２つの交換型リコネクション（IMF とローブ磁力線の繋ぎ変え、ローブ磁力線と閉磁力線の繋ぎ変え）から成ることから来ている。交換型リコネクションは、2 つのトポロジー領域がセパレータを除くセパラトリクス上で会するリコネクションである。南向き IMF 時のダンジーサイクルと北向き IMF 時の交換サイクルは一見排反のように思われるが、実は同時に存在し得る。その一例は、IMF 北向き時の夜側電離圏に時折出現する IMF By に依存した対流系である。これはダンジーサイクルの一部と解釈され、交換サイクルに特徴的で昼間側に現れる逆向き対流と共存している。我々はグローバル磁気流体シミュレーションで上述の IMF By に依存した対流系を再現し、いかにして２つの磁束循環が共存し得るかを調べた。IMF 北向き時の磁気圏磁場構造は、2 つの磁気零点とそれを結ぶ 2 本のセパレータから構成される。IMF が真北に近い時、磁気零点近傍において 2 本のセパレータは大きく湾曲している。この湾曲がダンジー型リコネクションと交換型リコネクションを零点近傍で共存させている。ただしこの時のダンジー型リコネクションの様相は、IMF 南向き時のダンジー型リコネクションとかなり異なっている。講演では、2 つの磁束循環を共起させるセパレータの形状について詳細に議論する。

R006-P03
ポスター 1 ：11/24　PM1/PM2 （13:15-18:15）

#中溝 葵 [1)], 吉川 顕正 [2)], 中田 裕之 [3)], 深沢 圭一郎 [4)], 田中 高史 [2)]
([1]NICT, [2] 九大/理学研究院, [3] 千葉大・工, [4] 京大・メディアセンター

Large-scale FAC pattern and SW-M-I coupling

#Aoi Nakamizo[1)], Akimasa Yoshikawa[2)], Hiroyuki Nakata[3)], Keiichiro Fukazawa[4)], Takashi Tanaka[2)]
([1]National Institute of Information and Communications Technology, [2]Department of Earth and Planetary Sciences, Kyushu University, [3]Graduate School of Engineering, Chiba University, [4]Academic Center for Computing and Media Studies, Kyoto University

The distribution of large-scale FAC shows different patterns depending for example on the IMF clock angle, basically reflecting the large-scale solar wind-magnetosphere (SW-M) interaction and magnetospheric convection. However, as with the ionospheric convection pattern, various asymmetries can be seen in the patterns. For example, the well-developed FAC distribution during the southward IMF Bz does not necessarily show a perfect dawn-dusk symmetric pattern.

As for the ionospheric potential pattern, the deformations and their causes are understood relatively well. For example, it is well known that the pattern rotates clockwise when IMF By is positive and anti-clockwise when IMF By is negative. In addition, Nakamizo & Yoshikawa [2019] pointed out that there is a bias of clockwise rotation that cannot be explained by the IMF By effect (external effect) alone, and they show that the bias is due to the Hall polarization field generated by the latitudinal conductance gradient, based on a test calculation using an ionospheric potential solver. In contrast, as for the FAC pattern, little is known so far about its asymmetry and its causes. So, we numerically investigate how and why the large-scale FAC pattern exhibits asymmetries. Since the large-scale FAC is generated by the solar wind-magnetosphere-ionosphere (SW-M-I) coupling, we use a global MHD model, which is a dynamic model whereas the ionospheric potential solver used in the ionospheric convection pattern study is a static one.

In the simulation runs, we set the y-components of solar wind velocity and IMF to zero, in order to eliminate external factors for the large-scale asymmetry. First, we perform simulation with ionospheric polarization effects turned off (with a finite constant ionospheric conductance) to extract the effects of SW-M interactions. Next, we perform a normal simulation (with normal non-uniform ionospheric conductance) and compare the results with those for the no ionospheric effect to extract the effect of M-I coupling (ionospheric polarization). Furthermore, we try to identify the effect of the M-I coupling process itself on the FAC pattern by comparing the simulation results of cases with the conventional coupling scheme and Alfvenic coupling scheme as the M-I coupling in the global MHD model.

R006-P04
ポスター１：11/24　PM1/PM2（13:15-18:15）

#Porunakatu Radhakrishna Shreedevi[1)], Miyoshi Yoshizumi[1)], Yu Yiqun[2,3)], Jordanova Vania[4)]
([1]ISEE, [2]School of Space and Environment, Beihang University, [3]Space Science Application, Los Alamos National Laboratory, Los Alamos, NM, [4]Space Science Application, Los Alamos National Laboratory, Los Alamos, NM

On the driving mechanisms for the high-speed westward flow channels in the dusk-side sub-auroral ionosphere: Simulation study

#Radhakrishna Porunakatu[1)], Yoshizumi Miyoshi[1)], Yiqun Yu[2,3)], Vania Jordanova[4)]
([1]Institute for Space Earth Environmental Research, [2]School of Space and Environment, Beihang University, [3]Key Laboratory of Space Environment Monitoring and Information Processing, Beijing, [4]Space Science Application, Los Alamos National Laboratory, Los Alamos, NM

The dusk-side mid-latitude ionosphere is characterized by fast, sunward flow channels of a few degrees in width, known as Sub-auroral Polarization Streams (SAPS). Occasionally, these regions exhibit distinct, latitudinally narrow enhancements in velocity, referred to as double-peak Sub-auroral Ion Drifts (DSAIDs). SAPS are associated with Region 2 Field-Aligned Currents (R2 FACs) that flow into the low-conductance sub-auroral ionosphere, while DSAIDs have been linked to the presence of a double-conductance trough in this region. A recent statistical study by Nishimura et al. (2022) demonstrated that sub-auroral ion drifts intensify in the presence of electromagnetic waves, with local plasma structures exerting greater control over the velocity characteristics of these westward flows than solar wind or global magnetospheric conditions. In this study, we investigated the occurrence of fast flows in the dusk-side sector during a geomagnetic storm event using the RAM-SCB model. We conducted two simulation studies, one with and one without EMIC waves, to explore the relationships between R2 FACs, electric fields, EMIC wave-particle interactions, proton precipitation, ionospheric conductance, and westward flows in the dusk-side sub-auroral ionosphere. The simulations confirmed that EMIC wave-induced proton precipitation leads to localized enhancements in conductivity, which, in turn, generates high-speed westward flows in the dusk-side sub-auroral ionosphere. Our findings reveal the significant role of wave-particle interactions in shaping ionospheric behavior during disturbed conditions.

R006-P05
ポスター 1 ：11/24　PM1/PM2 （13:15-18:15）

みちびき初号機と MAGDAS で同時観測される孤立型磁場変動の自動同定結果を用いた磁気圏-電離圏結合電流系の大規模統計解析

#浦 晴香 [1)], 河野 英昭 [2,4)], Moiseev Alexey[3)], Baishev Dmitry[3)], 魚住 禎司 [4)], 阿部 修司 [4)], 吉川 顕正 [4,5)]
([1] 九大・理・地惑, [2] 九大・理・地球惑星, [3] ロシア科学アカデミーシベリア支部ヤクート科学センター Yu.G. シャファー宇宙物理・超高層大気物理学研究所, [4] 九大 国際宇宙, [5] 九大/理学研究院

Statistical analysis of magneto-ionospheric currents using automatically-identified magnetic perturbations from QZS-1 and MAGDAS

#Haruka Ura[1)], Hideaki Kawano[2,4)], Alexey Moiseev[3)], Dmitry Baishev[3)], Teiji Uozumi[4)], Shuji Abe[4)], Akimasa Yoshikawa[4,5)]
([1]Department of Earth and Planetary Sciences, Graduate School of Science, Kyushu University, [2]Department of Earth and Planetary Sciences, Kyushu University, [3]Yu.G. Shafer Institute of Cosmophysical Research and Aeronomy SB RAS, [4]International Research Center for Space and Planetary Environmental Science, Kyushu University, [5]Department of Earth and Planetary Sciences, Kyushu University

Field-Aligned Currents (FACs) are currents that flow along the magnetic field lines within the magnetosphere. They are connected to ionospheric currents. They have a crucial role in understanding magnetosphere-ionosphere structures and disturbances such as substorms. In this study, we aim to investigate the magnetosphere-ionosphere coupling using magnetic field data observed by the QZS-1 satellite and the MAGDAS ground magnetometers. The QZS-1 satellite, having orbits at a distance nearly equivalent to that of a geostationary orbit but with a slightly modified inclination and eccentricity, allows the foot point of the satellite-magnetosphere field line to remain over Japan for extended periods. This means that the foot point of the magnetic field line passing through the satellite stays near the three MAGDAS observation points in Siberia (Kotelny (KTN), Tixie (TIK), Chokurdakh (CHD)) for long durations. Thus, long-term simultaneous observations of the magnetosphere-ionosphere current coupling system can be conducted using the magnetic field data from both the QZS-1 satellite and the three MAGDAS observation points. Previous research (Abematsu,2018) analyzed two and a half years of data. Based on predefined criteria, 76 isolated magnetic-field perturbation events, simultaneously observed by QZS-1 and MAGDAS, were visually identified, and the statistical analysis was conducted using these events. The analysis categorized the connections between the ionospheric currents and the FACs into four patterns, and the features of the categorized events were basically consistent with physical expectations. However, the number of analyzed events was too small to yield statistically significant results; the small number came from the consumption of time by visual identification process, which provably led to overlooking of many events, too. Therefore, in this study we automate the event identification process and construct the database with significantly larger number of events ensuring statistical significance. We then conduct large-scale statistical analyses of the magnetosphere-ionosphere coupling by using the database. We will present a few event studies and the initial results of the statistical analyses at the poster session.

Acknowledgement. In this study, we utilized MAM and orbit data of QZS-1 provided by the Space Environment & Effect System(SEES). We would like to express our gratitude to the JAXA research department for their cooperation.

FAC (沿磁力線電流) は磁気圏内で磁力線に沿って流れる電流であり、電離圏電流と繋がり、磁気圏電離圏構造やサブストームなどの擾乱現象を理解するために非常に重要なものである。本研究の目的は、みちびき衛星初号機と MAGDAS 地上磁力計それぞれの磁場観測データを使用し、磁気圏－電離圏結合電流系の様相を調べる事である。みちびき衛星の軌道は静止軌道とほぼ同じ地心距離を持つが軌道傾斜角と軌道離心率が少し変更されているため、地心－衛星間直線の foot point (地表に達する地点) が日本上空に長時間滞在する。これは、衛星を通る磁力線の foot point がシベリアの MAGDAS 3 観測点（Kotel ’ ny（KTN)、Tixie（TIK)、Chokurdakh（CHD)）の近くに長時間滞在する事を意味する。そのため、みちびき衛星と MAGDAS 3 観測点の磁場データから磁気圏－電離圏電流結合系の長時間同時観測が可能である。先行研究（安倍松修論 2018）では、みちびき衛星初号機と MAGDAS の 2 年半の同時観測データから、あらかじめ設定した基準に基づいて、目視により、みちびき衛星初号機-MAGDAS 同時観測 76 イベントが同定され、それを用いた統計解析が行われた。電離圏電流と FAC の繋がりを 4 パターンに場合分けし、選定されたイベントについて解析を行った結果、予想された変動と観測データは概ね当てはまる結果となっていた。しかし、解析されたイベント数があまりに少なく、有意な結果とは言い難い。またこの研究では大量のデータ中から目視でイベント同定されたため、目視に時間がかかって解析時間が不足し、また、見逃されたイベントも多いと考えられる。そこで本研究では、イベント同定を自動化するプログラムを作成することによりイベント数を大幅に増やして有意性を担保し、磁気圏-電離圏結合電流系の大規模解析を行う。会場にて、自動同定プログラムを用いて同定した同時観測 events からなる大規模データベースの event studies と初期統計解析について発表する。

謝辞: 本研究では、宇宙環境計測情報システム（SEES）から配信されている QZS-1 の MAM・軌道データを利用した。データの提供にご協力いただいた JAXA 研究部門に感謝いたします。

R006-P06
ポスター 1 ：11/24　PM1/PM2 （13:15-18:15）

沿磁力線電流の 3 次元分布に対する降下電子の影響

#金田 ことの [1)], 海老原 祐輔 [1)]
(1 京都大学生存圏研究所

Influence of precipitating electrons on three-dimensional distribution of field-aligned current

#Kotono Kaneda[1)], Yusuke Ebihara[1)]
(1Research Institute for Sustainable Humanosphere of Kyoto University

We used three-dimensional Hall-magnetohydrodynamics simulations to investigate influence of precipitating electrons in the upward field-aligned current region. To excite the Alfvén waves, electric field perturbation is applied to the upper boundary of the simulation box located at 1000 km altitude. The ionospheric ion density is enhanced to incorporate the influence of precipitating electrons. First, we calculated the upward field-aligned potential drop on the basis of the magnitude of the upward field-aligned currents with conductance previously suggested. Secondly, we calculated the characteristic energy precipitating electrons by using empirical equations. Thirdly, assuming energy flux of precipitating electrons, we calculated the ionization rate by using the empirical atmospheric model MSIS-E90. Fourthly, we increased the ion density in accordance with the ionization rate. The distribution of the upward field-aligned currents appears to be modulated by the precipitating electrons. We discuss the influence of the precipitating electrons on the temporalspatial evolution of the field-aligned current.

R006-P07
ポスター 1 ：11/24　PM1/PM2 （13:15-18:15）

磁気圏ー電離圏間の電場の投影について

#海老原 祐輔 [1)], 田中 高史 [2)]
[(1] 京大生存圏, [(2]REPPU 研

On the electric field ”mapping” between the magnetosphere and the ionosphere

#Yusuke Ebihara[1)], Takashi Tanaka[2)]
[(1]Research Institute for Sustainable Humanosphere, Kyoto University, [(2]REPPU code institute

The electric field is fundamental to transport of charged particles. In the inner magnetosphere, the electric field is responsible for the radial transport of hot ions to enhance the ring current, and hot electrons to excite whistler-mode waves. It has been widely assumed that the magnetic field lines are equipotential, and that the electric field can be mapped between the magnetosphere and the ionosphere along the magnetic field lines. However, if the electric field propagates as the Alfvén waves, it may not be straightforward that the assumption is always valid because of the presence of the plasma bulk flow and infinite travel time of the Alfvén waves. We traced the trajectories of the packets of the Alfvén waves from the equatorial plane to the ionosphere in the fields obtained by the global MHD simulation. We called them Alfvénic footprints. We also traced instantaneous magnetic field lines from the equatorial plane to the ionosphere, and called them magnetic footprints. We set the solar wind speed of 400 km/s and interplanetary magnetic field (IMF) of 5 nT or -5 nT, and calculated the difference between the Alfvénic footprints and the magnetic footprints in the ionosphere. When IMF is southward, the deviation is as high as ˜1 deg in magnetic latitude (MLAT) near midnight at $>$8 RE, and $>$0.5 hours in magnetic local time (MLT) on nightside except for midnight. When IMF is northward, the deviation is large at $>$10 RE. The deviation depends largely on plasma density and flow velocity, so these values are not definitive. We discuss the validity of the electric field ”mapping” on the basis of the MHD simulation under various solar wind conditions.

R006-P08
ポスター 1 ：11/24　PM1/PM2 （13:15-18:15）

Arase 衛星の衛星電位を用いた地球磁気圏における電子密度・温度導出の検討

#川潟 桂也 [1)], 笠羽 康正 [1)], 土屋 史紀 [1)], 風間 洋一 [2)], 城 剛希 [3)], 中川 朋子 [4)], 新堀 淳樹 [5)], 加藤 雄人 [3)]
([1] 東北大・理, [2]ASIAA, [3] 東北大・理・地球物理, [4] 東北工大・工・情報通信, [5] 名古屋大学宇宙地球環境研究所

Examination of electron density and temperature in the Earth's magnetosphere using the spacecraft potential observed by Arase

#Keiya Kawagata[1)], Yasumasa Kasaba[1)], Fuminori Tsuchiya[1)], Yoichi Kazama[2)], Koki Tachi[3)], Tomoko Nakagawa[4)], Atsuki Shinbori[5)], Yuto Katoh[3)]
([1]Planetary Plasma and Atmospheric Research Center, Graduate School of Science, Tohoku University, [2]Academia Sinica Institute of Astronomy and Astrophysics, [3]Department of Geophysics, Graduate School of Science, Tohoku University, [4]Information and Communication Engineering, Tohoku Institute of Technology, [5]Institute for Space-Earth Environmental Research, Nagoya University

Since March 2017, the Arase satellite has continuously acquired data that contributes to determining the electron density and temperature in the geospace over a period of about seven years. Density and temperature are fundamental information which defines the structure of the ionosphere, plasmasphere, and magnetosphere. These parameters also play a dominant role in the growth, decay, and propagation of waves through their influence on the dispersion relation.

On the Arase satellite, the electron density is determined using the electric field spectrum (10 kHz to 10 MHz) from the PWE/HFA (Plasma Wave Experiment/High Frequency Analyzer), where the UHR (Upper Hybrid Resonance) frequency is identified through a combination of automatic detection and manual inspection (temporal resolution: 1 min), in conjunction with the background magnetic field strength. This method can determine the electron density with high accuracy, including low temperature components below 10 eV. However, there are many regions where electron density cannot be determined, such as in areas where other strong waves are observed near the UHR frequency or in low-density regions where UHR waves are weak. While low-energy ion and electron data have been used on other satellites, the electrostatic plasma analyzers LEPe and LEPi on Arase have difficulty measuring energies below ~20 eV. In deriving density from particle measurements, assumptions are required for the distribution function of low-temperature plasma, which is abundant in the orbit of Arase near Earth.

Satellite potential can also serve as an indicator of electron density. The floating potential of a satellite in plasma is determined by the balance between photoelectron emission due to solar ultraviolet radiation and electron influx from the surrounding plasma. This potential is influenced by factors such as the efficiency of photoelectron and secondary electron emission depending on the satellite's surface material, the shape of satellite and orientation, and the surrounding electron temperature, which results in low accuracy for electron density inferred from satellite potential. However, since observational data can be obtained with a resolution of 1-spin (about 8 seconds) without relying on manual inspection or specific assumptions, it is possible to consistently derive electron density with a certain degree of reliability, except during shadow periods when there is no photoelectron emission.

Compared to the plasma density (determined by direct ion measurement) versus satellite potential relationship observed with the Geotail and Cluster satellites, the UHR-derived electron density versus satellite potential relationship on Arase shows particularly low accuracy below 1 /cc. This may be due to the low accuracy of UHR-derived electron density in low-density regions and the short antenna length of 15 m (Geotail and Cluster have 50 m), which in low-density regions where 'Debye length >antenna length' may cause the probe potential to be influenced by the satellite potential.

To verify these findings, we have conducted a comparison of plasma density derivation using multiple methods across the entire orbit of the Arase satellite and verified their accuracy. The study covers the period from April 2017 to April 2022, during which electron density information based on UHR frequencies is provided. We also evaluate the dependence on orbital position and aim to assess the impact of different plasma temperature environments on density estimation depending on the region. In our analysis so far, we have found cases where UHR-derived electron density is clearly underestimated in low-density regions, and we are examining specific cases. Additionally, there is better correlation during magnetically quiet periods compared to magnetically disturbed periods, particularly in low-density regions. Further investigation is needed from this perspective due to its potential impact on plasma temperature.

Based on the above, we will explore the causes of data that deviate from the theoretically predicted 'electron density exp(satellite potential)' relationship and from prior cases observed with Geotail and Cluster. Specifically, we will refer to the distribution functions of low-energy electrons and ions provided by LEPe and LEPi to clarify their relationship with plasma particle information. Furthermore, we plan to compare with the provisional low-temperature electron density and temperature data provided by LEPe to verify the consistency and reliability of different plasma density estimation methods.

We will also examine the comparison with the amount of bias current applied to the probe and its relation to solar UV flux, including verification of the stability of probe potential. This stability is also a factor in the accurate determination of electric fields in the magnetosphere and ionosphere as well as low-frequency waves. This research contributes to the pursuit of accuracy in Arase's electric field measurements, which have been the subject of heated debate, and also lays the foundation

for ensuring the accuracy of electron density and electric field measurements using similar probes on the BepiColombo/Mio Mercury exploration mission, which will begin orbiting in 2026.

Arase 衛星は、2017 年 3 月から約 7 年間に渡りジオスペースの電子密度・温度決定に資するデータを取得し続けている。密度・温度は、電離圏・プラズマ圏・磁気圏の構造を決める基本情報である。密度・温度は、分散関係への影響を通して波動の成長・減衰・伝搬にも支配的である。

Arase 衛星では、PWE/HFA（プラズマ波動計測器/高調波受信部）の電場スペクトル（10kHz〜10 MHz）から UHR（高域ハイブリッド共鳴波動）周波数を自動判定と目視の組み合わせで同定し（時間分解能：1 min)、背景磁場強度と併せて電子密度を決定している。この方法は、10eV 以下の低温成分を含む電子密度を高精度で決定できる。しかし、UHR 周波数近傍に他の強い波動が見られる領域や UHR 波動が弱い低密度領域で、電子密度が決定されない領域が多く生じる。他衛星では低エネルギーイオン・電子データが用いられてきたが、Arase の静電プラズマ分析器 LEPe・LEPi は〜20 eV 以下の計測が難しい。粒子計測からの密度導出では、地球に近い Arase 軌道で多い低温プラズマの分布関数に仮定が必要となる。

衛星電位も、電子密度の指標となりえる。プラズマ中における衛星の浮動電位は、太陽紫外線による光電子流出と周辺プラズマからの電子流入のバランスで決定される。衛星表面材料に依存する光電子・二次電子放出効率、衛星の形状・姿勢、および周辺電子温度に影響され、衛星電位から演繹される電子密度の精度は低い。しかし、目視や特定の仮定に依存することなく 1-spin（8sec 程度）の分解能で観測量を取得できるため、光電子放出が無い日陰時を除き、ある程度の信頼性を持った電子密度を常時導出することが可能である。

しかし、Geotail 衛星や Cluster 衛星におけるプラズマ密度（イオン直接計測で決定）- 衛星電位関係と比べると、Arase 衛星における UHR 由来電子密度 - 衛星電位関係は特に 1 /cc 以下で精度が低い。これは、低密度域で UHR 周波数由来電子密度の精度が低いことに加え、アンテナ長が 15 m と短く（Geotail・Cluster は 50 m）「Debye 長＞アンテナ長」となりやすい低密度域ではプローブ電位が衛星電位の影響下にありうることなどに起因しうる。

これらの検証のため、Arase 衛星の軌道全域にわたり、複数の手法を用いたプラズマ密度導出の比較とそれらの精度の検証を行ってきた。UHR 周波数に基づく電子密度情報が提供されている 2017 年 4 月から 2022 年 4 月を対象としている。軌道位置への依存性の評価も行い、領域によって異なるプラズマ温度環境が与える密度推定への影響評価も目指している。これまでの解析結果では、低密度域で明らかに UHR 由来電子密度が過小評価されている例を見出しており、具体的な事例について検討を加えつつある。また、磁気擾乱時と比較して磁気静穏時の方が、特に低密度領域において良好な相関を示す。プラズマ温度に影響ありえるため、この視点でさらなる検討を行う。

上記に基づき、Geotail や Cluster で行われた先行事例、および理論的に予測される「電子密度 $\propto$ exp(衛星電位)」の関係から逸脱するデータの原因を探る。具体的には、LEPe・LEPi による低エネルギー電子・イオンの分布関数を参照し、プラズマ粒子情報との関係を明確化する。さらに、LEPe が提供する暫定的な低温電子密度・温度データと比較し、異なるプラズマ密度推定手法の一貫性・信頼性を検証へ向かう予定である。

プローブに与えるバイアス電流量との比較や太陽 UV flux との関連も確認し、プローブ電位の安定度の検証も含む。この安定度は、磁気圏・電離圏電場および低周波波動の精度決定要因でもある。本研究は、喧々諤々の議論が続く Arase 電場計測の精度追求への一助であり、また 2026 年から周回観測を開始する BepiColombo/Mio 水星探査機における同型プローブを用いた電子密度・電場計測の精度保証の基盤となる。

R006-P09
ポスター 1 ：11/24　PM1/PM2 （13:15-18:15）

プラズマ波動観測と機械学習によるプラズマポーズ位置推定モデルの開発

#浅輪 優斗 [1)], 松田 昇也 [1)], 笠原 禎也 [1)], 三好 由純 [2)], 篠原 育 [3)]
([1] 金沢大, [2] 名大 ISEE, [3] 宇宙機構／宇宙研

An Empirical Plasmapause Model using Arase/PWE Data and Machine Learning

#Yuto Asawa[1)], Shoya Matsuda[1)], Yoshiya Kasahara[1)], Yoshizumi Miyoshi[2)], Iku Shinohara[3)]
([1]Kanazawa University, [2]Institute for Space-Earth Environement Research, Nagoya University, [3]Japan Aerospace Exploration Agency/Institute of Space and Astronautical Science

In the inner magnetosphere, the space around the Earth, there is a plasmasphere filled with low-temperature and high-density plasma. The plasmapause is a boundary that clearly separates the high-density plasmasphere from the low-density plasma trough region. Since the characteristics of plasma waves differ inside and outside the plasmasphere, accurate determination of the plasmapause location is important for understanding the dynamics of the inner magnetosphere. Plasmaspheric hiss is typically trapped inside the plasmasphere due to reflection at the plasmapause.

In this study, we focus on the characteristics of plasmaspheric hiss and propose a new method to identify the plasmapause location by considering the boundary of the plasmaspheric hiss. We develop a machine learning model to identify the plasmapause location based on the VGG16 model, which is a type of convolutional neural network. We use electric and magnetic field spectral data observed by the Onboard Frequency Analyzer (OFA) of the Plasma Wave Experiment (PWE) aboard the Arase satellite. We investigate plasmapause locations using approximately six years data and derived an empirical plasmapause model using the least squares method, with the Kp index, magnetic local time (MLT), and magnetic latitude (MLAT) as parameters. We successfully represent the typical plasmapause locations as functions of MLT and MLAT under the different geomagnetic conditions.

In this presentation, we introduce our approach for determining plasmapause location, discuss the statistical results of plasmapause locations derived from the long-term measurement data observed by the Arase satellite and the modeling method of plasmapause locations.

地球近傍の宇宙空間である内部磁気圏には、低温で高密度のプラズマで満たされたプラズマ圏が存在する。プラズマポーズとは高密度のプラズマ圏と低密度のプラズマトラフ領域を明確に分ける境界である。プラズマ波動の性質はプラズマ圏の内側と外側で異なるため、プラズマポーズ位置を正確に把握することは、内部磁気圏のダイナミクスを理解する上で重要である。プラズマ圏内では、プラズマ圏ヒスと呼ばれるプラズマ波動が存在することが知られ、典型的にはプラズマポーズを境界として反射する特性があることから、プラズマ圏内に閉じ込められたように観測される。

本研究ではプラズマ圏ヒスの特徴に着目し、プラズマ圏ヒスの観測境界をプラズマポーズとみなしてプラズマポーズ位置を同定する方法を提案する。あらせ衛星に搭載されたプラズマ波動・電場観測器（PWE）のサブシステムの 1 つである機上周波数分析器 (OFA) で観測された電磁界スペクトルデータを用い、畳み込みニューラルネットワークモデルの一つである VGG16 モデルによってプラズマポーズ位置を同定する方法を開発した。あらせ衛星の約 6 年間分の観測データを用いてプラズマポーズ位置を調べ、Kp 指数、磁気地方時、磁気緯度をパラメータとする経験的プラズマポーズモデルを最小二乗法によって導いた。これにより地磁気活動度の変化に伴いプラズマポーズが収縮する特徴や、磁気地方時毎の非対称性の特徴をモデルにより表現することができた。

本発表では、電磁界スペクトルデータを用いたプラズマポーズ位置の判定手法、プラズマポーズ位置の統計解析結果、プラズマポーズ位置のモデル化手法と各パラメータの対応関係について議論する。

R006-P10
ポスター１：11/24　PM1/PM2（13:15-18:15）

取下げ

R006-P11
ポスター 1 ：11/24　PM1/PM2 （13:15-18:15）

#酒井 啓伍 [1)], 加藤 雄人 [1)], 熊本 篤志 [1)]
[1 東北大・理・地球物理

Test Particle Simulations of Ion Acceleration by BBELF waves at Ionospheric Altitudes

#Keigo Sakai[1)], Yuto Katoh[1)], Atsushi Kumamoto[1)]
[1Department of Geophysics, Graduate School of Science, Tohoku University

The Earth's ionospheric ions flow out from the polar regions, particularly in the cusp region, through the heating process caused by low-frequency plasma waves. In this process, ions are heated perpendicular to a magnetic field line and then accelerated parallel to the field line by conserving the first adiabatic invariant [Yau and André, 1997]. Among the waves considered to contribute to this heating, the most common is the BroadBand Extremely Low Frequency (BBELF) wave, characterized by a smooth power spectrum that follows a power-law distribution from DC to the lower hybrid resonance frequency. Previous studies, such as those by Shen et al. (2020), have conducted simulations to investigate how BBELF waves heat ions. However, detailed heating mechanisms, including in the presence of magnetic field gradient, remain only partially understood.

In this research, test particle simulations were conducted to investigate how waves with BBELF spectra heat O+ and H+ ions in the plasma and magnetic field environment of the polar region. The altitude range was set between 400 and 2000 km, above the peak density of the ionosphere, and the three-dimensional equations of motion of ions were numerically solved using the fourth-order Runge-Kutta method. Ions outflowing from the cusp region undergo bulk upward motion at low altitudes due to bipolar diffusion resulting from electron precipitation and frictional heating by convection. As these ions ascend, they eventually reach wave-heating regions, where they gain additional energy. To examine how the velocity of bulk upflow affects wave heating, initial conditions were set such that the ions had an energy of 0-20 eV in the parallel direction and 0.2 eV in the perpendicular direction. The wave electric field was assumed to be purely perpendicular to the background magnetic field and was modeled by superimposing multiple waves with different frequencies, possessing a power spectrum that follows a power-law distribution to represent the BBELF spectrum.

We focus on the time scale of pitch angle changes due to the mirror force and the different responses of O+ and H+ ions to energy input by BBELF waves.

R006-P12
ポスター１：11/24　PM1/PM2（13:15-18:15）

あらせ衛星で観測されたイオン３次元速度分布関数の統計解析

#式守 隆人[1)], 篠原 育[2)], 浅村 和史[3)], 三好 由純[4)], 横田 勝一郎[5)], 笠原 慧[6)], 桂華 邦裕[7)], 堀 智昭[8)], 松岡 彩子[9)], 寺本 万里子[10)], 山本 和弘[11)]
([1] 東大, [2] 宇宙機構／宇宙研, [3] 宇宙研, [4] 名大 ISEE, [5] 大阪大, [6] 東京大学, [7] 東大・理, [8] 名大 ISEE, [9] 京都大学, [10] 九工大, [11] 名大 ISEE

Statistical survey of Ion 3D velocity distribution functions observed by the Arase satellite

#Takahito Shikimori[1)], Iku Shinohara[2)], Kazushi Asamura[3)], Yoshizumi Miyoshi[4)], Shoichiro Yokota[5)], Satoshi Kasahara[6)], Kunihiro Keika[7)], Tomoaki Hori[8)], Ayako Matsuoka[9)], Mariko Teramoto[10)], Kazuhiro Yamamoto[11)]
([1]The University of Tokyo, [2]Japan Aerospace Exploration Agency/Institute of Space and Astronautical Science, [3]Japan Aerospace Exploration Agency, [4]Institute for Space-Earth Environemental Research, Nagoya University, [5]Osaka University, [6]The University of Tokyo, [7]Department of Earth and Planetary Science, Graduate School of Science, The University of Tokyo, [8]Institute for Space-Earth Environmental Research, Nagoya University, [9]Graduate School of Science, Kyoto University, [10]Kyushu Institute of Technology, [11]Institute for Space-Earth Environmental Research (ISEE), Nagoya University

Recently, it has become evident that wave-particle interactions play a crucial role in the inner magnetosphere. However, due to the difficulty of measuring plasma in the radiation belts, how the ion velocity distributions in the inner magnetosphere evolve and become unstable for exciting plasma waves remains observationally unclear. This study aims to investigate how unstable ion velocity distributions that excite plasma waves are formed by examining the characteristics of three-dimensional ion velocity distributions in the inner magnetosphere. For example, it is known that ring/shell distributions can excite magnetosonic waves, and temperature anisotropy can excite EMIC waves. However, it remains unclear under what conditions and variations these unstable velocity distributions appear. Using data observed by the ion experiments, LEP-i (30 eV – 25 keV) and MEP-i (10 keV – 100 keV), onboard the Arase satellite, we investigate the ion velocity distributions in the inner magnetosphere. We have identified several characteristic velocity distributions during the investigation of temperature anisotropy. We will discuss the initial results of these specific distribution functions.

近年、内部磁気圏において波動ー粒子相互作用が重要な役割を担っていることが明らかになってきている。これまで、放射線帯領域におけるプラズマの計測が困難であったために、プラズマ波動観測の研究は多く行われてきたが、その波を励起させる原因であるプラズマ観測の比較的少く、内部磁気圏に存在するイオンの速度分布関数がどのように発展し、不安定するか、については観測的にはまだよくわかっていない。そこで、本研究では、プラズマ波動を励起するプラズマの不安定な速度分布がどのように形成されるかを調べることを目的に、内部磁気圏におけるイオンの 3 次元速度分布関数の特長を調べる。例えば、シェル分布やリング分布が磁気音波を励起することや、温度非等方分布が EMIC 波を励起させることが知られているが、こうした不安定な速度分布がどのようなバリエーションをもち、どのような条件の時に現れるのかについて、あらせ衛星搭載のイオン分析器 LEP-i (30eV～25keV)　と MEP-i (10keV~100keV) のデータを使用して、内部磁気圏におけるイオンがどのような速度分布をしているかを調べている。これまで、温度異方性に着目して速度分布を調べるなかで、いくつかの特徴的な速度分布が見つかった。本講演では、その結果を元に初期結果を報告する。

R006-P13
ポスター 1 ：11/24　PM1/PM2 （13:15-18:15）

#西田 結衣 [1)], 三好 由純 [1)], 浅村 和史 [2)], Kistler Lynn[1,3)], 篠原 育 [2)]
([1] 名大 ISEE, [2] 宇宙研, [3] ニューハンプシャー大学

Variations of He++ Ions in the inner magnetosphere at Different L-Shells: Arase LEP-i Observations

#Yui Nishida[1)], Yoshizumi Miyoshi[1)], Kazushi Asamura[2)], Lynn Kistler[1,3)], Iku Shinohara[2)]
([1]ISEE/Nagoya University, [2]Japan Aerospace Exploration Agency, [3]University of New Hampshire

He++ ions in the inner magnetosphere mainly originate from the solar wind. He++ in the inner magnetosphere can serve as a tracer of solar wind-origin ions. However, since there have been few satellites that continuously observed He++ ions in the inner magnetosphere, the detailed variations of these ions are still not well understood. An ion analyzer LEP-i onboard the Arase satellite has high mass resolution and can discriminate different ion groups, including He++. In this study, we analyzed Time-of-Flight (TOF) data from LEP-i with 10-min time resolution to investigate the long-term variations of He++ ions in the inner magnetosphere as well as their dependence on L-shell, which covers the declining phase of Solar Cycle 24 through the rising phase of Solar Cycle 25. Analyzing the observational data LEP-i/TOF, we found the L-shell dependence of He++ ion count. During the southward IMF, the He++ ion count at $L<4.5$ largely increase, suggesting that the enhanced convection causes transportation.

We will discuss how the geomagnetic and solar wind parametery dependencies of He++ vary with the L-shell.

R006-P14
ポスター 1 ：11/24　PM1/PM2 （13:15-18:15）

内部磁気圏における 1 keV 以下の低エネルギー O+ プラズマの空間分布

#能勢 正仁 [1)], 浅村 和史 [2)], 三好 由純 [3)], 松岡 彩子 [4)], 寺本 万里子 [5)], 熊本 篤志 [6)], 土屋 史紀 [6)], 笠原 禎也 [7)], 新堀 淳樹 [3)], 篠原 育 [2)]
([1] 名市大・DS 学部, [2] 宇宙研, [3] 名大 ISEE, [4] 京都大学, [5] 九工大, [6] 東北大・理・地球物理, [7] 金沢大

Spatial distribution of low-energy (<1 keV) O+ plasma in the inner magnetosphere

#Masahito Nose[1)], Kazushi Asamura[2)], Yoshizumi Miyoshi[3)], Ayako Matsuoka[4)], Mariko Teramoto[5)], Atsushi Kumamoto[6)], Fuminori Tsuchiya[6)], Yoshiya Kasahara[7)], Atsuki Shinbori[3)], Iku Shinohara[2)]
([1]School of Data Science, Nagoya City University, [2]Japan Aerospace Exploration Agency, [3]Institute for Space-Earth Environement Research, Nagoya University, [4]Graduate School of Science, Kyoto University, [5]Kyushu Institute of Technology, [6]Department of Geophysics, Graduate School of Science, Tohoku University, [7]Emerging Media Initiative, Kanazawa University

The ion composition of background plasma in the magnetosphere is a very important parameter, because it significantly alters the nature of various electromagnetic phenomena occurring there, such as solar wind-magnetospheric coupling, magnetic reconnection, Kelvin-Helmholtz instability, electromagnetic ion cyclotron wave, and Alfvén wave. O+ ions, which are 16 times heavier than H+ ions, have a significant impact on the plasma mass density of the background plasma; thus, it is necessary to investigate when, where, and how low-energy O+ ion fluxes change. Recent studies by Chappell [2008] and Lee and Angelopoulos [2014] reported presence of low-energy (10 eV–a few keV) ions, called “warm plasma cloak”, at L$>$6 from midnight to the dawn and morning sides. Further low-energy ($<$50 eV) plasma, consisting mainly of O+ ions, has also been reported to be localized around L=3–5 on the dawn to morning side [Nosé et al. 2018, 2020]. This lower-energy O+ plasma is called “oxygen torus”. However, since these studies were based on observations in the outer magnetosphere at L>6 or event analysis, we need to perform a statistical study to reveal characteristics of the warm plasma cloak and the oxygen torus in the inner magnetosphere.

In this study, we investigated the spatial distribution of low-energy O+ plasma in the inner magnetosphere using data from the Arase satellite collected over a 3.7-year period from April 2017 to December 2020. We statistically analyzed the omnidirectional ion flux of 50–300 eV O+ observed by the LEP-i instrument onboard the Arase satellite. Our findings include: (1) peaks in O+ ion flux are frequently observed near the plasmapause; (2) the average O+ flux is significantly higher in the region of 21–09 MLT and L=4–5; (3) the pitch angle distribution of the O+ flux is cigar-shaped. These statistical results of low-energy O+ plasma align well with the expected temporal evolution of field-aligned low-energy O+ ions (FALEO) that flow from the ionosphere to the inner magnetosphere during substorms, suggesting that FALEO is the source of the low-energy O+ plasma.

磁気圏において、背景プラズマのイオン組成は、太陽風-磁気圏結合、磁力線繋ぎ変え、ケルビン-ヘルムホルツ不安定性、電磁イオンサイクロトロン波動、電磁流体波動など、その場で生じる様々な電磁気的現象の性質を大きく変化させるため、非常に重要なパラメターである。特に O+ イオンは H+ に比べて 16 倍の質量を持ち、背景プラズマの質量密度に大きな影響を与えるため、その低エネルギーフラックスがいつ、どこで、どのように変化するかを調べる必要がある。近年の研究によれば、真夜中から朝側・午前側にかけて、L>6 の磁気圏には、Warm plasma cloak と呼ばれる比較的低エネルギー (10 eV–数 keV) のイオンが存在している [Chappell, 2008; Lee and Angelopoulos, 2014]。また、朝側から午前側の L=3–5 あたりには、Oxygen torus と呼ばれる、さらに低エネルギー (<50 eV) で主に O+ からなるプラズマが局在化していることも分かってきた [Nosé et al., 2018, 2020]。ただ、こうした研究は、L>6 の外部磁気圏での観測や、イベント解析に基づくものであるため、Warm plasma cloak および Oxygen torus の内部磁気圏での統計的な調査が望まれる。

そこで、この研究では、2017 年 4 月から 2020 年 12 月の約 3.7 年間にわたって蓄積されたあらせ衛星のデータを用いて、低エネルギー O+ イオンが卓越するプラズマが内部磁気圏のどこで観測されやすいかを調査した。あらせ衛星搭載の LEP-i が観測した 50 – 300 eV の O+ 全方向イオンフラックスについて統計解析を行った結果、(1) O+ イオンフラックスのピークはプラズマ圏のすぐ近くでよく観測される、(2) O+ フラックスの平均値は、21–09 MLT, L=4–5 で大きな値を持つ、(3) O+ フラックスのピッチ角分布は、磁力線方向に偏った cigar-type である、ことが分かった。こうした低エネルギー O+ プラズマの統計観測結果は、サブストーム時に電離圏から内部磁気圏へ流出し、磁力線に沿って動く低エネルギー O+ イオン (Field-aligned low-energy O+ ion, FALEO) の時間発展から予想される結果とよく一致しており、低エネルギー O+ プラズマの供給源が FALEO であることを示唆している。

R006-P15
ポスター 1 ：11/24　PM1/PM2 （13:15-18:15）

#山川 智嗣 [1)], 関 華奈子 [2)], 三好 由純 [3)], 中溝 葵 [4)], 山本 和弘 [5)]
([1] 名古屋大学 ISEE, [2] 東大理・地球惑星科学専攻, [3] 名大 ISEE, [4]NICT, [5] 名大 ISEE

Variation of ring current ions during magnetic storms on 22 July 2009 based on the GEMSIS magnetosphere-ionosphere coupled model

#Tomotsugu Yamakawa[1)], Kanako Seki[2)], Yoshizumi Miyoshi[3)], Aoi Nakamizo[4)], Kazuhiro Yamamoto[5)]
([1]Institute for Space-Earth Environmental Research, Nagoya University, [2]Department of Earth and Planetary Science, Graduate School of Science, University of Tokyo, [3]Institute for Space-Earth Environement Research, Nagoya University, [4]National Institute of Information and Communications Technology, [5]Institute for Space-Earth Environmental Research ([ISEE), Nagoya University

During magnetic storms, energetic particles are injected on the nightside and westward ring current is formed in the inner magnetosphere. Understanding the dynamics of ring current particles is essential for both the inner magnetosphere and ionosphere, since the ring current causes the variation of the magnetic field and transports the energy from the magnetosphere to the ionosphere through the field aligned current (FAC). The distribution of the ring current during magnetic storms depends on its transport, acceleration, and loss [e.g., Fok et al., 2001]. Recently, Yamakawa et al. [2023] reproduced the formation of ring current and plasmasphere during substorms based on the GEMSIS magnetosphere-ionosphere coupled model. However, this simulation was performed under simplified and static conditions for Region-1 FAC and ion injection on the nightside, which are not true for the inner magnetosphere. The purpose of this study is to investigate the variation of ring current particles during magnetic storms with the input of time-varying Region-1 FAC and ion injection, which are based on the observed solar wind parameters.

In this study, we focused on a magnetic storm on 22 July 2009 and compared simulation results with previous ring current model (CRCM) [Fok et al., 2001] and spacecraft observations. On 22 July 2009, the Dst dropped nearly -80 nT at 07:00 and 10:00 UT [Fok et al., 2010]. We investigated the variation of the inner magnetosphere based on the magnetosphere-ionosphere coupled model between GEMSIS-RC [Amano et al., 2011] and GEMSIS-POT [Nakamizo et al., 2012]. GEMSIS-RC model solves 5-D drift-kinetic equation for ion PSD and Maxwell equations self-consistently. GEMSIS-POT is a 2-D potential solver in the ionosphere. We included the loss term of ring current ions due to charge exchange. The coupled model enabled us to simulate the transport, acceleration, and loss of ring current ions and formation of the plasmasphere. The density and temperature of energetic ions at outer boundary on the nightside are based on the empirical model [Tsyganenko and Mukai, 2003] and the distribution of Region-1 FAC is given by the Weimer model [Weimer, 2001] as well as previous ring current model [Fok et al., 2010]. In this study, the latitudinal distribution of the FAC between lat = 65° and 80° was fitted with a Gaussian function at each MLT grid. By fitting the FAC, we obtained the smoothed distribution of Region-1 FAC, which was used for potential calculation in GEMSIS-POT. Simulation results suggest that intensity of FAC strongly depends on IMF Bz. The GEMSIS coupled model reproduced the shrink of the plasmapause on the nightside and formation of the plasmaspheric drainage plume on the dayside associated with the development of the ring current in the inner magnetosphere. In this event, THEMIS-D observed the inner magnetosphere and Pc5 ULF waves (3 mHz) were observed on the duskside from 09:00 UT to 10:00 UT. In this presentation, we will discuss the variation of ring current and the excitation of ULF waves by ring current ions by comparing with the results of CRCM model and THEMIS observations.

R006-P16
ポスター 1 ：11/24　PM1/PM2 （13:15-18:15）

大規模磁気嵐中の電離圏起源リングカレントイオンのエネルギースペクトル変動

#桂華 邦裕 [1)], 関 華奈子 [2)], 笠原 慧 [3)], 横田 勝一郎 [4)], 三好 由純 [5)], 堀 智昭 [6)], 篠原 育 [7)], 松岡 彩子 [8)]
([1] 東大理・地球惑星科学専攻, [2] 東大理・地球惑星科学専攻, [3] 東大理・地球惑星科学専攻, [4] 大阪大, [5] 名大 ISEE, [6] 名大 ISEE, [7] 宇宙機構／宇宙研, [8] 京都大学

Energy-spectral evolution of ring current ions of ionospheric origin during intense magnetic storms

#Kunihiro Keika[1)], Kanako Seki[2)], Satoshi Kasahara[3)], Shoichiro Yokota[4)], Yoshizumi Miyoshi[5)], Tomoaki Hori[6)], Iku Shinohara[7)], Ayako Matsuoka[8)]
([1]Department of Earth and Planetary Science, Graduate School of Science, The University of Tokyo, [2]Department of Earth and Planetary Science, Graduate School of Science, University of Tokyo, [3]Department of Earth and Planetary Science, Graduate School of Science, University of Tokyo, [4]Osaka University, [5]Institute for Space-Earth Environemental Research, Nagoya University, [6]Institute for Space-Earth Environmental Research, Nagoya University, [7]Japan Aerospace Exploration Agency/Institute of Space and Astronautical Science, [8]Graduate School of Science, Kyoto University

O+ ions significantly influence plasma pressure in Earth's inner magnetosphere during magnetic storms. This is primarily due to the increased supply of O+ from the ionosphere and the preferential energization of O+ in the magnetotail. Our previous study, which analyzed approximately 40 moderate magnetic storms, revealed the statistical characteristics of energetic ions that predominantly contribute to the ring current. The radial profile of the pressure-contributing first adiabatic invariant (mu_max) indicates that lower-mu O+ ions dominate at L <4, while higher-mu O+ ions dominate at L >6, compared to H+ ions. The dominance of lower-mu O+ in the lower L-shells highlights the importance of Earth-origin low-energy (<a few hundred eV) O+ ions in the plasma sheet, sometimes called warm cloak, for building up the inner ring current. Conversely, the contribution of higher-mu O+ in the higher L-shells emphasizes the vital role of preferential energization in enhancing the outer ring current.

The present study extends our analysis to intense storms with a minimum Dst smaller than -100 nT that occurred in 2023 and later. Additionally, we incorporate measurements of other ionospheric-origin ion species, such as He+ and O++, into our database. We utilize data from the Medium-Energy Particle experiments - ion mass analyzer (MEP-i), which measures ions with energies ranging from ˜10 to 180 keV/q and differentiates between ion species. We have confirmed that the MEP-i energy range can cover typical contributing mu values, from 0.05 to 0.5 keV/nT, across a wide range of radial distances. Our goal is to identify the relative contributions of the supply of low-mu O+ and the generation of high-mu O+ to the buildup of the ring current. Furthermore, we aim to examine how these contributions depend on the storm intensity.

R006-P17
ポスター 1 ：11/24　PM1/PM2 （13:15-18:15）

プロトンの等方的降りこみは磁気圏プロトンの等方的分布と対応するのか?

#今城 峻 [1)], 三好 由純 [2)], 笠原 慧 [3)], 横田 勝一郎 [4)], 松岡 彩子 [1)], 桂華 邦裕 [3)], 堀 智昭 [2)], 篠原 育 [5)], 塩川 和夫 [2)]
([1] 京大・地磁気センター, [2] 名大 ISEE, [3] 東京大学, [4] 大阪大, [5] 宇宙機構／宇宙研, [6] 名大 ISEE, [7] 宇宙機構／宇宙研, [8] 京都大学, [9] 東大・理, [10] 名大宇地研

Does isotropic proton precipitation correspond to an isotropic distribution of magnetospheric protons?

#Shun Imajo[1)], Yoshizumi Miyoshi[2)], Satoshi Kasahara[3)], Shoichiro Yokota[4)], Ayako Matsuoka[1)], Kunihiro Keika[3)], Tomoaki Hori[2)], Iku Shinohara[5)], Kazuo Shiokawa[2)]
([1]Graduate School of Science, Kyoto University, [2]Institute for Space-Earth Environement Research, Nagoya University, [3]The University of Tokyo, [4]Osaka University, [5]Japan Aerospace Exploration Agency/Institute of Space and Astronautical Science, [6]Institute for Space-Earth Environmental Research, Nagoya University, [7]Japan Aerospace Exploration Agency/Institute of Space and Astronautical Science, [8]Graduate School of Science, Kyoto University, [9]Department of Earth and Planetary Science, Graduate School of Science, The University of Tokyo, [10]Institute for Space-Earth Environmental Research, Nagoya University

It is not clear from previous low-altitude observations of energetic particle fluxes whether the magnetospheric plasma is also isotropic on the field line of isotropic precipitation. In this study, we have distinguished the low-latitude boundaries of the loss cone filling and the isotropic distribution of energetic protons in an energy range of 10-180 keV/q using meddle-altitude off-equatorial observations (3-5 Re geocentric distances) from the Arase satellite. The isotropic distribution boundary is defined by the ratio of proton fluxes at pitch angles of 0 – 45 deg and 45 – 90 deg for the northern hemisphere. The latitude of the isotropic distribution boundary has an energy dependence such that higher energy protons became isotropic at lower latitudes, implying isotropization of protons by the magnetic field line curvature. Around the isotropic distribution boundary, the downgoing loss cone (within 5 deg from the ambient magnetic field) was filled, while the corresponding upgoing loss cone was unfilled due to atmospheric loss. The low-latitude boundary of the loss cone filling was not always at the same latitude as the isotropic distribution boundary, and the loss cone filling tended to start at ˜0.1 – 0.4 deg lower latitude from the isotropic distribution boundary. This suggests that the magnetic field curvature required to isotropize the magnetospheric proton distribution is greater than that required for isotropic precipitation.

R006-P18
ポスター 1 ：11/24　PM1/PM2 （13:15-18:15）

#田中 良昌 [1,2,3], 小川 泰信 [1,2,3], 吹澤 瑞貴 [1], 門倉 昭 [1,2,3], 細川 敬祐 [4], 津田 卓雄 [4]
([1] 極地研, [2]ROIS-DS, [3] 総研大, [4] 電通大

Improvement in efficiency of auroral 3D analysis

#Yoshimasa Tanaka[1,2,3], Yasunobu Ogawa[1,2,3], Mizuki Fukizawa[1], Akira Kadokura[1,2,3], Keisuke Hosokawa[4], Takuo Tsuda[4]
([1]National Institute of Polar Research, [2]Research Organization of Information and Systems, Joint Support-Center for Data Science Research, [3]The Graduate University for Advanced Studies, SOKENDAI, [4]University of Electro-Communications

Generalized-auroral computed tomography (G-ACT) is a method to reconstruct three-dimensional (3D) distribution of auroral emission from multi-instrument data, such as monochromatic images taken at multi-point imager network and ionospheric electron density from radars. This method is expected to be useful for auroral 3D research by combining multiple auroral images with the electron density data obtained by the EISCAT_3D radar, which is planned to be operated in the near future. On the other hand, the 3D analysis of aurora has been limited to case studies because it takes a long time to process data and solve the inverse problem. In this study, therefore, we examine how to make this G-ACT calculation more efficient and faster. In particular, hyper-parameters associated with the weights between different data types and the regularization cannot be fixed because they depend on observation conditions such as auroral shape, position, and noise level, and also they are time consuming to calculate. Thus, hyper-parameters are pre-calculated under various conditions using model simulations and compiled into a database to automatically determine the appropriate hyper-parameters for the observed data. The simulations also enable us to estimate errors in the analysis results.

R006-P19
ポスター 1 ：11/24　PM1/PM2 （13:15-18:15）

#西野 真木 [1)], 宮下 幸長 [2,3)], 細川 敬祐 [4)], ツァイ レイ [5)], 長谷川 洋 [1)], 齋藤 義文 [1)]
([1] 宇宙航空研究開発機構宇宙科学研究所, [2]KASI, [3]KUST, [4] 電気通信大学, [5] フィンランド・オウル大学

High-latitude dayside aurora and transpolar arcs observed during low Alfvén Mach number solar wind

#Masaki N. Nishino[1)], Yukinaga Miyashita[2,3)], Keisuke Hosokawa[4)], Lei Cai[5)], Hiroshi Hasegawa[1)], Yoshifumi Saito[1)]
([1]Japan Aerospace Exploration Agency, Institute of Space and Astronautical Science, [2]Korea Astronomy and Space Science Institute, [3]Korean University of Science and Technology, [4]Graduate School of Informatics and Engineering, University of Electro-Communications, [5]Space Physics and Astronomy, University of Oulu, Finland

The high-latitude dayside aurora (HiLDA) and the transpolar arcs (TPAs) usually appear in the polar cap under the northward interplanetary magnetic field (IMF). Previous statistical studies showed that the strength of the solar wind magnetic field or the magnetic energy does not affect the occurrence of TPAs. On the other hand, it has not been studied whether the TPAs and HiLDAs appear when the solar wind density is very low, and thus, its Alfvén Mach number (M_A) is very low (~2 – 3). Here, based on multi-spacecraft observations, we show a case of HiLDA and TPAs during very low M_A solar wind that followed multiple TPAs during high-density solar wind. The brightness of HiLDA was typical (1 – 10 kR) even under the low M_A solar wind condition. In contrast, the TPA under low M_A solar wind was typically single and faint, while multiple TPAs with complicated structures appeared in some periods. The magnetopause locations encountered by ARTEMIS P1 and P2 in the mid-distant magnetotail suggest a strong distortion of the magnetotail that might be related to the shape of the TPAs.

R006-P20
ポスター 1 ：11/24　PM1/PM2 （13:15-18:15）

DMSP 衛星観測データを用いた表面帯電を引き起こすプラズマ環境の調査

#升野 颯人 [1)], 寺本 万里子 [1)], 荒木 大智 [1)], 北村 健太郎 [1)], 奥村 哲平 [2)], 古賀 清一 [2)], 岡本 博之 [2)], 谷嶋 信貴 [2)]
([1] 九工大, [2]JAXA

Investigation of the Plasma Environment Responsible for Spacecraft Surface Charging Using DMSP Satellite Observations

#Hayato Masuno[1)], Mariko Teramoto[1)], Daichi Araki[1)], Kentarou Kitamura[1)], Teppei Okumura[2)], Kiyokazu Koga[2)], Hiroyuki Okamoto[2)], Nobutaka Tanishima[2)]
([1]Kyushu Institute of Technology, [2]Japan Aerospace Exploration Agency

Surface charging on low Earth orbit (LEO) satellites, the subject of this study, is induced by electrons with energies ranging from a few keV to several tens of keV. This research focuses on auroral activity because the plasma responsible for surface charging is generated during the auroral process, Clarifying the relationship between auroral activity and satellite surface charging will allow more accurate predictions of surface charging. This study aims to elucidate the plasma environmental conditions that lead to surface charging in LEO, particularly during plasma precipitation in polar regions. The data used in this study were obtained from the plasma sensor (Special Sensor for Precipitating Particles: SSJ) onboard the polar-orbiting DMSP F-16 satellite during Solar Cycle 24 (2009-2019). The SSJ observed the energy flux data of precipitating ions and electrons in the range of 30 eV to 30 keV. During surface charging events, the SSJ often detected an elevated ion flux corresponding to the charging potential of the satellite (e.g., Anderson, 2012). Therefore, we identified events in which a particular energy channel among the 18 energy channels (30 eV to 30 keV) detected significantly elevated ion flux. In addition, because surface charging is induced by electrons with energies greater than a few keV, we also examined the conditions of electron energy flux that cause charging. The plasma environmental conditions examined were: (1) the threshold for the sudden increase in ion flux, (2) the electron energy flux and energy during charging events, and (3) the duration of ion lines. The analysis revealed the following conditions for the plasma environment during surface charging: (1) the peak value of energy flux in the ion energy channel showing a sudden increase exceeded 1 × 10^7 [eV cm^-2 s^-1 sr^-1 eV^-1], (2) the electron energy flux exceeded 1 × 10^8 [eV cm^-2 s^-1 sr^-1 eV^-1] at energies above 14 keV, and (3) both (1) and (2) persisted for at least 2 seconds. Among the events detected under these conditions, only those where continuous ion lines corresponding to the charging potential were observed were identified. As a result, of the 2,435 events detected, ion lines were confirmed in 868 cases. The fact that 76% of the detected charging events occurred on the duskside (18:00-24:00 MLT) suggests that satellite charging is induced by discrete auroras. In addition, as the charging potential increased, the location of the charging event sifted from the dusk side to around midnight (24:00 MLT). However, charging potentials above -300V accounted for only about 5.5%, indicating that high-potential charging events were relatively rare. In this presentation, we will report on the plasma conditions that lead to surface charging, as revealed by this study.

本研究での研究対象である低軌道を飛行する人工衛星の表面帯電は、数 keV〜数十 keV 程度のエネルギーを持つ電子により引き起こされる。表面帯電の要因となるプラズマは、オーロラ発生の過程で生成されるため、本研究では焦点をオーロラに当てている。オーロラ活動と衛星の表面帯電の関係性を明確にできれば、表面帯電の正確な予測が可能になる。

そこで本研究は、極地でのプラズマ降下によって引き起こされる表面帯電の予測に向け、低高度軌道での表面帯電が引き起こされる際のプラズマ環境の条件を明らかにすることを目的とする。

使用したデータは、太陽活動第 24 周期の 2009 年から 2019 年の 11 年間に極軌道衛星である DMSP 衛星 F-16 号機に搭載されたプラズマ計測器（Special Sensor for Precipitating Particles：SSJ）が観測した 30 eV〜30 keV の降下イオン・電子のエネルギーフラックスデータを使用した。表面帯電時には、SSJ が衛星帯電電位に対応するエネルギーのイオンフラックスを多く観測する (e.g. Anderson, 2012)。そのため、30 eV〜30 keV の 18 エネルギーチャンネルのうち、ある特定のエネルギーチャンネルのみにイオンフラックスが極端に多い事象を検出した。また、表面帯電は、数 keV 以上のエネルギーを持つ電子により引き起こされるため、帯電を引き起こす電子エネルギーフラックスの条件についても検討した。

検討したプラズマ環境の条件は (1) イオンの急激な増加の閾値、(2) 帯電時の電子のエネルギーフラックスとエネルギー、(3) イオンラインの継続時間、の 3 つである。検討した結果、帯電時のプラズマ環境の条件は、それぞれ (1) 急激な降り込みが見られたイオンのエネルギーチャンネルで、エネルギーフラックスのピークの値が 1 × 10^7 [eV cm^-2 s^-1 sr^-1 eV^-1] 以上 (2) 14 keV 以上の電子のエネルギーフラックスが 1 × 10^8 [eV cm^-2 s^-1 sr^-1 eV^-1] 以上 (3) 少なくとも (1)、(2) が 2 秒以上継続、と定めた。この帯電条件で検出したイベントのうち、帯電時に起こるとされる、帯電電位に対応するイオンのフラックスの増加が継続しているイオンラインが確認できるもののみを検出した。結果、検出したイベント 2435 例の内、実際にイオンラインが確認されるものは、868 例となった。上記の条件で検出された帯電イベントの 76% は日暮れ側 (18 時〜24 時磁気地方時) に存在したことから、本研究の結果はディスクリートオーロラにより衛星帯電が引き起こされていることを示唆している。また、帯電イベントの発生場所は、帯電電位が上がるほど、日暮れ側から真夜中前後 (24 時磁気地方時) に遷移した。しかし、-300V 以下の帯電は 5.5% ほどであり、高電位での帯電はそれほど見られなかった。

本講演では本研究によって明らかにした表面帯電を引き起こすプラズマの条件について報告する。

R006-P21
ポスター 1 ：11/24　PM1/PM2 （13:15-18:15）

DMSP 衛星とあらせ衛星の観測データの解析による衛星表面帯電とコーラス波動の関係の調査

#荒木 大智 [1)], 寺本 万里子 [1)], 升野 颯人 [1)], 笠原 禎也 [2)], 熊本 篤志 [3)], 松岡 彩子 [4)], 松田 昇也 [2)], 堀 智昭 [5)], 新堀 淳樹 [5)], 山本 和弘 [5)], 三好 由純 [5)], 篠原 育 [6)], 奥村 哲平 [7)], 古賀 清一 [7)], 岡本 博之 [7)], 谷嶋 信貴 [7)], 北村 健太郎 [1)], 土屋 史紀 [3)]
([1] 九工大, [2] 金沢大, [3] 東北大, [4] 京都大, [5] 名古屋大, [6] 宇宙機構／宇宙研, [7]JAXA

Investigation of the relationship between satellite surface charging and chorus waves using DMSP and Arase satellite data

#Daichi Araki[1)], Mariko Teramoto[1)], Hayato Masuno[1)], Yoshiya Kasahara[2)], Atsushi Kumamoto[3)], Ayako Matsuoka[4)], Shoya Matsuda[2)], Tomoaki Hori[5)], Atsuki Shinbori[5)], Kazuhiro Yamamoto[5)], Yoshizumi Miyoshi[5)], Iku Shinohara[6)], Teppei Okumura[7)], Kiyokazu Koga[7)], Hiroyuki Okamoto[7)], Nobutaka Tanishima[7)], Kentarou Kitamura[1)], Fuminori Tsuchiya[3)]
([1]Kyushu Institute of Technology, [2]Kanazawa University, [3]Tohoku University, [4]Kyoto University, [5]Nagoya University, [6]Japan Aerospace Exploration Agency/Institute of Space and Astronautical Science, [7]Japan Aerospace Exploration Agency

The presence of a surrounding plasma environment can result in surface charging for satellites in space. Surface charging and discharges represent typical examples of satellite malfunctions induced by the space environment. The avoidance of risks associated with charging and discharges represents a crucial aspect of ensuring the safe operation of satellites. It is therefore anticipated that the prediction of satellite surface charging will become a reality in the near future. The present study investigates the relationship between satellite surface charging and chorus waves, which are postulated to be a factor in increasing the number of energetic electrons that cause surface charging, with a view to achieving the aforementioned prediction.

Chorus waves are a type of naturally occurring plasma wave in space. Chorus waves precipitate energetic electrons along the magnetic field lines through pitch angle scattering. In contrast, satellite surface charging can occur when the flux of high-energy electrons in the range of several keV to tens of keV increases in the plasma environment surrounding the satellite. Consequently, one potential scenario is that surface charging occurs when a satellite passes through regions where high-energy electrons are precipitated along magnetic field lines due to chorus waves.

In this study, we used plasma observation data from the DMSP (Defense Meteorological Satellite Program) F16 satellite to identify surface charging events on low-Earth orbit satellites. Furthermore, we analyzed data from the Arase satellite to examine the potential role of plasma waves in surface charging. The data from these satellites were statistically analyzed over the period from March 2017, when nominal observations by the Arase satellite began, through December 2022.

To identify surface charging events, we utilized the event list for 2017-2022 identified by the following criteria, which is applied in Meng et al. [2017], : 1) a distinct ion line structure is visible in the ion spectrogram, 2) the flux of high-energy electrons (above 14 keV) exceeds 10^8 electrons cm^(-2) s^(-1) sr^(-1), 3) the satellite's charging potential is between -2040 V and -95 V, and 4) the duration of the surface charging event was 3 seconds or longer. Arase-DMSP conjunctions were defined as instances where the two satellites were on the same magnetic field line. Surface charging events that occurred concurrently with conjunctions were designated as surface charging-conjunction events. Additionally, we checked whether the Arase satellite observed chorus waves during these events.

The analysis revealed that 21 of the 24 detected surface charging-conjunction event exhibited valid data. Among these, 8 events were identified in which the Arase satellite observed chorus waves. The locations of the Arase satellite during these observations were near the magnetic equator, in the morning sector (MLT around 1-7 hours), and 4 - 6 RE. This region is consistent with generation regions of the chorus waves. Furthermore, for 2 of the 8 events where electron density data were available, we estimated the energy of electrons resonating with chorus waves from the magnetic equator to the satellite's position. The estimated energies were 7.41-81.20 keV and 3.28-10.29 keV, respectively. We also confirmed that the electron flux observed by the electrostatic analyzer (SSJ5) onboard the DMSP F16 satellite in the corresponding energy range increased. These findings indicate that electrons in the energy range responsible for surface charging precipitate into the Earth's atmosphere due to chorus waves. This suggests that surface charging may be caused by electrons originating from precipitation induced by chorus waves.

宇宙空間を飛行する人工衛星は、周辺のプラズマ環境に応じて表面帯電が起こることがある。表面帯電と、表面帯電によって引き起こされる放電は、宇宙環境が原因となる衛星障害の代表例である。人工衛星を安全に運用する上で、帯電・放電によるリスクとそれを未然に防ぐことは重要な課題であり、将来的な衛星表面帯電予測の実現が期待される。そこで、本研究では予測の実現に向けて、衛星表面帯電とそれを引き起こす高エネルギー電子を増加させる要因として考えられるコーラス波動の関係を調査した。

コーラス波動は、宇宙空間で自然発生するプラズマ波動の一種である。コーラス波動は、ピッチ角散乱によって磁力線沿いに高エネルギー電子を降り込ませる。一方で、衛星の表面帯電は、衛星周辺のプラズマ環境において数 keV～数十 keV の高エネルギー電子のフラックスが増加することで起こることがある。そのため、コーラス波動によって高エネルギー電子が磁力線沿いに降り込むとき、その降り込み先を衛星が通過することで表面帯電が起こるシナリオが考えられ

る。

本研究では、低軌道衛星の表面帯電イベントを検出するために、DMSP(Defense Meteorological Satellite Program: 防衛気象衛星計画) 衛星 F16 のプラズマ観測データを用いた。加えて、表面帯電を引き起こすと考えられるプラズマ波動を解析するために、あらせ衛星の観測データを用いた。それぞれの衛星の観測データについて、あらせ衛星の定常観測が開始した 2017 年の 3 月以降、2022 年 12 月までを統計的に解析した。

表面帯電イベントについて、Meng et al. [2017] で定義された条件のもと、2017〜2022 年のイベントを検出した。検出条件は、1) イオンスペクトログラムのイオンラインの構造を確認できること、2)14 keV 以上の高エネルギー電子のフラックスが 10^8 electrons cm^(-2) s^(-1) sr^(-1) より大きいこと、3) 衛星の帯電電位が-2040 V ~-95 V であること、4) 表面帯電イベントの継続時間が 3 秒以上であること、をすべて満たすとき表面帯電イベントとして検出した。２つの衛星が同一磁力線上にある conjunction を定義し、conjunction イベントを検出した。表面帯電と conjunction が同時発生しているイベントを表面帯電-conjunction として検出し、このとき、あらせ衛星がプラズマ波動を観測しているかどうかを確認した。

解析の結果、検出された表面帯電-conjunction イベント全 24 回のうち、有効データの揃った 21 回のイベントについて、あらせ衛星がコーラス波動を観測しているイベントを 8 回検出することができた。このとき、あらせ衛星の観測位置は、磁気赤道面付近、朝側領域（MLT が 1~7 時付近）、地球中心から地球半径の 4〜6 倍の距離であり、過去の研究によって確かめられたコーラス波動の発生領域と一致していることを確認できた。また、コーラス波動を観測している８例のイベントのうち、電子密度のデータのある２例のイベントにおいて、磁気赤道面〜衛星位置までのコーラス波動と共鳴する電子が持つエネルギーを推定したところ、それぞれ 7.41〜81.20keV、3.28〜10.29keV となった。また、これらの電子の降り込む DMSP 衛星 F16 に搭載された静電分析器（SSJ5）において、対応するエネルギー帯の電子のフラックスが増加していることを確認できた。以上より、表面帯電を引き起こすエネルギー帯の電子がコーラス波動によって地球大気へと降り込んでおり、コーラス波動による降下電子由来の表面帯電の発生を示唆している。

R006-P22
ポスター 1 ：11/24　PM1/PM2 （13:15-18:15）

高時空間分解能光学観測を用いたオーロラ微細構造に関する研究

#Winn Wandal[1)], 細川 敬祐 [1)], 大山 伸一郎 [2)], 三好 由純 [2)], 小川 泰信 [3)], 田中 良昌 [3)]
([1] 電通大, [2] 名大 ISEE, [3] 極地研

Study of Auroral Fine Scale Structure Using High Spatio-Temporal Resolution Optical Observations

#Wandal Winn[1)], Keisuke Hosokawa[1)], Shin ichiro Oyama[2)], Yoshizumi Miyoshi[2)], Yasunobu Ogawa[3)], Yoshimasa Tanaka[3)]
([1]University of Electro-Communications, [2]Institute for Space-Earth Environement Research, Nagoya University, [3]National Institute of Polar Research

Auroras are classified into two broad categories: the discrete aurora, which has a distinct arc-like shape, and the diffuse aurora, which has an indistinct patchy shape. Most of the diffuse auroras are known to show a quasi-periodic luminosity modulation called pulsating aurora (PsA). Recent observations with high temporal resolution have been advancing our understanding of the physical mechanisms causing PsA. The main driver of PsA are chorus waves (Nishimura et al., 2010), a type of electromagnetic wave which is generated near the equatorial magnetosphere. As electrons in the magnetosphere travel along geomagnetic field lines, they can resonate with chorus waves, giving them enough energy to reach Earth's atmosphere and generate PsA. Thus, patches of PsA in the Earth's atmosphere have a one-to-one spatial and temporal correlation with patches of chorus waves in the magnetosphere. However, the origin or formation process of these complex spatial structures remain unclear, which is mainly due to the insufficient spatial resolution of conventional fisheye lens-based all-sky camera systems used for auroral imaging.

To solve this problem, we have recently set up a high resolution optical system in Skibotn, Norway (a village in the northern Scandinavian Peninsula at 69° 23′ 27″ N 20° 16′ 02″ E) to resolve the fine-scale spatial structure of PsA in greater detail. This system is comprised of a Hamamatsu Photonics C15550-20UP (ORCA-Quest qCMOS camera) with a narrow field-of-view F1.4 lens (Kowa LM8HC). The C15550-20UP camera has spatial resolution of 4096 × 2304 pixels, which will allow us to resolve sub-kilometer scale structures of auroras near the zenith. We put a wide-band optical filter (BG3 glass filter) on top of the lens to remove contributions of slower aurora emissions, such as the ones at 557.7 nm and 630.0 nm, and capture sub-second fast modulations of aurora. Since the installation in October 2023, the camera has been routinely operated at a rate of 20 frames-per-second (FPS), which is accurately synchronized by GNSS. We have also begun initial analyses of the images transferred from Norway. We utilized the star constellations in the background of the images to determine the camera's field of view in the sky, a process called astrometric calibration. Combining this information with the time of the image and the camera's geographical coordinates, we were able to map the images from the camera onto the geographic coordinate system at a 100 km altitude. Upon inspecting the images from the camera, we identified a 10 minute segment for further investigation. At 00:53 UT on Nov 21, 2023, a PsA patch emerges and lasts approximately 15 seconds, corresponding to a single ON phase of the main pulsation. During this ON phase, while the center of the patch remains stable, the edges show sub-second modulations in brightness. Upon generating a keogram, the PsA patch appears to modulate at roughly 3 Hz. Further investigation may reveal how general this behavior is to all PsA patches, and reveal the composition of the chorus wave patches in the magnetosphere which cause them. In the presentation we will introduce the above-mentioned procedures of astrometric calibration, along with initial findings in the PsA imagery from the arctic.

R006-P23
ポスター 1 ：11/24　PM1/PM2 （13:15-18:15）

#野田 大晟 [1)], 三好 由純 [1)], 細川 敬祐 [2)], 浅村 和史 [3)], 坂野井 健 [4)], Marc Lessard[5)], Alison Jaynes[6)], Mike Shumko[7)], Alexa Halford[8)], 滑川 拓 [9)], 三谷 烈史 [3)], 能勢 正仁 [10)], Geoff McHarg[11)], Vincent Ledvina[12)], Don Hampton[12)]
([1] 名大 ISEE, ([2] 電通大, ([3] 宇宙研, ([4] 東北大・理・PPARC, ([5] ニューハンプシャー大学, ([6] アイオワ大学, ([7] ジョンズ・ホプキンス大学応用物理研究所, ([8]NASA ゴダード宇宙飛行センター, ([9]NICT, ([10] 名市大・DS 学部, ([11] 空軍士官学校, ([12] アラスカ大学フェアバンクス校

Over-darking of diffuse/pulsating aurora: LAMP sounding rocket observation

#Taisei Noda[1)], Yoshizumi Miyoshi[1)], Keisuke Hosokawa[2)], Kazushi Asamura[3)], Takeshi Sakanoi[4)], Lessard Marc[5)], Jaynes Alison[6)], Shumko Mike[7)], Halford Alexa[8)], Taku Namekawa[9)], Takefumi Mitani[3)], Masahito Nose[10)], McHarg Geoff[11)], Ledvina Vincent[12)], Hampton Don[12)]
([1]Institute for Space-Earth Environmental Research, Nagoya University, ([2]University of Electro-Communications, ([3]Institute of Space and Astronautical Science, JAXA, Sagamihara, Japan, ([4]Planetary Plasma and Atmospheric Research Center, Graduate School of Science, Tohoku University, ([5]University of New Hampshire, Durham, US, ([6]University of Iowa, Iowa, US, ([7]Applied Physics Laboratory, Johns Hopkins University, Maryland, US, ([8]Goddard Space Flight Center, NASA, Maryland, US, ([9]The National Institute of Information and Communications Technology, ([10]School of Data Science, Nagoya City University, ([11]The United States Air Force Academy, Colorado, US, ([12]University of Alaska, Fairbanks, US

Pulsating aurora is a kind of diffuse aurora that modulate their luminosity from a few seconds to 10 seconds. The over-darking, in which the brightness is decreased by several tens of percent against background, has been observed just after the luminosity enhancement during the pulsation “ON” time. There have been various reports on over-darkening after pulsating auroras, but details about the over-darking have not yet been revealed. We have studied the over-darking phenomena associated with the pulsating aurora using the observation data of electron observations (EPLAS) and optical observations (AIC) onboard the LAMP sounding-rocket experiments, which was launched on March 5, 2022 at Poker Flat Research Range. EPLAS can observe electrons in the 10eV-20keV energy range, and AIC can observe optical emissions in the 667-680nm and 844-848nm wavelength ranges. An event of the over-darking is observed during the flight operation of the LAMP sounding rocket. The optical aurora emission at the footprint of the LAMP rocket observed by AIC decreased from 3,000 Rayleigh to 1,300 Rayleigh, and the downward energy flux observed by EPLAS decreased by ˜50%. The energy flux significantly decreases above 5 keV, especially the flux at 6.6 keV decreased ˜40%. Considering the resonance condition with whistler mode chorus waves, the attenuation of precipitation at high-energy electros is caused by decrease of the pitch angle scattering with the chorus waves. In the presentation, we will show detail variations of energy spectrum and pitch angle distribution of precipitating electrons during the over-darking and discuss possible mechanisms.

R006-P24
ポスター 1 ：11/24　PM1/PM2 （13:15-18:15）

#伊藤 ゆり [1,2)], 小川 泰信 [1,2)], 田中 良昌 [1,2,3)], 門倉 昭 [2,3)], 吹澤 瑞貴 [2)], 細川 敬祐 [4)], 三好 由純 [5)], 堀 智昭 [5)], 笠原 禎也 [6)], 松田 昇也 [6)], 篠原 育 [7)]
([1 総研大, ([2 極地研, ([3ROIS-DS, ([4 電通大, ([5 名大 ISEE, ([6 金沢大, ([7 宇宙機構／宇宙研

Statistical analysis of pulsating auroras and high-latitude propagation of chorus waves

#Yuri Ito[1,2)], Yasunobu Ogawa[1,2)], Yoshimasa Tanaka[1,2,3)], Akira Kadokura[2,3)], Mizuki Fukizawa[2)], Keisuke Hosokawa[4)], Yoshizumi Miyoshi[5)], Tomoaki Hori[5)], Yoshiya Kasahara[6)], Shoya Matsuda[6)], Iku Shinohara[7)]
([1The Graduate University for Advanced Studies, ([2National Institute of Polar Research, ([3Research Organization of Information and Systems, Joint Support-Center for Data Science Research, ([4University of Electro-Communications, ([5Institute for Space-Earth Environmental Research, Nagoya University, ([6Kanazawa University, ([7Japan Aerospace Exploration Agency/Institute of Space and Astronautical Science

Pulsating auroras (PsA) are considered to be caused by precipitation of a few to a few tens of keV electrons. The energetic electrons are scattered by lower-band chorus (LBC) waves, which are one of the whistler-mode waves in the magnetosphere, through the cyclotron resonance. Past study has suggested that, during PsA, relativistic electrons causing ozone depletion simultaneously precipitate into the ionosphere [Miyoshi et al., 2021]. Observational studies also suggested that, relativistic/sub-relativistic electrons precipitate to lower altitudes when PsA has a patchy structure and that PsA patches tend to develop towards the morning side [Tesema et al., 2020; 2022]. Our previous study proposed that the relationship between the PsA shape and the energy of precipitating electrons is controlled by presence of magnetospheric density ducts and associated high-latitude propagation of chorus waves [Ito et al., 2024]. However, the background mechanism of how density ducts are generated, and the universality of the proposed model have not been clarified yet.

In order to understand the detailed development process of density ducts and quantitatively evaluate the universality, we are in the progress of a statistical analysis of PsA patches simultaneously observed by the multipoint optical instruments in the northern Europe and the Arase satellite. The survey period is from March 2017 to March 2024. We count the appearance of patches at the footprint of Arase as a single sample and investigate the spatiotemporal development of PsA patches, propagation latitudes of chorus waves. In this presentation, we will report the details of the analysis method, the observed data, and the initial results and discuss the statistical relationship between the PsA morphology, magnetospheric density ducts and high-latitude propagation of chorus waves.

R006-P25
ポスター 1 ：11/24　PM1/PM2 （13:15-18:15）

#村瀬 清華 [1)], 西山 尚典 [1)], 吹澤 瑞貴 [1)], 藤井 良一 [1)]
([1] 極地研

Statistical analysis of internal modulations in pulsating aurorae with a large dataset of a high-speed imager

#Kiyoka Murase[1)], Takanori Nishiyama[1)], Mizuki Fukizawa[1)], Fujii Ryoichi[1)]
([1]National Institute of Polar Research

Pulsating aurorae are a major type of diffuse aurora, characterized by quasi-periodic pulsations in brightness ranging from a few seconds to several tens of seconds. They sometimes coexist with shorter-period variations of a few Hz, called ”internal modulations.” The hierarchy of these periods has observationally shown to correspond to the intensity variations in chorus wave which is responsible for electron precipitation causing pulsating aurorae. However, the number of reports on internal modulation is limited due to the high sampling rates (>10 Hz) required for optical observations to investigate internal modulation. The factors controlling the presence or absence of internal modulation has not been well understood.

This study aims to statistically investigate how the periodicity of chorus wave activity, which determines the presence of internal modulation, is controlled in the magnetosphere, and how this results in differences in characteristics such as the morphology of the pulsating aurora and the energy of the precipitating electrons. This has been made possible by the recently published dataset of 10-Hz sampling images obtained by the High-speed Auroral Imaging (HAI) system at Syowa Station. We first tried a frequency filtering to determine the timings and regions with internal modulations for an example data. It is confirmed that a simple way of subtracting running average from the original auroral intensity shows enough performance to detect the modulation. This method of detecting internal modulation is applied to a three-year data set from 2017 to provide a statistical view of the internal modulation, with a particular focus on its relationship to auroral morphology.

R006-P26
ポスター 1 ：11/24　PM1/PM2 （13:15-18:15）

内部磁気圏で観測された昼側降下電子の統計的解析

#髙原 璃乃[1)], 篠原 育[2)], 笠原 慧[3)], 浅村 和史[4)], 横田 勝一郎[5)], 桂華 邦裕[6)], 風間 洋一[7)], Wang Shiang Yu[7)], Tam Sunny Wing-Yee[8)], 田 采祐[9)], 堀 智昭[10)], 松岡 彩子[11)], 寺本 万里子[12)], 山本 和弘[13)], 笠原 禎也[14)], 松田 昇也[15)], 熊本 篤志[16)], 新堀 淳樹[17)], 土屋 史紀[18)], 三好 由純[19)]
([1] 東大, [2] 宇宙機構／宇宙研, [3] 東京大学, [4] 宇宙研, [5] 大阪大, [6] 東大・理, [7]ASIAA, [8]NCKU, [9] 名大 ISEE 研, [10] 名大 ISEE, [11] 京都大学, [12] 九工大, [13] 名大 ISEE, [14] 金沢大, [15] 金沢大学, [16] 東北大・理・地球物理, [17] 名古屋大学宇宙地球環境研究所, [18] 東北大・理・惑星プラズマ大気, [19] 名大 ISEE

Statistical Survey of Dayside Energetic Electron Precipitation Observed In-Situ in the Inner Magnetosphere

#Rino Takahara[1)], Iku Shinohara[2)], Satoshi Kasahara[3)], Kazushi Asamura[4)], Shoichiro Yokota[5)], Kunihiro Keika[6)], Yoichi Kazama[7)], Shiang Yu Wang[7)], Sunny Wing-Yee Tam[8)], ChaeWoo Jun[9)], Tomoaki Hori[10)], Ayako Matsuoka[11)], Mariko Teramoto[12)], Kazuhiro Yamamoto[13)], Yoshiya Kasahara[14)], Shoya Matsuda[15)], Atsushi Kumamoto[16)], Atsuki Shinbori[17)], Fuminori Tsuchiya[18)], Yoshizumi Miyoshi[19)]
([1]The University of Tokyo, [2]Japan Aerospace Exploration Agency/Institute of Space and Astronautical Science, [3]The University of Tokyo, [4]Japan Aerospace Exploration Agency, [5]Osaka University, [6]Department of Earth and Planetary Science, Graduate School of Science, The University of Tokyo, [7]Academia Sinica Institute of Astronomy and Astrophysics, [8]Institute of Space and Plasma Sciences, National Cheng Kung University, [9]Institute for Space-Earth Environmental Research, [10]Institute for Space-Earth Environmental Research, Nagoya University, [11]Graduate School of Science, Kyoto University, [12]Kyushu Institute of Technology, [13]Institute for Space-Earth Environmental Research (ISEE), Nagoya University, [14]Emerging Media Initiative, Kanazawa University, [15]Kanazawa University, [16]Department of Geophysics, Graduate School of Science, Tohoku University, [17]Institute for Space-Earth Environmental Research, Nagoya University, [18]Planetary Plasma and Atmospheric Research Center, Graduate School of Science, Tohoku University, [19]Institute for Space-Earth Environement Research, Nagoya University

Energetic (hundreds of eV – tens of keV) electrons originating from the magnetosphere precipitate into the Earth's upper atmosphere and modify ionospheric conditions, consequently influencing the magnetospheric convection pattern. Pitch angle (PA) scattering by plasma waves plays an important role in magnetospheric electron precipitation. The quantitative evaluation of precipitating electrons by wave-particle interactions is therefore crucial for understanding the effects of magnetospheric electron precipitation on the magnetosphere-ionosphere coupling system.

Since the loss cone angle in the magnetosphere is only a few degrees, in-situ observation of precipitating electrons in the inner magnetosphere was enabled recently by the energetic electron analyzers with high pitch-angular resolution onboard the Arase satellite. Kasahara et al. (2018) provided for the first time a direct observational evidence of PA scattering by showing a close correlation between the appearance of whistler mode chorus waves and the modulation of electron fluxes inside the loss cone (PA<2°) when pulsating auroras were observed. Based on these results, we carry out a statistical survey of electrons inside the loss cone with energies of 67 eV – 88 keV from March 2017 to March 2022 observed in-situ by the medium- and low-energy electron analyzers (MEP-e and LEP-e) onboard the Arase satellite to understand the contribution of wave-particle interactions to electron precipitation.

We found out the occurrence probability of electron precipitation is high from the nightside to the dawnside around L ~6, which is consistent with the region where chorus waves are frequently detected. While chorus waves around the magnetic equator is suggested as the main contributor of electron precipitation around MLT ~22 – 6, the effects of higher latitude propagating chorus waves and dayside chorus waves generated at higher latitudes are implied from the dawnside to the dayside (MLT >3). In this study, we discuss the contribution of high-latitude chorus waves based on the difference in the occurrence frequency and the generation region of electron precipitation at different latitudes.

磁気圏を起源とする数百 eV – 数十 keV の電子が地球上層大気へ降下すると、電離圏の電子密度や電導度が変動し、磁気圏の対流パターンが変化する。磁気圏の電子降下は、主にプラズマ波動との共鳴によるピッチ角（PA）散乱が引き起こしており、波動粒子間相互作用によって生成された降下電子の定量的評価は、磁気圏電子降下による磁気圏-電離圏結合システムへの影響を理解する上で重要である。

磁気圏の降下電子のピッチ角は数度程度であり、磁気圏「その場」での降下電子観測は、あらせ衛星搭載の高角度分解能を持つ電子分析器群によって近年漸く達成された。Kasahara et al. (2018) は、脈動オーロラ発生時にあらせ衛星が観測したロスコーン内（PA<2° ）電子フラックス強度が、ホイッスラーコーラス波動の出現に合わせて変化していることを示し、PA 散乱による降下電子の生成を初めて実証した。これらを踏まえ、我々は波動粒子間相互作用による電子降下の寄与を明らかにすることを目的として、2017 年 3 月から 2022 年 3 月にあらせ衛星の低・中エネルギー電子分析器（LEP-e, MEP-e）が磁気圏「その場」で観測した 67 eV – 88 keV の降下電子の統計的解析を行っている。

これまでの研究結果により、降下電子は L ~6 の真夜中から朝方領域で生成頻度が高く、これはコーラス波動の観測

領域と整合的であることが明らかになった。中でも MLT ~22 – 2 では、磁気赤道付近のコーラス波動の寄与が大きいことが示唆された一方で、MLT ~3 以降の朝方～昼側領域については、高緯度伝搬するコーラス波動や、高緯度で生成される昼側コーラス波動の効果が窺われた。本研究では、降下電子の緯度ごとでの生成頻度や生成領域の違いから高緯度コーラス波動の寄与を考察する。

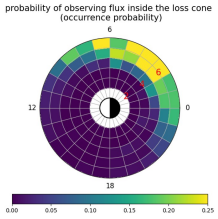

Average resonance energy
at the magnetic equator

$$W_{||res} = \frac{B_{eq}^2}{2\mu_0 n_{eq}} \left(1 - \frac{f_{eq}}{f_{ce}}\right)^3 \frac{f_{ce}}{f_{eq}}$$

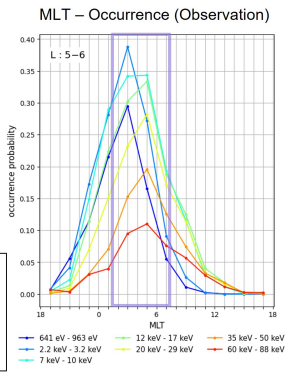

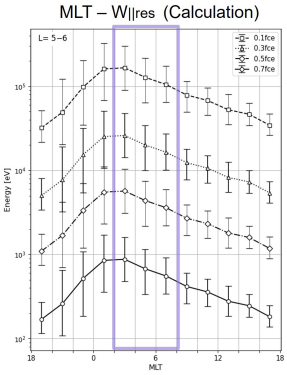

R006-P27
ポスター 1 ：11/24　PM1/PM2 （13:15-18:15）

REP イベント発生時のオーロラ観測と発光高度の推定

#柳澤 球大朗 [1)], 片岡 龍峰 [2)], 関 華奈子 [3)], 三好 由純 [4)], 塩川 和夫 [5)], Martin Connors[6)], 中平 聡志 [7)], 鳥居 祥ニ [8)]
([1] 東大院理地惑, [2] 極地研, [3] 東大理・地球惑星科学専攻, [4] 名大 ISEE, [5] 名大宇地研, [6] アサバスカ大学, [7] 宇宙研, [8] 早稲田大学理工学術院

Observation of auroral emission altitude during relativistic electron precipitation events

#Kyutaro Yanagisawa[1)], Ryuho Kataoka[2)], Kanako Seki[3)], Yoshizumi Miyoshi[4)], Kazuo Shiokawa[5)], Connors Martin[6)], Satoshi NAKAHIRA[7)], Shoji Torii[8)]
([1]The University of Tokyo, Graduate School of Science, Department of Earth and Planetary Science, [2]National Institute of Polar Research, [3]Department of Earth and Planetary Science, Graduate School of Science, University of Tokyo, [4]Institute for Space-Earth Environemental Research, Nagoya University, [5]Institute for Space-Earth Environmental Research, Nagoya University, [6]Athabasca University, [7]Institute of Space and Astronautical Science, Japan Aerospace Exploration Agency, [8]Faculty of Science and Engineering, Waseda University

High-energy electrons trapped in the radiation belt can sometimes precipitate into the atmosphere. This phenomenon is known as relativistic electron precipitation (REP) events. The possible mechanisms include the interaction with plasma waves such as electromagnetic ion cyclotron (EMIC) waves and chorus waves(Kataoka et al., JGR,2020). This study investigates what kind of auroras are visible from the ground when REP events occur in magnetic conjunctions. The REP events are identified by the CALorimetric Electron Telescope (CALET) experiment on-board the ISS (JAXA, “CALorimetric Electron Telescope (CALET)”, humans-in-space.jaxa.jp, 2021, https://humans-in-space.jaxa.jp/en/biz-lab/experiment/theme/detail/000932.html) above the observation site. The emission altitude of the aurora depends on the energy of precipitating electrons or protons, which can contribute to identifying the possible wave mode to cause REP as well.The experiment will be carried out at two observation points in Athabasca, Canada, approximately 25 km apart. The two points are Athabasca University Geophysical Observatory (AUGO), 54.71N and 113.31W,and Athabasca University Geospace Observatory (AUGSO), 54.60N and 113.64W. To estimate the emission altitude, the stereoscopic approach will be adopted by using identical all-sky cameras with a wavelength of 427.8 nm.The installation will start from August 28, 2024, and the observation will continue for a few years. We will report the latest results of the ground-based observations, when the ISS/CALET observe REP events, based on the data obtained from September to November, 2024.

放射線帯に捕捉された高エネルギー電子が、大気中に降り注ぐことがある。この現象は相対論的電子降下（REP）現象と呼ばれている。そのメカニズムとしては、電磁イオンサイクロトロン（EMIC）波やコーラス波などのプラズマ波との相互作用が考えられている (Kataoka et al., JGR,2020)。本研究では、同一磁力線上で REP 現象が発生した場合、地上からどのようなオーロラが見えるかを調べる。REP 現象は、ISS に搭載された CALET（CALorimetric Electron Telescope）実験（JAXA,「CALorimetric Electron Telescope (CALET)」, humans-in-space.jaxa.jp, 2021, https://humans-in-space.jaxa.jp/en/biz-lab/experiment/theme/detail/000932.html）によって観測地点の上空で同定される。オーロラの発光高度は、降下する電子やプロトンのエネルギーに依存するため、REP を引き起こす可能性のある波動モードの特定にも貢献する。実験は、カナダのアサバスカにある約 25km 離れた 2 つの観測地点で実施される。アサバスカ大学地球物理天文台（AUGO）の北緯 54.71 度、西経 113.31 度と、アサバスカ大学地球宇宙天文台（AUGSO）の北緯 54.60 度、西経 113.64 度である。観測は 2024 年 8 月 28 日から数年間行われる予定であり、観測高度を推定するために、波長 427.8nm の同一の全天カメラを用いた立体視アプローチを用いる。本発表では、2024 年 9 月から 11 月までのデータをもとに、ISS/CALET が REP イベントを観測した際の最新の地上観測結果を報告する予定である。

R006-P28
ポスター 1 ：11/24　PM1/PM2 （13:15-18:15）

#新井 まどか [1)], 加藤 雄人 [2)], 片岡 龍峰 [3)], 寺本 万里子 [4)], 熊本 篤志 [2)], 土屋 史紀 [5)], 笠羽 康正 [6)], 三好 由純 [7)], 笠原 禎也 [8)], 松田 昇也 [9)], 篠原 育 [10)], 山本 和弘 [11)], 松岡 彩子 [12)], 堀 智昭 [13)], 新堀 淳樹 [14)], 鳥居 祥二 [15)], 赤池 陽水 [15)]
([1] 東北大学, [2] 東北大・理・地球物理, [3] 極地研, [4] 九工大, [5] 東北大・理・惑星プラズマ大気, [6] 東北大・理, [7] 名大 ISEE, [8] 金沢大, [9] 金沢大学, [10] 宇宙機構／宇宙研, [11] 名大 ISEE, [12] 京都大学, [13] 名大 ISEE, [14] 名古屋大学宇宙地球環境研究所, [15] 早稲田大学

Repetition period of REP and chorus observed during the conjunction event of ISS/CALET and the Arase satellite

#Madoka Arai[1)], Yuto Katoh[2)], Ryuho Kataoka[3)], Mariko Teramoto[4)], Atsushi Kumamoto[2)], Fuminori Tsuchiya[5)], Yasumasa Kasaba[6)], Yoshizumi Miyoshi[7)], Yoshiya Kasahara[8)], Shoya Matsuda[9)], Iku Shinohara[10)], Kazuhiro Yamamoto[11)], Ayako Matsuoka[12)], Tomoaki Hori[13)], Atsuki Shinbori[14)], Shoji Torii[15)], Yosui Akaike[15)]
([1]Tohoku university, [2]Department of Geophysics, Graduate School of Science, Tohoku University, [3]National Institute of Polar Research, [4]Kyushu Institute of Technology, [5]Planetary Plasma and Atmospheric Research Center, Graduate School of Science, Tohoku University, [6]Planetary Plasma and Atmospheric Research Center, Graduate School of Science, Tohoku University, [7]Institute for Space-Earth Environemental Research, Nagoya University, [8]Emerging Media Initiative, Kanazawa University, [9]Kanazawa University, [10]Japan Aerospace Exploration Agency/Institute of Space and Astronautical Science, [11]Institute for Space-Earth Environmental Research ([ISEE), Nagoya University, [12]Graduate School of Science, Kyoto University, [13]Institute for Space-Earth Environmental Research, Nagoya University, [14]Institute for Space-Earth Environmental Research, Nagoya University, [15]Graduate School of Science, Waseda University

Relativistic electron precipitation (REP) is the enhancement of downward electron counts in the MeV energy range detected at the LEO orbit. The pitch angle scattering by chorus emissions in the magnetosphere is one of the mechanisms responsible for REP. The percentage of each type of wave that causes REP has yet to be identified. Kandar et al. (2023) reported distributions of the repetition periods of REP. They compared them with the distribution of repetition periods of rising tone chorus elements derived by Shue et al. (2015) in different magnetic local time categories. Results of the comparison indicated close agreement between REP and chorus in the night, dawn, and day MLT sectors where chorus emissions are frequently observed. Ozaki et al. (2018) showed agreement between the intensity modulation of chorus and pulsating aurora caused by keV electrons. In the present study, we explore the characteristic of REP caused by chorus emissions by analyzing the conjunction event of ISS/CALET and the Arase satellite.

We analyze observation data of ISS CALET/CHD for REP and Arase PWE/OFA for chorus. ISS CALET/CHD consists of two orthogonal layers of plastic scintillators, with CHD-X and CHD-Y thresholds corresponding to $\geq$ 1.6 MeV and $\geq$ 3.6 MeV electrons, respectively. From count rate ratio of CHD-X to CHD-Y, we defined the REP event when the ratio $\geq$ 1.2. We defined the criteria of the conjunction between ISS and Arase as the period when Arase's footprint was within $\pm$ 2.5 degrees of latitude and within $\pm$ 15 degrees of longitude from ISS while REP was occurring. We identified the 103 conjunction events in the observation data from February 2017 to December 2023. Among them, there were 23 events where chorus was observed. In this paper, we focus on an event in 18:31:00-18:37:00 on April 24, 2017, one of three events treated by Kataoka et al. (2020) in which REP and plasma wave occurred simultaneously and chorus was observed. In this event, the Arase satellite observed chorus at -23 degrees of the magnetic latitude within L=4.62-4.73, and 0.15-0.30 MLT ranges. The observed chorus appeared in the frequency range from 0.4 to 3 kHz. We estimated the cyclotron resonance energy and found that waves in the frequency range from 0.9-3 kHz can resonate with 1.6-3.6 MeV electrons. We analyzed the repetition period of REP, defined as the interval between points where the gradient of count rates ratio is $\geq$ +0.25 /time duration. We identified three enhancements (spikes) of REP during this conjunction. While the repetition periods of the observed chorus were commonly in 2-5 sec, we found that the REP occurred with similar repetition periods. Since the interval of the REP event contains a small number of data per spike, we present the result of a multiple case study to reveal the statistical relationship between chorus and REP.

R006-P29
ポスター 1 ：11/24　PM1/PM2 （13:15-18:15）

#寺本 万里子 [1)], 片岡 龍峰 [2)], 三好 由純 [3)], 鳥居 祥二 [4)], 笠原 禎也 [5)], 松岡 彩子 [6)], 三宅 晶子 [7)], 中平 聡志 [8)], 松田 昇也 [5)], 尾崎 光紀 [5)], 山本 和弘 [3)], 篠原 育 [8)], 北村 健太郎 [1)]
([1] 九工大, [2] 極地研, [3] 名大 ISEE, [4] 早稲田大, [5] 金沢大, [6] 京都大学, [7] 岐阜高専, [8] 宇宙研

Characteristics of MeV Electron Precipitation Observed by CALET/CHD for Geomagnetic Disturbances

#Mariko Teramoto[1)], Ryuho Kataoka[2)], Yoshizumi Miyoshi[3)], Shoji Torii[4)], Yoshiya Kasahara[5)], Ayako Matsuoka[6)], Shoko Miyake[7)], Satoshi NAKAHIRA[8)], Shoya Matsuda[5)], Mitsunori Ozaki[5)], Kazuhiro Yamamoto[3)], Iku Shinohara[8)], Kentarou Kitamura[1)]
([1]Kyushu Institute of Technology, [2]National Institute of Polar Research, [3]Institute for Space-Earth Environement Research, Nagoya University, [4]Waseda University, [5]Emerging Media Initiative, Kanazawa University, [6]Graduate School of Science, Kyoto University, [7]National Institute of Technology, Gifu College, [8]Institute of Space and Astronautical Science, Japan Aerospace Exploration Agency

Relativistic electron precipitation (REP) from the outer radiation belt into the Earth's atmosphere is caused by electron resonance interaction with the whistler mode and electromagnetic ion cyclotron (EMIC) waves via pitch angle scattering. The characteristics of the energy spectra of the precipitating MeV electrons are not fully understood.

We investigate the spatial distributions of precipitating MeV electrons and their geomagnetic dependence. To detect REP events, the CALET (Calorimetric Electron Telescope)/CHD (Charge Detector) on board the International Space Station (ISS) was utilized. CALET is the instrument for observing GeV-TeV electrons, nuclei in Z = 1-40, gamma rays above 1 GeV, and gamma ray bursts. The CALET-CHD consists of two orthogonal layers, CHD-X and CHD-Y, of plastic scintillator charge measurement modules. The two layers determine the incident position of the cosmic rays. The trigger counter signals are counted and the accumulated numbers are recorded every 1 s. Kataoka et al. (2016, 2020) show that the count rate observed by CHD can be used for REP studies. CHD-X and CHD-Y observe $>$1.6 MeV and $>$3.6 MeV electrons, respectively. We use the data from March 2017 to December 2023 to identify periods of abrupt changes in the CHD count rate and identified them as REP events. To investigate the dependence of the geomagnetic disturbances on the REP at $>$1.6 MeV and $>$3.6 MeV, the SME$*$at the REP events is calculated, which is the average of the SME index of the identified REP events up to 1 h before. In addition, we calculate R_{XY} , which is the ratio of the CHD-X count rate to the CHD-Y count rate. High R_{XY} values indicate that the energy spectra of REP events are soft. During geomagnetic quiet periods (SME$*<$200 nT) the high R_{XY} regions appear at Lm $>$5 and mainly on the night side (21-03 MLT). As the degree of geomagnetic disturbance increased, the high R_{XY} regions spread to the dawn and dusk side at Lm $<$5. We also find that the high R_{XY} regions appear outside the plasmapause, while R_{XY} is low inside the plasmapause. We identify REP events with good Arase-ISS conjunction and found that the Arase satellite observed chorus waves on the dawnside during some REP events. These results indicate that REP events near the plasmapause and outside the plasmapause are caused by the EMIC waves and chorus waves, respectively.

R006-P30
ポスター 1 ：11/24　PM1/PM2 （13:15-18:15）

科学衛星あらせによって観測された狭帯域低周波波動の自動抽出

#三浦 雅也 [1)], 三宅 壮聡 [2)], 笠原 禎也 [3)]
([1] 富山県大, [2] 富山県大, [3] 金沢大

Automatic extraction of narrowband low-frequency waveforms observered by ARASE

#Masaya Miura[1)], Taketoshi Miyake[2)], Yoshiya Kasahara[3)]
([1]Toyama Prefectural University, [2]Faculty of Engineering, Toyama Prefectural University, [3]Emerging Media Initiative, Kanazawa University

Various type of low frequency waves are observed by Electric Field Detector (EFD) onboard satellite. In this study, we are going to detect narrowband low frequency waves from EFD data, classify these waves into several type by using Machine learning method. At first, we applied R-CNN method to 1 hours of EFD spectrum data form March 21, 2017 to August 31, 2022, and detect 3876 narrowband low frequency waves. We automatically get these time of occurrence, frequency band and center frequency at the same time. Next, we try to classify narrowband low frequency waves into several types by clustering method. We apply K-means method and hierarchical clustering method to the EFD spectrum data and the numerical data, which are the frequency range and center frequency, image features, respectively. We found 10 types of narrowband low frequency with different characteristics. This will enable detailed analysis of narrowband low-frequency waves, and we hope to clarify the relation the characteristics of the narrowband low-frequency waves with the plasma environment around the satellite.

本研究では、科学衛星あらせに搭載された電場観測器 (EFD) によって宇宙空間で観測された狭帯域な特徴を持つ低周波波動の分類を行う。最初に R-CNN 法を用いて 2017 年 3 月 23 日〜2019 年 11 月 22 日の期間で 24 時間周期の EFD の観測データから低周波波動を検出し、発生時間と周波数帯、中心周波数を取得した。次に、取得したデータに K-means 法、取得した数値データに階層型クラスタリングを用いて 5 種類に分類した。その後、分類した狭帯域低周波波動 280 個に対して観測位置、磁場強度、磁場擾乱の調査、イオンサイクロトロン周波数、低域混成周波数との比較イオンエネルギーの解析を行ったところ狭帯域低周波波動は周波数変化が周囲のプラズマ環境に影響を受けていることが確認できた。しかし、狭帯域低周波波動のデータ数が 280 個と少なかったため発生源の特定に必要な特徴を見つけられなかった。また、24 時間周期で波動を検出したため波動の細かい特徴や継続時間の短い波動を見落としている可能性がある。そこで期間を 2017 年 3 月 21 日〜2022 年 8 月 31 日までとし、細かい特徴を見るために 1 時間周期で機械学習を適用し、さらに分類手法を改良したところ 3876 個の狭帯域低周波波動を検出した。次に、検出した狭帯域低周波波動を R-CNN 法を用いて取得した数値データをもとに階層型クラスタリングで分類を行った結果、10 種類の特徴を持つ狭帯域低周波波動に分類することができた。これによって狭帯域低周波波動の詳しい解析が可能となり、衛星周辺のプラズマ環境との関係を明らかにしていきたいと考えている。また、狭帯域なスペクトルを持つ波動には人工ノイズが含まれている可能性が高いと考えられているので自然な波動と人工ノイズを区別できるのか検討する。

R006-P31
ポスター 1 ：11/24　PM1/PM2 （13:15-18:15）

科学衛星あらせによって観測された特徴的な低周波波動の自動抽出

#宍野 蒼雅 [1)], 三宅 壮聡 [2)], 笠原 禎也 [3)]
[(1] 富山県立大院工, [(2] 富山県大, [(3] 金沢大

Automatic Extraction of Characteristic Low-Frequency Waves observed by ARASE

#Soga Shishino[1)], Taketoshi Miyake[2)], Yoshiya Kasahara[3)]
[(1]Graduate School of Engineering, Toyama Prefectual University, [(2]Faculty of Engineering, Toyama Prefectural University, [(3]Emerging Media Initiative, Kanazawa University

In this study, we extract and classify low-frequency plasma waves observed by Electric Field Detector (EFD) onboard the scientific satellite Arase.

We applied improved machine learning method to low-frequency plasma waves with relatively broadband spectra, and extracted 175 characteristic waves from 2017.3.21 to 2022.8.31.

Next, we used the k-means clustering method and the hierarchical clustering method with the numerical data, which are observed time, frequency bandwidth, and center frequency, and classified these extracted waves into 6 types.

As a result, we succeed to extract and classify the characteristic low-frequency plasma waves, which are visually classified, by using machine learning method.

We are going to analyze the relation between the classified low-frequency plasma waves and the other observation data, such as satellite position, magnetic data and frequency data.

本研究では、科学衛星あらせに搭載された電場観測機 (EFD) によって観測された低周波プラズマ波動スペクトルを自動抽出したのち、そのスペクトルの特徴によって分類を行う。これまでの研究では、まず目視による抽出・分類を行い、比較的広帯域なスペクトルを持つ 3 種類の特徴的な波動が観測されていることが確認できた。次に、膨大な量のデータを目視で分類するのは非効率的であるため、機械学習を利用して低周波波動の抽出・分類を行ったところ、2017 年 3 月 21 日から 2019 年 10 月 29 日までに観測された EFD データから 373 個の波動を抽出し、抽出した波動をスペクトルの特徴から 8 種類に分類できた。しかし、この機械学習による分類では、目視では見落としていた波動を抽出できた一方で、最初に目視で行った分類を再現できておらず、特徴的な波動を上手く抽出できていなかった。そこで、比較的広帯域なスペクトルを持つ波動に対して機械学習を適用してさらに細かく分類を行い、目視による特徴的な波動の抽出・分類の再現を試みた。その結果、2017 年 3 月 21 日から 2022 年 8 月 31 日までのスペクトル画像 1987 枚から 175 個のスペクトル波動を抽出することができた。得られた波動の継続時間と周波数帯、中心周波数のデータを用いて k-means クラスタリングと階層型クラスタリングを行うことで、抽出した画像の中に含まれる対象波動の確認できないものを取り除き、抽出した波動を 6 種類に分類した。その結果、低周波プラズマ波動に対して機械学習を適用して、目視による特徴的な波動の抽出・分類を再現することができた。今後は分類された低周波波動と観測位置、地場強度、地場擾乱、イオンサイクロトロン周波数、低域混成周波数などとの関係について解析を行っていく。

R006-P32
ポスター 1 ：11/24　PM1/PM2 （13:15-18:15）

#風間 洋一 [1)], 三好 由純 [2)], 加藤 雄人 [3)], 笠羽 康正 [4)], 栗田 怜 [5)], 笠原 禎也 [6)], 小嶋 浩嗣 [7)], 桂華 邦裕 [8)], 松田 昇也 [9)], 田 采祐 [10)], 堀 智昭 [11)], Wang Bo-Jhou[1)], Wang Shiang-Yu[1)], Tam Sunny[12)], 浅村 和史 [13)], 松岡 彩子 [14)], 寺本 万里子 [15)], 篠原 育 [16)]
([1]ASIAA, [2] 名大 ISEE, [3] 東北大・理・地球物理, [4] 東北大・理, [5] 京都大学 生存研, [6] 金沢大, [7] 京大, [8] 東大・理, [9] 金沢大学, [10] 名大 ISEE 研, [11] 名大 ISEE, [12]Institute of Space and Plasma Sciences, National Cheng Kung University, [13] 宇宙研, [14] 京都大学, [15] 九工大, [16] 宇宙機構／宇宙研

Noon-midnight difference in latitudinal occurrence of whistler-mode chorus waves observed by the Arase satellite

#Yoichi Kazama[1)], Yoshizumi Miyoshi[2)], Yuto Katoh[3)], Yasumasa Kasaba[4)], Satoshi Kurita[5)], Yoshiya Kasahara[6)], Hirotsugu Kojima[7)], Kunihiro Keika[8)], Shoya Matsuda[9)], ChaeWoo Jun[10)], Tomoaki Hori[11)], Bo-Jhou Wang[1)], Shiang-Yu Wang[1)], Sunny Tam[12)], Kazushi Asamura[13)], Ayako Matsuoka[14)], Mariko Teramoto[15)], Iku Shinohara[16)]
([1]Academia Sinica Institute of Astronomy and Astrophysics, [2]Institute for Space-Earth Environement Research, Nagoya University, [3]Department of Geophysics, Graduate School of Science, Tohoku University, [4]Planetary Plasma and Atmospheric Research Center (PPARC), Tohoku University, [5]Research Institute for Sustainable Humanosphere, Kyoto University, [6]Emerging Media Initiative, Kanazawa University, [7]Kyoto university, [8]Department of Earth and Planetary Science, Graduate School of Science, The University of Tokyo, [9]Kanazawa University, [10]Institute for Space-Earth Environmental Research, [11]Institute for Space-Earth Environmental Research, Nagoya University, [12]Institute of Space and Plasma Sciences, National Cheng Kung University, [13]Japan Aerospace Exploration Agency, [14]Graduate School of Science, Kyoto University, [15]Kyushu Institute of Technology, [16]Japan Aerospace Exploration Agency/Institute of Space and Astronautical Science

We present spatial occurrence distributions of whistler-mode chorus waves and their correlation with low-energy electrons, based on 5.1-year observations of the Arase satellite. The detailed statistical analysis indicates that strong chorus waves are predominantly observed near the magnetic equator in the postmidnight sector, and the active region of chorus waves shifts to higher latitudes with moderate chorus emissions as electrons drift eastward toward the noon sector. The differences in chorus intensity and latitudinal occurrence between noon and midnight can be explained by the nonlinear growth theory of whistler waves. Specifically, these differences are influenced by threshold amplitude controlled by hot electron density and magnetic field inhomogeneity determined by geomagnetic field configuration.

R006-P33
ポスター 1 ：11/24　PM1/PM2 （13:15-18:15）

#篠原 育 [1)], 楊 敬軒 [2)], 風間 洋一 [3)], Wang Shiang-Yu[3)], Tam Sunny W. Y.[4)], 田 采祐 [5)], 笠原 慧 [6)], 横田 勝一郎 [7)], 桂華 邦裕 [8)], 山本 和弘 [9)], 堀 智昭 [10)], 浅村 和史 [11)], 三好 由純 [12)], 三谷 烈史 [13)], 笠原 禎也 [14)], 松田 昇也 [15)], 松岡 彩子 [16)], 寺本 万里子 [17)]
([1] 宇宙機構／宇宙研, ([2] 東大・理・地惑, ([3]ASIAA, ([4]NCKU, ([5] 名大 ISEE 研, ([6] 東京大学, ([7] 大阪大, ([8] 東大・理, ([9] 名大 ISEE, ([10] 名大 ISEE, ([11] 宇宙研, ([12] 名大 ISEE, ([13] 宇宙研, ([14] 金沢大, ([15] 金沢大学, ([16] 京都大学, ([17] 九工大

Chorus wave activity observed at marginal condition of electron temperature anisotropy instability in the inner magnetosphere

#Iku Shinohara[1)], Jingxuan Yang[2)], Yoichi Kazama[3)], Shiang-Yu Wang[3)], Sunny W. Y. Tam[4)], ChaeWoo Jun[5)], Satoshi Kasahara[6)], Shoichiro Yokota[7)], Kunihiro Keika[8)], Kazuhiro Yamamoto[9)], Tomoaki Hori[10)], Kazushi Asamura[11)], Yoshizumi Miyoshi[12)], Takefumi Mitani[13)], Yoshiya Kasahara[14)], Shoya Matsuda[15)], Ayako Matsuoka[16)], Mariko Teramoto[17)]
([1]Japan Aerospace Exploration Agency/Institute of Space and Astronautical Science, ([2]Earth and Planetary Science, The University of Tokyo, ([3]Academia Sinica Institute of Astronomy and Astrophysics, ([4]National Cheng Kung University, ([5]Institute for Space-Earth Environmental Research, ([6]The University of Tokyo, ([7]Osaka University, ([8]Department of Earth and Planetary Science, Graduate School of Science, The University of Tokyo, ([9]Institute for Space-Earth Environmental Research (ISEE), Nagoya University, ([10]Institute for Space-Earth Environmental Research, Nagoya University, ([11]Japan Aerospace Exploration Agency, ([12]Institute for Space-Earth Environemental Research, Nagoya University, ([13]Japan Aerospace Exploration Agency, Institute of Space and Astronautical Science, ([14]Emerging Media Initiative, Kanazawa University, ([15]Kanazawa University, ([16]Graduate School of Science, Kyoto University, ([17]Kyushu Institute of Technology

Whistler chorus mode waves observed in the inner magnetosphere are believed to be caused by the free energy of electron temperature anisotropy, which is created by injections or plasma convection from the magnetotail. To investigate this, we analyzed electron temperature anisotropy data from the Arase satellite, specifically electron data (LEP-e and MEP-e) observed from March 2017 to October 2019. As presented in the last SGEPSS meeting, we identified the marginal condition of the whistler anisotropy instability in the data obtained near the magnetic equator. The data points near the marginal condition are found within a limited region of Lm=5~6, MLT=23~6, and MLAT=-10~+10, which is consistent with the higher occurrence region of the whistler chorus wave in the inner magnetosphere. Moreover, the duration during which the marginal condition is only a few minutes. In our presentation, we will report a statistical analysis of chorus wave activity observed by the PWE when the marginal condition is identified.

R006-P34
ポスター 1 ：11/24　PM1/PM2 （13:15-18:15）

あらせ衛星で観測されたコーラス波が駆動する静電波の周波数スペクトル構造の解析

#吉田 永遠 [1)], 栗田 怜 [2)], 小嶋 浩嗣 [3)], 笠原 禎也 [4)], 松田 昇也 [5)], 松岡 彩子 [6)], 三好 由純 [7)], 堀 智昭 [8)], 寺本 万里子 [9)], 山本 和弘 [10)], 篠原 育 [11)]
([1] 京大・工・電気, [2] 京都大学 生存研, [3] 京大, [4] 金沢大, [5] 金沢大学, [6] 京都大学, [7] 名大 ISEE, [8] 名大 ISEE, [9] 九工大, [10] 名大 ISEE, [11] 宇宙機構／宇宙研

Analysis of frequency spectral structure of electrostatic waves driven by chorus waves observed by the Arase satellite

#Towa Yoshida[1)], Satoshi Kurita[2)], Hirotsugu Kojima[3)], Yoshiya Kasahara[4)], Shoya Matsuda[5)], Ayako Matsuoka[6)], Yoshizumi Miyoshi[7)], Tomoaki Hori[8)], Mariko Teramoto[9)], Kazuhiro Yamamoto[10)], Iku Shinohara[11)]
([1]Faculty of Engineering, Kyoto University, [2]Research Institute for Sustainable Humanosphere, Kyoto University, [3]Kyoto university, [4]Emerging Media Initiative, Kanazawa University, [5]Kanazawa University, [6]Graduate School of Science, Kyoto University, [7]Institute for Space-Earth Environement Research, Nagoya University, [8]Institute for Space-Earth Environmental Research, Nagoya University, [9]Kyushu Institute of Technology, [10]Institute for Space-Earth Environmental Research (ISEE), Nagoya University, [11]Japan Aerospace Exploration Agency/Institute of Space and Astronautical Science

Whistler-mode chorus waves are electromagnetic waves that are excited in the Earth's magnetosphere. Chorus waves are observed in the frequency range of 0.1 to 0.8 times the electron cyclotron frequency. Chorus waves resonate with electrons in various energy bands and accelerate electrons. Reinleitner et al. (1983) reported that the acceleration of these electrons excites electrostatic waves which oscillate parallel to the magnetic field lines. Chorus waves which propagate obliquely to the magnetic field lines have an electric field component parallel to the field lines. The beam-mode electrostatic waves are excited by Landau resonance between the electric field of the chorus wave and electrons. Li et al. (2017) also reported that a beam with a velocity matching the phase velocity of the chorus wave exists in observed electron distribution functions. However, in these previous studies, the wave instruments covered only up to ˜10 kHz and did not accurately the high frequency components of electrostatic waves. In addition, only few cases have been analyzed by past studies.

In order to further examine the electrostatic waves associated with chorus waves, we perform a statistical analysis on them on the basis of plasma wave data obtained by the Arase satellite, which can measure waves up to 20 kHz. We analyzed bandwidths of the electrostatic waves associated with chorus waves observed by the Waveform Capture (WFC) of the Plasma Wave Experiment (PWE) instrument onboard the Arase satellite. The occurrence distribution for the bandwidths has a peak at about 1 kHz and spread from 2 kHz to about 10 kHz. The bandwidths of electrostatic waves associated with each band of chorus waves are different. Especially in lower-band-chorus (LBC), many electrostatic waves have bandwidths wider than 2 kHz. This result suggests that resonance with electrons by LBC is important in this phenomenon.

To understand the distribution of the bandwidth, we also analyzed the electric field and magnetic field waveforms observed by WFC. The result shows that many periodic bursts of electrostatic waves were observed in association with the electric field in parallel direction of chorus waves. On the other hand, in narrow bandwidth of about 1 kHz, the periodic structure was rarely observed. From these observations, the excitation of electrostatic waves associated with LBC is different from the excitation of electrostatic waves associated with other chorus wave frequency bands.

ホイッスラーモードコーラス波は、地球磁気圏内で励起される電磁波であり、電子サイクロトロン周波数の 0.1 倍から 0.8 倍程度の周波数帯で観測される。コーラス波は様々なエネルギー帯の電子と共鳴し、これらの電子の加速を生じる。Reinleitner et al. (1983) においては、これらの電子の加速により磁力線平行方向に振動する静電波が励起することが報告されている。磁力線に対して斜めに伝搬するコーラス波では、磁力線平行方向に電界の成分をもつ。このコーラス波の電界とランダウ共鳴した電子が加速され、ビームモードの静電波が励起される。これより、励起される静電波は、コーラス波の磁力線平行方向の電界成分によって変調された波形となっている。Li et al. (2017) においては、位相空間密度にコーラス波の位相速度と一致する速度のビームが存在していることも報告されている。しかし、これらの先行研究においては、観測器の上限周波数が 10 kHz 程度となっており、高い周波数成分をもつ静電波が正確に捉えられていない。加えて、議論されている事例が数例となっているため、この現象の包括的な理解には至っていない。よって、私たちは波形観測器の上限周波数が 20 kHz であるあらせ衛星の観測データを用いて統計解析を行った。

あらせ衛星に搭載されたプラズマ波動観測器 (PWE) の 1 つである波形観測器 (WFC) によって観測されたデータを用いて、コーラス波に関連した静電波の周波数帯域幅に関する解析を行った。これらの静電波の帯域幅に関する頻度分布は、約 1 kHz をピークとし、2 kHz から 10 kHz 程度まで広がった分布となっていた。また、各帯域のコーラス波に関連した静電波の帯域幅の分布は、コーラス波の周波数帯域によって大きく異なっていた。特に Lower-Band-Chorus(LBC) においては、帯域幅が 2 kHz 以上の静電波が多く観測されていた。このことより、LBC による電子との共鳴が、本現象において重要となっていると考えられる。

これらの静電波の帯域幅の分布を理解するために、WFC で観測された電界・磁界波形についても詳細に解析した。そ

の結果、帯域幅が広い静電波では、コーラス波の磁力線平行方向の電界成分に対応して静電波の周期的なバーストが多く観測された。一方、1 kHz 程度の狭い帯域幅をもつ静電波においては、そのような周期的な構造はほとんど確認されなかった。このことより、LBC に伴う電波と、それ以外のコーラス波の周波数帯に関連した静電波では発生メカニズムが異なることが考えられる。

R006-P35
ポスター 1 ：11/24　PM1/PM2 （13:15-18:15）

#宮下 隼輔 [1)], 加藤 雄人 [1)], 熊本 篤志 [1)], 土屋 史紀 [2)], 笠羽 康正 [2)], 笠原 禎也 [3)], 松田 昇也 [3)], 松岡 彩子 [4)], 三好 由純 [5)], 堀 智昭 [5)], 新堀 淳樹 [5)], Santolik Ondrej[6,7)]
([1] 東北大・理・地球物理, [2] 東北大・理・惑星プラズマ大気, [3] 金沢大, [4] 京都大学, [5] 名大 ISEE, [6] チェコ共和国 ASCR 大気物理学研究所, [7] カレル大学数物学部

Study of propagation characteristics of EMIC wave using multipoint observation by Arase and Cluster

#Shunsuke Miyashita[1)], Yuto Katoh[1)], Atsushi Kumamoto[1)], Fuminori Tsuchiya[2)], Yasumasa Kasaba[2)], Yoshiya Kasahara[3)], Shoya Matsuda[3)], Ayako Matsuoka[4)], Yoshizumi Miyoshi[5)], Tomoaki Hori[5)], Atsuki Shinbori[5)], Santolik Ondrej[6,7)]
([1]Department of Geophysics, Graduate School of Science, Tohoku University, [2]Planetary Plasma and Atmospheric Research Center, Graduate School of Science, Tohoku University, [3]Emerging Media Initiative, Kanazawa University, [4]Graduate School of Science, Kyoto University, [5]Institute for Space-Earth Environement Research, Nagoya University, [6]Institute of Atmospheric Physics ASCR, Prague, Czech Republic, [7]Faculty of Mathematics and Physics, Charles University, Prague, Czech Republic

Electromagnetic ion cyclotron (EMIC) waves are important for the loss of radiation belt electron and ring current ions. After being excited by an instability driven by the temperature anisotropy followed by nonlinear wave-particle interactions occurring near the magnetic equator of the inner magnetosphere, EMIC waves propagate parallel along the magnetic field lines with left-handed polarization. As the waves propagate to higher latitudes, their wave normal angles with respect to the magnetic field increase. At latitudes where the wave frequency is the same as the crossover frequency, the polarization changes from left-handed to right-handed, called polarization reversal. Polarization reversal is one of the mechanisms that allow EMIC waves to propagate to the ground without being reflected in the magnetosphere (Chen et al.2014). The crossover frequency at which polarization reversal occurs depends highly on the surrounding plasma environment. To investigate the polarization reversal in the magnetosphere, conjugate observation, in which the same event is observed at different latitudes, is useful for discussing the propagation process of plasma waves and changes in the surrounding plasma environment. However, few previous studies have observed and analyzed an identical wave in different latitudes, and there is a spatial spread (Engebretson et al. 2018).

In this study, we analyzed EMIC waves simultaneously observed by the Arase and Cluster satellites. We used the electric and magnetic field waveform data observed by the PWE-EFD and MGF onboard the Arase satellite and the magnetic field waveform data observed by STAFF onboard the C1 satellite. By analyzing the properties of the same wave at different latitudes, we study the surrounding plasma environment and wave characteristics in detail. The event of interest was observed from 21:20 to 21:40 UT on July 25,2020, with the same L-value-(L=6) and MLT-(12.9 MLT). In the spectra observed by Arase located in the equatorial region (MLAT=5°), we identified the enhancement of electromagnetic waves in the frequency range from 0.65Hz to 1.1Hz, corresponding to the proton-band EMIC waves. The same EMIC wave was observed by C1 in the region away from the equator-(MLAT=-24°). While the frequency range of the EMIC wave observed at Arase was higher than the local helium cyclotron frequency, the EMIC wave observed at C1 appeared in the spectra close to the local helium cyclotron frequency. Considering the cold plasma dispersion relation, it was suggested that polarization reversal may have occurred during the wave propagation process from the equatorial region at Arase to the higher latitude at C1. Also, to investigate polarization properties, we have performed the Singular Value Decomposition (SVD) method (Santolik et al. 2003) for each satellite data. This method allows us to derive polarization properties, Poynting vectors, etc., and to investigate how the waves change in the propagation process. In this presentation, we present the analysis result of these polarization characteristics and the surrounding environment in which the waves are propagating.

R006-P36
ポスター 1 ：11/24　PM1/PM2 （13:15-18:15）

あらせ衛星観測に基づく磁気音波の空間分布解析

#山﨑 貴司 [1)], 松田 昇也 [1)], 笠原 禎也 [1)], 笠羽 康正 [2)], 熊本 篤志 [2)], 土屋 史紀 [2)], 堀 智昭 [3)], 新堀 淳樹 [3)], 三好 由純 [3)], 篠原 育 [4)]
([1] 金沢大, [2] 東北大, [3] 名古屋大, [4] 宇宙機構／宇宙研

Spatial Distribution of Magnetosonic Waves Observed by the Arase Satellite

#Takashi Yamazaki[1)], Shoya Matsuda[1)], Yoshiya Kasahara[1)], Yasumasa Kasaba[2)], Atsushi Kumamoto[2)], Fuminori Tsuchiya[2)], Tomoaki Hori[3)], Atsuki Shinbori[3)], Yoshizumi Miyoshi[3)], Iku Shinohara[4)]
([1]Kanazawa University, [2]Tohoku University, [3]Nagoya University, [4]Japan Aerospace Exploration Agency/Institute of Space and Astronautical Science

Magnetosonic waves are a type of plasma wave observed at frequencies below several hundred Hz and play a role in accelerating ions through wave-particle interactions. Investigating the characteristics and spatial distribution of magnetosonic waves is important for understanding energy transport processes in geospace. Magnetosonic waves are classified into two types based on the properties of their amplitude modulation: one is the structureless magnetosonic wave, which does not exhibit periodic amplitude modulation, and the other one is the rising tone magnetosonic wave which repeatedly shows a periodic amplitude modulation with a period of a few minutes. Several previous studies using Van Allen Probes data have conducted event analyses on these two types of magnetosonic waves. However, the factors contributing to their different spectral structures have not yet been clarified. In order to clarify them, we conduct a statistical analysis of the two types of magnetosonic waves using data obtained by the Electric Field Detector (EFD), a sub-instrument of Plasma Wave Experiment (PWE) aboard the Arase satellite. We examined 1546 events of magnetosonic waves from the electric field spectra obtained by PWE/EFD, using over five years data from March 2017 to January 2022, and investigated their occurrence frequency and average intensity distribution. We found that rising tone magnetosonic waves were mainly observed outside the plasmasphere while structureless magnetosonic waves were observed both inside and outside the plasmasphere. This suggests the presence of a clear boundary in the distribution of the two types of magnetosonic waves. In this presentation, we focus on the relationship between the characteristics of magnetosonic waves and the plasmapause location, as well as their correlation with geomagnetic indices, and discuss the factors that change the characteristics of magnetosonic waves.

R006-P37
ポスター 1 ：11/24　PM1/PM2 （13:15-18:15）

#謝 怡凱 [1)], 大村 善治 [1)]
([1] 京大生存研

Energetic electron dynamics caused by whistler-mode chorus emissions in the Earth's inner magnetosphere

#Yikai Hsieh[1)], Yoshiharu Omura[1)]
([1]Research Institute for Sustainable Humanosphere, Kyoto University

Energetic electron accelerations and precipitations in the Earth's inner magnetosphere and outer radiation belt are highly associated with wave-particle interactions between whistler-mode chorus emissions and electrons. Two nonlinear processes, which change the energy and pitch angle of electrons effectively, take place in whistler mode wave-particle interactions. One is the nonlinear scattering, which smaller the electron energy slightly. The other is the nonlinear trapping, which makes effective energy gain of the resonant electrons. We utilized the Green's function method to reproduce the wave-particle interactions in the inner magnetosphere and investigate the electron acceleration and precipitation interacting with both parallel and obliquely propagating chorus emissions. The formation processes and the loss processes of the outer radiation belt electron fluxes interacting with consecutive chorus emissions are traced by applying the convolution integrals for the Green's functions. In the acceleration parts, MeV electrons are generated promptly due to the combination of cyclotron resonance and Landau resonance of oblique chorus waves. We compare the precipitation phenomena between parallel waves and oblique waves, and the results show that oblique chorus emissions lead to more electron precipitation than that led by parallel chorus emissions. Furthermore, we found that the acceleration process is stronger than the loss process, indicating that the radiation belt becomes stronger under the wave-particle interactions between chorus emissions and electrons comprehensively.

R006-P38
ポスター 1 ：11/24　PM1/PM2 （13:15-18:15）

あらせ衛星に搭載された磁力計が測定した地球近傍地磁気データの精度評価

#久田 大生 [1)], 寺本 万里子 [1)], 松岡 彩子 [2)], 山本 和弘 [3)], 三好 由純 [3)], 篠原 育 [4)], 北村 健太郎 [1)]
([1] 九工大, [2] 京都大学, [3] 名大 ISEE, [4] 宇宙機構／宇宙研

Accuracy evaluation of near-earth geomagnetic data measured by magnetic field experiment on board the Arase Satellite

#Taiki Hisada[1)], Mariko Teramoto[1)], Ayako Matsuoka[2)], Kazuhiro Yamamoto[3)], Yoshizumi Miyoshi[3)], Iku Shinohara[4)], Kentarou Kitamura[1)]
([1]Kyushu Institute of Technology, [2]Graduate School of Science, Kyoto University, [3]Institute for Space-Earth Environmental Research（ISEE), Nagoya University, [4]Japan Aerospace Exploration Agency/Institute of Space and Astronautical Science

In recent years, there has been an increasing demand for geomagnetic field measurements near the Earth at altitudes of 500~5,000 km for applications such as observing disturbances in the ionosphere. The Arase satellite is one of the satellites observing the geomagnetic field at this altitude. The Magnetic Field Experiment(MGF)[Matsuoka et.al., 2018] aboard the Arase satellite observes the geomagnetic field at altitudes ranging from 440 km to 32,000 km. Given that the geomagnetic field near the Earth is stronger than that at a location far from the Earth, MGF has been designed with two measurement ranges: ± 60,000 nT and ± 8,000 nT. In the ± 8,000 nT range, the calibration parameters are calculated under the assumption that the geomagnetic field remains constant during a spin of the Arase satellite. In contrast, the geomagnetic field observed during a spin in the ± 60,000 nT range exhibit significant variation due to satellite motion. Consequently, the application of the calibration method utilized in the ± 8,000 nT to the ± 60000 nT range is likely to yield erroneous, resulting in a reduction in the accuracy of the geomagnetic field in the ± 60,000 nT range. However, the accuracy of the geomagnetic field measurements taken in the ± 60,000 nT range has yet to be evaluated.

To evaluate the accuracy of the geomagnetic field measured in the ± 60,000 nT range, we compared the model magnetic field generated by the IGRF-13 model with the observed geomagnetic field data from the MGF. We used data observed on the 5 quiet days between April 2017 and December 2022. A positive correlation was identified between the geomagnetic fields and those of the IGRF-13 model in each of three components. Therefore, a linear fit was performed using the least squares method to obtain the slope and intercept of the approximate line. The slopes and intercepts obtained from the approximate straight lines exhibit a range of values from 0.951 to 1.062 and from -286.8 nT to 214.4 nT, respectively, indicating a degree of variation. The region observed in the ± 60,000 nT range is at low altitude and the ± 60,000 nT range is considered to be unaffected by magnetospheric disturbances. It can thus the postulated that the variation in the slope and intercept is the result of a geomagnetic disturbance caused by currents generated in the ionospheric region. In this presentation, we report on the data processing method used to compare the IGRF model with the MGF observations and present the results of the above analysis.

近年、電離圏の擾乱の観測などの用途から、高度 500〜5000km の地球近傍における地磁気測定の需要が高まってきている。あらせ衛星はこの領域における地磁気測定を行っている衛星の一つであり、あらせ衛星に搭載された Magnet Field Experiment(MGF)[Matsuoka et.al., 2018] は、高度 440~32000km の範囲で地磁気の測定を行っている。地磁気の強度は地球に近いほど強くなることから、あらせ衛星の MGF は地球に接近しているときは± 60000nT、地球から遠ざかっているときは± 8000nT の 2 つの測定レンジで運用をおこなっている。あらせ衛星が 1 回スピンする間で観測する地磁気は一定であるという仮定をおいて較正パラメータを算出しているが [Matsuoka et.al., 2019]、MGF の測定範囲を± 60000nT として運用する領域では、衛星の移動によりあらせ衛星が 1 スピンする間に観測される地磁気は大きく変化する。そのため、± 8000nT レンジで用いている較正方法を± 60000nT レンジに適用した場合、較正パラメータが適切に算出されず精度が低くなる可能性があるが、± 60000nT レンジはあらせ衛星の磁場観測精度要求の対象の外であるため ± 60000nT レンジで測定された地磁気の精度の評価は行われていない。

本研究では MGF の± 60000nT レンジにおける測定地磁気の精度を評価するため、IGRF-13 モデルから算出されたモデル磁場と MGF が測定した地磁気の値の比較を行った。解析には 2017 年 4 月から 2022 年 12 月の期間の地磁気静穏日に観測されたデータを用いた。MGF が観測した地磁気 3 成分それぞれに対し、IGRF モデルとの比較を行ったところ正の相関が見られた。そこで、最小二乗法を用いた直線フィッティングを行い、近似直線の傾きと切片を求めた。近似直線で導出された傾きは 0.951~1.062、切片は-286.8nT~214.4nT の範囲となり、ばらつきが見られた。± 60000nT レンジで観測している領域は、低高度であり± 60000nT レンジの観測は磁気圏の擾乱の影響を受けないと考えられ、傾きと切片に見られるばらつきは、電離圏領域に作られる電流由来の地磁気擾乱であると推測される。本発表では、IGRF モデルと MGF の観測値を比較する際に行ったデータ処理方法と上記解析の結果について報告する。

超小型衛星に搭載可能な小型のベクトル・スカラー磁力計を用いた磁力計較正システムの開発

#福元 笑美乃 [1)], 寺本 万里子 [1)], 魚住 禎司 [2)], 北村 健太郎 [1)]
([1] 九工大, [2] 九大/国際宇宙惑星環境研究センター

Development of Magnetometer Calibration System Using a Small Vector and Scalar Magnetometer for CubeSats

#Emino Fukumoto[1)], Mariko Teramoto[1)], Teiji Uozumi[2)], Kentaro Kitamura[1)]
([1]Kyushu Institute of Technology, [2]International Research Center for Space and Planetary Environmental Science, Kyushu University

In the field of space weather, an importance of the precise geomagnetic field observations associated with the solar wind variations has been leading a continuous improvement of the accuracy of magnetic field observations by the satellites. The European Space Agency (ESA) has previously developed and operated conventional large satellites, such as CHAMP and SWARM, to conduct high-precision geomagnetic field observations using vector and scalar magnetometers. On the other hand, with the increasing of CubeSats since the 2000s, that can be developed in a short period of two or three years and at low cost, they have also come to be used in the scientific observations. In the field of geomagnetic observation, CubeSats observation has not been developed due to the cost of high-precision magnetometers and the low accuracy of small magnetometers. If the magnetometer system developed by ESA can be applied to CubeSats, high-precision magnetometer calibration system can be developed, mass production at low cost will be possible, and simultaneous observation of the geomagnetic field at multiple locations will become feasible. There is significant potential for contributing to the field of space weather through the miniaturization of highly accurate magnetometer calibration systems. The study aims to develop a small, highly accurate magnetometer calibration system that can be mounted on an CubeSat. The magnetometer system to be developed consists of a measurement system and a calibration system. A fluxgate magnetometer (Spacemag-Lite, Bartington) is used for the vector magnetometer and an optical pumping magnetometer for the scalar magnetometer (OTFA-13M, QuSpin).

This study involves verifying the operation of Breadboard Models (BBMs) of magnetometers that can be mounted on Cubesats, developing control programs for simultaneous measurements, and conducting numerical analysis of the calibration program based on previous research. After developing the control program, a 10-minute indoor measurement was conducted, during which simultaneous measurements were mostly successful, although a few instances of extremely low values were observed in the scalar magnetometer readings.

The calibration program was then validated for accuracy based on the method used by Fan and Lühr [2011] to calibrate the CHAMP magnetometers. This calibration principle allows estimating the necessary calibration parameters for the vector magnetometer based on the scalar magnetometer observations, and the error in the total magnetic field total B calculated from the calibrated vector magnetometer is less than 0.5 nT.

A validation program was created to evaluate the accuracy of this calibration principle, and the analysis was performed assuming that the December 3, 2019 data from the geomagnetic observation data provided by the Geospatial Information Authority of Japan (Kuju Observatory) was the true magnetic field data, resulting in an error Δ B of 252.275 nT for the total B of the total magnetic field. The error before calibration was 3459.71 nT, confirming a significant improvement in total B after calibration compared to before calibration. However, since the requirement of the magnetometer system to be developed in this study is a accuracy within 50 nT (within 1°), the calculated error does not meet the requirement. Therefore, the offset of the calibration parameter was changed and the values before and after calibration were compared again using the verification program. When the offset was changed from the original setting of several thousand nT to several tens of nT, the error was found to be 0.10 nT, which is within the requirement. This confirmed that the calibration accuracy varies greatly depending on the parameter range.

In this session, the results of continuous measurements of fluxgate magnetometers and optical pumping magnetometers and the evaluation of the accuracy of the calibration program will be presented.

宇宙天気分野において、太陽風の影響による地球磁場変動を観測することは、非常に重要であり、精度の高い継続的な磁場観測が求められている。欧州宇宙機関は、ベクトル磁力計とスカラー磁力計を用いた高精度の磁場観測を行う大型衛星 CHAMP や SWARM を開発・運用をおこなってきた。一方、2000 年代以降、短期間・低コストで開発可能な超小型衛星の開発が増加してきており、科学分野への利用も始まっている。しかし、高精度かつ安価な磁力計が開発されていないため、地磁気観測分野において超小型衛星を用いた観測例は多くはない。欧州宇宙機関がおこなった磁力計較正システムを超小型衛星に適用させ、小型・高精度の磁力計較正システムを開発することができれば、低コストで大量生産が可能であり、地磁気の同時観測への応用が期待される。そのため、磁力計較正システムの小型化は宇宙天気分野への貢献に繋がる。

本研究では、超小型に搭載可能な小型の高精度の磁力計較正システムの開発を目的としている。開発する磁力計システムは、計測系と較正システム系の２つで構成されており、ベクトル磁力計にはフラックスゲート磁力計（Spacemag-Lite, Bartington 社）、スカラー磁力計（OTFA-13M, QuSpin 社）には光ポンピング磁力計を使用する。本研究ではまず、２つの磁力計の Bread Board Model(BBM) を用いた動作確認及び同時計測に向けた制御プログラムの作成、較正プログラムの検証を行った。開発した制御プログラムを、室内にて 10 分間計測を行ったところ、スカラー磁力計で極端に小さな観測値が数例見られたものの、計測期間の大半で同時計測を行うことができた。続いて較正用プログラムの検証を実施した。Fan and Lühr [2011] が行った CHAMP の磁力計較正に使用されていた手法をもとに精度の検証を行った。この較正原理では、スカラー磁力計の観測値を基準として、ベクトル磁力計に必要な較正パラメータを推定することができ、較正のベクトル磁力計から算出される全磁場 total B の誤差は 0.5 nT 以下となる。この較正原理の精度を評価する検証プログラムを作成し、国土地理院が発行する地磁気観測データ（久住観測所）の、2019 年 12 月 3 日のデータを真の磁場データと仮定して、解析を行ったところ、全磁場 total B の誤差 Δ B が 252.275 nT となった。較正前の誤差は 3459.71 nT であり、較正前と比較して較正後の total B は大きく改善することが確認できた。しかし本研究で開発する磁力計システムの要求は、精度 50nT 以内（1° 以内）であるため、算出された誤差は要求を満たしてない。そこで、較正パラメータのオフセットを変化させ、再度検証プログラムを用いて較正前後の値を比較した。オフセットを元の数千 nT から数十 nT に設定にすると、誤差が 0.10 nT と要求内であることが分かった。よって、パラメータのレンジによって較正精度が大きく変化することが確認された。

本発表では、フラックスゲート磁力計と光ポンピング磁力計の連続計測結果と較正プログラムの精度評価について報告する。

R006-P40
ポスター 1 ：11/24　PM1/PM2 （13:15-18:15）

キューブサット搭載用超小型・省電力プラズマ波動受信器の開発

#山本 康輔 [1)], 頭師 孝拓 [1)], 小嶋 浩嗣 [2)]
([1] 奈良高専, [2] 京大

Development of the miniaturized and low-power plasma wave receiver for use on CubeSat

#Kosuke Yamamoto[1)], Takahiro Zushi[1)], Hirotsugu Kojima[2)]
([1]National Institute of Technology, Nara College, [2]Kyoto university

In the field of plasma wave observation, the use of CubeSat has been increasing in recent years. CubeSat is a standardized small satellite of 10 cm cubic size. Its small size allows for increased observation opportunities and high-precision observations through simultaneous multi-point measurements. However, due to the limited size and power constraints of CubeSat, it is difficult to equip it with conventional high-performance plasma wave observing equipment.

To address this challenge, we are developing a new plasma wave receiver suitable for CubeSat. This receiver is ultra-compact and power-efficient, significantly smaller than traditional devices. By dividing the observed frequency band being observed into three parts and particularly reducing the sampling frequency in the low-frequency band, the structure allows for a dramatic reduction in power consumption. The analog circuit has been developed as Application-Specific Integrated Circuits (ASICs), resulting in significant miniaturization compared to conventional designs.

We also use a low-power microcontroller called the RP2040 for digital signal processing and overall system control. The RP2040 is equipped with a Cortex M0+ CPU, which, while low in power consumption, does not have high computing performance. To address this, we leverage a module called PIO to control the system directly without going through the CPU.

We are currently advancing the development of a breadboard model. This breadboard model includes a one-channel analog integrated circuit, six-channel A/D converters, and a microcontroller. In my presentation, we will show the results of the power consumption measurements and present the results of evaluating the overall receiver performance with a breadboard model including analog circuits.

プラズマ波動観測の分野において、近年、CubeSat の利用が増加している。CubeSat は、10cm 立方の小型規格衛星であり、その小型軽量性を活かして、観測機会の増加や多点同時観測による高精度観測を行うことを可能にする。しかし、CubeSat の限られた大きさや電力の制約により、従来の高性能なプラズマ波動観測装置を搭載することは困難である。

この課題を解決するため、我々は CubeSat に適した新しいプラズマ波動受信器の開発を行っている。この受信器は、超小型かつ省電力で、従来の装置よりもはるかに小型化されている。観測する周波数帯域を 3 つに分割し、特に低周波帯域でのサンプリング周波数を減らすことで、消費電力を劇的に削減できる構造となっている。アナログ回路部分は、専用集積回路として開発されており、その結果、従来に比べて大幅な小型化を実現した。

さらに、デジタル信号処理やシステム全体の制御には、RP2040 という省電力なマイクロコントローラを使用している。このマイクロコントローラに搭載されている Cortex M0+ CPU は低消費マイクロコントローラである一方、演算性能は高くないため、PIO と呼ばれる機能を活用して、CPU を介さずに直接制御を行っている。

現在、我々はブレッドボードモデルの開発を進めている。このブレッドボードモデルは 1ch のアナログ集積回路と 6ch の A/D コンバータ、マイクロコントローラを搭載している。発表においては、アナログ回路を含めたブレッドボードモデルにおける消費電力の測定と、受信器全体の性能の評価を行い、結果を示す。

R006-P41
ポスター 1 ：11/24　PM1/PM2 （13:15-18:15）

宇宙プラズマ分析器における視野掃引用軌道偏向機構の形状設計

#北村 悠稀 [1)], 横田 勝一郎 [1)], 笠原 慧 [2)], 寺田 健太郎 [1)]
([1] 大阪大, [2] 東京大学

Geometry design of orbit deflection mechanisms for field-of-view sweeping in space plasma analyzers.

#Yuuki Kitamura[1)], Shoichiro Yokota[1)], Satoshi Kasahara[2)], Kentarou Terada[1)]
([1]Osaka University, [2]The University of Tokyo

In-situ observations using plasma analyzers on board exploration satellites are an important tool for understanding the behavior of plasma in space. Energy analyzers such as Top-Hat electrostatic analyzers are used as plasma analyzers.

To understand the behavior of the plasma, it is necessary to study the three-dimensional distribution in detail, but as the energy analyzer has only a two-dimensional field of view, a three-dimensional field of view is obtained either by using the satellite's spinning motion or by installing an orbital deflector at the plasma injection point.

While there is a limit to the voltage value that can be applied to a Deflector, there is a similar upper limit to the energy value of the plasma that can sweep the field of view for most Deflectors in relation to the applied voltage value, which poses a challenge in ensuring a complete 3-D field of view in the high energy band.

One of the reasons for this is the lack of investigation of the parameters that affect performance and the establishment of a theory to evaluate performance compared to electrostatic analyzers using spherical polar plates.

Therefore, in this study, we conducted simulations with various pole shapes to theoretically evaluate this deflector performance, and investigated in detail how the pole shapes affect the performance.

Specifically, the Deflector and energy analyzer geometry was set up in 3-D cylindrical coordinate space, and the Successive Over-Relaxation method was used to simulate the propagation of potentials. Next, ion trajectories were simulated for this space using a second-order Runge-Kutta method.

The results show that the performance depends especially on the length L of the deflector and the distance G between the pole plates.

It was also found that if the L/G ratio is kept constant, the performance is similar without size dependence.

宇宙空間におけるプラズマの挙動を理解する上で、探査衛星に搭載されたプラズマ分析器を使用したその場観測は重要な手段となる。プラズマ分析器としては Top-Hat 型の静電分析器などのエネルギー分析器が用いられる。

プラズマの挙動を理解するためには 3 次元的な分布を詳細に調べる必要があるが、エネルギー分析器は 2 次元的な視野しか持たないため、探査衛星の自転運動を利用するか、プラズマ入射部に軌道偏向機構 (Deflector) を搭載することによって 3 次元的な視野を獲得する。

Deflector に印加できる電圧値には制限がある一方で、多くの Deflector について印加電圧値に対する視野掃引可能なプラズマのエネルギー値に同程度の上限が存在しており、高エネルギー帯における完全な 3 次元視野の確保に課題がある。

この原因の一つとして、球殻極板を用いた静電分析器に比べて性能に対して影響を与えるパラメータの調査や、性能評価を行うための理論の確立が不十分であることが挙げられる。

そこで本研究では、この Deflector 性能の理論的な評価に向けて様々な極板形状でのシミュレーションを行い、その極板形状が性能にどのような影響を与えるのかを詳細に調査した。具体的には、3 次元円筒座標空間上で Deflector およびエネルギー分析器形状を設定し、Successive Over-Relaxation 法を用いて電位の伝播をシミュレーションした。次にこの空間に対して 2 次の Runge-Kutta 法を用いてイオン軌道をシミュレーションした。

その結果、性能は特に Deflector の長さ L と極板同士の距離 G に大きく依存することが分かった。また、L/G 比を一定に保つと、サイズ依存性無く同様の性能を示すことが分かった。

R006-P42
ポスター 1 ：11/24　PM1/PM2 （13:15-18:15）

プラズマ粒子観測器向け多機能 ASIC の開発

#高橋 士門 [1)], 菊川 素如 [1)], 浅村 和史 [2)], 頭師 孝拓 [3)], 栗田 怜 [1)], 横田 勝一郎 [4)], 小嶋 浩嗣 [1)]
([1 京大, ([2 宇宙研, ([3 奈良高専, ([4 大阪大

Development of a Multifunctional ASIC for Plasma Particle Detectors on board Satellites

#Shimon Takahashi[1)], Motoyuki Kikukawa[1)], Kazushi Asamura[2)], Takahiro Zushi[3)], Satoshi Kurita[1)], Shoichiro Yokota[4)], Hirotsugu Kojima[1)]
([1Kyoto University, ([2Japan Aerospace Exploration Agency, ([3National Institute of Technology（KOSEN), Nara College, ([4Osaka University

Space plasma is characterized by its extremely low density, where energy exchange through particle collisions is negligible. Nevertheless, significant changes in particle kinetic energy, such as heating and acceleration of electrons and ions, are observed. These phenomena are mediated by plasma waves through a process known as wave-particle interaction. Detailed observations of these interactions are crucial for comprehending the electromagnetic environment of the universe. To elucidate the energy transport processes facilitated by wave-particle interactions in spatially inhomogeneous space plasmas, simultaneous multi-point observations are essential. Nano-satellite constellations offer a promising approach to achieve this goal. However, conventional plasma analyzers are often too large and resource-intensive for widespread deployment on ultra-compact satellites, highlighting the urgent need for miniaturized analyzers. This study aims to miniaturize the electronic circuitry of particle analyzers using Application-Specific Integrated Circuit (ASIC) technology. We have developed an analog front-end circuit for a Time-of-Flight (TOF) based ion energy-mass spectrometer. Ion beam irradiation experiments have confirmed that this circuit possesses sufficient time resolution to discriminate ion species typical of the Earth's magnetosphere. To ensure space environment compatibility, we conducted comprehensive environmental tests. Temperature tests ranging from -20 ℃ to 60 ℃ and radiation tests up to 300krad demonstrated the ASIC's reliability under space-like conditions. Furthermore, we have integrated a counting function into the newly developed ASIC, enabling simultaneous output of TOF signals and accumulated particle counts over specified time intervals.

宇宙空間のプラズマ無衝突プラズマであり、粒子同士の衝突によるエネルギー交換はほとんど生じない。しかし、実際には電子やイオンの加熱・加速などの運動エネルギーの変化は発生しており、その現象にはプラズマ波動が媒体として関与している。この現象は波動粒子相互作用と呼ばれ、その詳細な観測は宇宙電磁環境を理解する上で非常に重要である。空間的に非一様性が強い宇宙プラズマにおいて、波動粒子相互作用によるエネルギーの輸送過程を理解するには、超小型衛星による同時多点観測が必要とされる。しかし、従来の観測装置は回路規模が大きく、同時多点観測を実現するためのリソースが非常に多く必要となることから観測装置の小型化が求められている。そこで本研究では、粒子観測器の電子回路部を特定用途向け集積回路 (ASIC) 技術によって小型化することを目的としている。TOF (Time-of-Flight) 型イオン質量分析器向けに開発したアナログフロントエンド回路は、イオンビーム照射実験により、地球磁気圏のプラズマイオンを識別するために十分な時間分解能を持つことが確認された。また、-20 ℃から 60 ℃までの温度試験および 300krad までの放射線試験を実施し、宇宙環境下においても信頼性を保つことが実証された。さらに、新たに開発した ASIC には粒子カウンタが統合されており、TOF 信号と一定時間に蓄積された粒子数を同時に出力できる機能を備えている。

R006-P43
ポスター 1 ：11/24　PM1/PM2 （13:15-18:15）

#滑川 拓 [1)], 坂口 歌織 [1)], 大辻 賢一 [1)], Park Inchun[1)], 齊藤 慎司 [1)], 三谷 烈史 [2)]
([1] 情報通信研究機構, [2] 宇宙研

Development of Radiation Monitor for Space weather measuring Electrons (RMS-e) for Himawari-10

#Taku Namekawa[1)], Kaori Sakaguchi[1)], Kenichi Otsuji[1)], Inchun Park[1)], Shinji Saito[1)], Takefumi Mitani[2)]
([1]National Institute of Information and Communications Technology, [2]Japan Aerospace Exploration Agency, Institute of Space and Astronautical Science

Radiation Monitor for Space weather measuring Electrons (RMS-e) is an electron detector that will be installed on the next geostationary meteorological satellite Himawari-10 to provide continuous observations of high-energy electrons in the geostationary satellite orbit over Japan. Current space weather forecasting in Japan is based on observations from the GOES satellites, which have different conditions from the space environment around the geostationary satellite orbits over Japan. RMS-e will provide continuous observations of energetic electrons in geostationary satellite orbits over Japan, which are critical for improving the accuracy of space weather forecasts in Japan.

RMS-e consists of two sets of layered solid-state detectors (SSDs) made of silicon semiconductors called RMS-e lo and RMS-e hi. RMS-e lo and RMS-e hi are designed to measure electrons with energies in the range of 50 keV to 1300 keV and 0.8 to 5 MeV, respectively. The energy resolution of RMS-e lo is 26 % for 50 keV electrons and that of RMS-e hi is than 15.8 % for 1 MeV electrons based on evaluation tests.

Currently, we are completing the development of the engineering model (EM) of RMS-e and preparing for the development of the proto flight model (PFM) of RMS-e.

In this presentation, we report the current status of the instrument development and test results of RMS-e.

R006-P44
ポスター 1 ：11/24　PM1/PM2 （13:15-18:15）

LAMP1 ロケット搭載カメラのオーロラ観測成果と LAMP2 ロケット搭載カメラ開発と地上観測初期報告

#坂野井 健 [1)], 浅村 和史 [2)], 三好 由純 [3)], 細川 敬祐 [4)], 滑川 拓 [5)], 大山 伸一郎 [6)], 西山 尚典 [7)], 吹澤 瑞貴 [7)], 石井 智士 [8)], ジェーンズ アリソン [9)]
[1 東北大・理・PPARC, [2 宇宙研, [3 名大 ISEE, [4 電通大, [5NICT, [6 名大 ISEE, [7 極地研, [8 立教大, [9 アイオワ大学

Results of the auroral camera on the LAMP1 rocket and development of the LAMP2 rocket camera

#Takeshi Sakanoi[1)], Kazushi Asamura[2)], Yoshizumi Miyoshi[3)], Keisuke Hosokawa[4)], Taku Namekawa[5)], Shin ichiro Oyama[6)], Takanori Nishiyama[7)], Mizuki Fukizawa[7)], Satoshi Ishii[8)], Jaynes N. Allison[9)]
[1PPARC, Graduate School of Science, Tohoku University, [2Japan Aerospace Exploration Agency, [3Institute for Space-Earth Environement Research, Nagoya University, [4Graduate School of Informatics and Engineering, University of Electro-Communications, [5The National Institute of Information and Communications Technology, [6Institute for Space-Earth Environmental Research, Nagoya University, [7National Institute of Polar Research, [8Rikkyo University, [9The University of Iowa

We report the recent results of a multi-spectral auroral camera AIC on the NASA's LAMP rocket launched from Poker Flat at 11:27:30 UT on March 5, 2022. The purpose of LAMP rocket mission is to clarify the relationship between pulsating aurora and microbursts. AIC measured two auroral emissions in the E-region at 670 nm (N2 1PG) and mainly in the F-region at 845 nm (OI) using two CMOS cameras called AIC1 and AIC2. Two cameras took images simultaneously with a time resolution of ˜10 frame/s. The field-of-view (FOV) of AIC1 was 29 deg x 29 deg directed to the magnetic footprint covering 180 km x 180 km area with a resolution of 3 km x 3 km at the apex altitude (˜430 km altitude). FOV of AIC2 was 106 deg diameter circle covering the wide range from nadir to limb of the Earth.

The LAMP rocket was successfully launched into active pulsating auroral patches, and AIC and its despun platform worked satisfactorily throughout the flight. From AIC1 data, we compared auroral images with high- and low-energy electrons, and ground auroral images obtained at Venetie and Fort Yukon, and found good correspondence between them even for the sub-second variations.

From the AIC2 data, we estimated the altitude distribution of oxygen 845nm emission with the three methods and verified the peak altitude in association with precipitating electron energy obtained by the LAMP1 rocket. (1) Differential emission intensities in the direction of the magnetic footprint. (2) Emission intensities in the horizontal direction. (3) Auroral image in the limb direction around the apex attitude. From these analyses, we estimated the emission peaks in the altitude range from 160km to 330km. The estimated emission altitudes are consistent with the electron precipitation in the energy range of a few keV obtained by the rocket.

Although the LAMP1/AIC succeeded to observe pulsating auroral continuously, the sub-second (˜3Hz) modulation of pulsating aurora was not obvious. In addition, the sensitivity was not sufficient for the faint oxygen 845nm emission. In the next rocket project LAMP2, therefore, we plan to develop auroral cameras which have higher sensitivity and faster imaging capability. LAMP2 rocket mission is a NASA's project which is planned to be launched in the winter of 2026. We are now designing and developing new auroral cameras AIC2 with a sampling of 15 frame/s. We selected a larger-sized CMOS (ASI-432MM, 1.1", global shutter) which has higher sensitivity than LAMP/AIC (ASI-183MM, 1", rolling shutter). As established in the previous LAMP1 rocket, the single board computer NanoPiM4V2 is used for primary processing of camera. We developed an engineering model (EM) of AIC2 using the same objective lens as the flight model, filters (N2 670nm and oxygen 845nm), and CMOS sensors, and carried out the optical tests with blinking LED arrays. We verified the time accuracy even at 20 fps (50 ms exposure) image data. The AIC2 EM cameras are now installed at the Skibton station, and ready for the automatic operation during the winter period this year. The operation is scheduled to start in the end of this September and obtain the image data for 30 min around the midnight every day. The data and the instruments will be recovered by the next spring in 2024. In this presentation, we give the first result of image data obtained by AIC2 EM camera at Skibton.

R006-P45
ポスター 1 ：11/24　PM1/PM2 （13:15-18:15）

地球磁気圏 X 線撮像計画 GEO-X の現状

#江副 祐一郎 [1)], 船瀬 龍 [2,3)], 永田 晴紀 [4)], 三好 由純 [5)], 中嶋 大 [6)], 三石 郁之 [5)], 石川 久美 [1)], 沼澤 正樹 [1)], 佐藤 佑樹 [6)], 川端 洋輔 [3)], 布施 綾太 [3)], 中島 晋太郎 [2)], Boden Ralf[2)], Kamps Landon[7)], 信原 佑樹 [7)], 平井 翔太 [7)], 米山 友景 [8)], 萩野 浩一 [3)], 松本 洋介 [9)], 細川 敬祐 [10)], 笠原 慧 [3)], 伊師 大貴 [2)], 平賀 純子 [11)], 満田 和久 [12)], 藤本 正樹 [2)], 上野 宗孝 [2)], 山崎 敦 [2)], 長谷川 洋 [2)], 三谷 烈史 [2)], 川勝 康弘 [2)], 岩田 隆浩 [2)]
([1 東京都立大学, ([2JAXA 宇宙研, ([3 東京大学, ([4 北海道大学, ([5 名古屋大学, ([6 関東学院大学, ([7Letara 株式会社, ([8 中央大学, ([9 千葉大学, ([10 電気通信大学, ([11 関西学院大学, ([12 高エネルギー加速器研究機構

Status of GEO-X mission

#Yuichiro Ezoe[1)], Ryu Funase[2,3)], Harunori Nagata[4)], Yoshizumi Miyoshi[5)], Hiroshi Nakajima[6)], Ikuyuki Mitsuishi[5)], Kumi Ishikawa[1)], Masaki Numazawa[1)], Yuki Satoh[6)], Yosuke Kawabata[3)], Ryota Fuse[3)], Shintaro Nakajima[2)], Ralf Boden[2)], Landon Kamps[7)], Yuki Nobuhara[7)], Shota Hirai[7)], Tomokage Yoneyama[8)], Koichi Hagino[3)], Yosuke Matsumoto[9)], Keisuke Hosokawa[10)], Satoshi Kasahara[3)], Daiki Ishi[2)], Junko Hiraga[11)], Kazuhisa Mitsuda[12)], Masaki Fujimoto[2)], Munetaka Ueno[2)], Atsushi Yamazaki[2)], Hiroshi Hasegawa[2)], Takefumi Mitani[2)], Yasuhiro Kawakatsu[2)], Takahiro Iwata[2)]
([1Tokyo Metropolitan University, ([2ISAS/JAXA, ([3The University of Tokyo, ([4Hokkaido University, ([5Nagoya University, ([6Kanto Gakuin University, ([7Letara, ([8Chuo University, ([9Chiba University, ([10University of Electro-Communications, ([11Kwansei Gakuin University, ([12KEK

GEO-X (GEOspace X-ray imager) is a small satellite mission aiming at visualization of the Earth's magnetosphere by X-rays and revealing dynamical couplings between solar wind and magnetosphere. In recent years, X-ray astronomy satellite observations discovered soft X-ray emission originated from the magnetosphere due to charge exchange between solar wind ions and exospheric neutrals. From observational and theoretical studies, this emission is expected to increase largely in the sheath region because of the large ambient plasma density. Therefore, the boundary region between the bow shock and the magnetopause will be detected with the strong soft X-ray emission.

We are developing GEO-X to realize this global imaging of the magnetosphere by X-ray observations (Ezoe et al. 2023 JATIS). It is a small satellite within 50 kg and 50 cm cube carrying a novel compact X-ray imaging spectrometer. The satellite has a propulsion system to increase an altitude from piggyback launch to Geo Transfer Orbit or Trans Lunar Injection orbit. A wide FOV (5x5 deg) and a good spatial resolution (10 arcmin) X-ray (0.3-2 keV) imaging spectrometer allows us to take snapshots of the magnetosphere and X-ray spectra of the solar wind charge exchange emission. These data will greatly advance our understanding of the magnetospheric structures and their response to solar activities. We aim to launch the satellite around the peak of the 25th solar cycle (~2025-27). In this paper, we report on the status of the GEO-X mission.

GEO-X (GEOspace X-ray imager) は地球磁気圏の X 線撮像とそれによる太陽風に対する磁気圏応答の理解を目指す超小型衛星計画である。近年、X 線天文衛星「すざく」などによって地球の周辺から軟 X 線が放射されていることが分かってきた。太陽風に含まれる多価イオンが地球の超高層大気である外圏の中性物質から電子を奪い、奪われた電子がイオン中で基底準位に落ちる中で発光する電荷交換反応によるものである。こうした中、観測および理論予測から、太陽風プラズマ密度は衝撃波通過後の遷移領域で高まることから、X 線を用いた昼側磁気圏のグローバル撮像が可能であることが示唆されてきた。

我々はそこで世界に先駆けて磁気圏 X 線撮像を狙う超小型衛星 GEO-X の開発を進めてきた (Ezoe et al. 2023 JATIS)。衛星は目標 約 50 kg 以内かつ約 50 cm 立方以内と小型であり、そこに超軽量・広視野・高感度の独自の X 線撮像分光装置を搭載する。衛星はジオトランスファ軌道や月遷移軌道等への相乗りから、推進系を使って軌道変換を行なって放射源である磁気圏の外からの俯瞰的な観測を行う。観測装置は広視野 (5x5 deg) かつ優れた角度分解能 (10 arcmin) を実現し、磁気圏構造の微細構造の分解および X 線放射スペクトルの取得を可能とし、我々の磁気圏構造とその太陽活動に対する応答の理解の深化に大きく資すると期待できる。打ち上げは第二十五太陽周期の極大付近 (2025-27 年頃) を目指しており、検討中である。本講演では計画の現状について報告する。

R006-P46
ポスター 1 ：11/24　PM1/PM2 （13:15-18:15）

#桑原 正輝 [1)], 吉岡 和夫 [2)], 村上 豪 [3)], 吉川 一朗 [4)]
([1] 立教大学, [2] 東大・新領域, [3]ISAS/JAXA, [4] 東大

The observation of the Earth's plasmasphere in extreme ultraviolet from a nano-spacecraft

#Masaki Kuwabara[1)], Kazuo Yoshioka[2)], Go Murakami[3)], Ichiro Yoshikawa[4)]
([1]Rikkyo University, [2]The University of Tokyo, [3]Japan Aerospace Exploration Agency, [4]University of Tokyo

The Plasmaspheric Helium ion Observation by Enhanced New Imager in eXtreme ultraviolet (PHOENIX) onboard EQUilibriUm Lunar-Earth point 6U Spacecraft (EQUULEUS) is an ultra-small instrument for observing the Earth's plasmasphere from a meridian view. The PHOENIX instrument is a normal-incidence telescope optimized for observing He II emission at 30.4 nm. It comprises an Mo/Si multilayer-coated mirror, an Al/C metallic thin filter, and a 2-D photon-counting device with microchannel plate and resistive anode. In May 2023, PHOENIX successfully conducted imaging observations of the Earth's plasmasphere while EQUULEUS was en route to the Earth-Moon Lagrange point 2, revealing the density structure formed along the dipole-shaped magnetic field lines. This marks the first instance of imaging the entire Earth's plasmasphere using an ultra-small instrument onboard a nano-spacecraft. In this presentation, an overview of the PHOENIX instrument and the observation results of the Earth's plasmasphere will be shown. Future applications of PHOENIX for planetary exploration will also be discussed.